2011

OPTIMIZATION OF COAGULATION AND SYNERESIS PROCESSES IN CHEESEMAKING USING A LIGHT BACKSCATTER SENSOR TECHNOLOGY

Tatiana Gravena Ferreira
University of Kentucky, tatianagravena@yahoo.com.br

ABSTRACT OF THESIS

OPTIMIZATION OF COAGULATION AND SYNERESIS PROCESSES IN CHEESEMAKING USING A LIGHT BACKSCATTER SENSOR TECHNOLOGY

Curd syneresis, a critical step in cheesemaking, directly influences the quality of cheese. The syneresis process is empirically controlled in cheese manufacturing plants. A sensor technology for this step would improve process control and enhance cheese quality. A light backscatter sensor with a Large Field of View (LFV) was tested using a central composite design over a broad range of cheese process conditions including milk pH, calcium chloride addition level, milk fat to protein ratio, temperature, and a cutting time factor (β). The research objectives were to determine if the LFV sensor could monitor coagulation and syneresis steps and provide information for predicting pressed curd moisture. Another objective was to optimize cheese yield and quality. The LFV sensor was found to monitor coagulation and syneresis and provide light backscatter information for predicting curd moisture content. A model for relating final curd moisture content with light backscatter response was developed and tested. Models for predicting whey fat losses, pressed curd moisture, and cheese yield were successfully developed ($R^2>0.75$) using the test factors as independent variables. This was the first attempt to develop a technology for controlling pressed curd moisture using a sensor to monitor the syneresis step.

KEYWORDS: sensor, syneresis, curd moisture control, cheese production optimization, cheese quality.

Tatiana Gravena Ferreira

May 17, 2011

OPTIMIZATION OF COAGULATION AND SYNERESIS PROCESSES IN CHEESEMAKING USING A LIGHT BACKSCATTER SENSOR TECHNOLOGY

By

Tatiana Gravena Ferreira

Dr. Fred Payne
Co-Director of Thesis

Dr. Manuel Castillo
Co-Director of Thesis

Dr. Dwayne Edwards
Director of Graduate Studies

May 17, 2011
Date

RULES FOR THE USE OF DISSERTATIONS

Unpublished dissertations submitted for the Master's degree and deposited in the University of Kentucky Library are as a rule open for inspection, but are to be used only with due regard to the rights of the authors. Bibliographical references may be noted, but quotations or summaries of parts may be published only with permission of the author, and with the usual scholarly acknowledgements.

Extensive copying or publication of the thesis in whole or in part also requires the consent of the Dean of the Graduate School of the University of Kentucky.

A library that borrows this dissertation for use by its patrons is expected to secure the signature of each user.

Name	Date

THESIS

Tatiana Gravena Ferreira

The Graduate School
University of Kentucky
2011

OPTIMIZATION OF COAGULATION AND SYNERESIS PROCESSES IN CHEESEMAKING USING A LIGHT BACKSCATTER SENSOR TECHNOLOGY

THESIS

A thesis submitted in partial fulfillment of the
requirements for the degree of Master of Science in
Biosystems and Agricultural Engineering
At the University of Kentucky

By

Tatiana Gravena Ferreira

Lexington, Kentucky

Co-Directors: Dr. Manuel Castillo, Associate Adjunct Professor
and Dr. Fred Payne, Professor of Biosystems Agricultural Engineering

Lexington, Kentucky
2011

This thesis is dedicated to my parents,
my brothers and my fiancé
for their love and support
that helped me to realize my dreams.

ACKNOWLEDGMENTS

It is a pleasure to be able to thank the many people who made this thesis possible, but it is difficult to transform my thoughts into words.

First, I want to thank God because he is the reason why things happen.

I would like to express my sincere gratitude to my advisors, Dr. Fred Payne and Dr. Manuel Castillo, for their patience, motivation, guidance, and especially because they believed that I could get here and they helped make this happen.

Besides my advisors, I would like to thank Dr. Czarena Crofcheck and Dr. Clair Hicks for their questions and really good comments.

I cannot forget Colette Fagan because without her help and knowledge it would have been much more difficult to get through this process.

My appreciation also goes to Sarah Short, Travis Darden, Emily Grieser, Lloyd Dunn, Burl Fannin, Franklin Jones, and Joseph Redwine for their valuable help during my tests. I want to extend my appreciation to the whole BAE family who always made my life easier. This departmental environment helped me to wake up every day wanting to go to work.

I am grateful to many new friends that I made, especially Jennifer Frederick, Levi dos Santos, Lucas Melo, Rodrigo Zandonadi, Maira Amaral,

Juliana Tenorio, and Felipe Porto who helped me as I was so far away from many people that I love. A special thanks to my "roommates" Tathyana Mello, Gabriela Morello, Igor Lopes, Enrique Alves, and Joe Luck, who obligated me to get out of my house and have some fun time. I also want to thank my old friends Maria Luiza Fortes and Leticia Guidi.

I want to thank the Trotter family where I lived during this time for their love, comprehension, and especially for making me feel at home. A special thanks to my Aunt Adriana who was my adviser, friend, and mom. Thanks for being patient with me, for listening to me, and especially for being with me throughout this process.

I wish to thank my entire family for providing a loving environment. My brothers: Tiago, Leandro, Gustavo, and Rafael; and my sister-in-law Giovana. I would like to extend my gratitude to my aunts, uncles, and cousins, especially my godmother Renata Giampietri.

I would like to thank my mom for all the emotional support that she has given me and for her medical support. To my dad: thanks for being rude when it was necessary. Without you I wouldn't even be a Food Engineer.

Last but not least, I would like to dedicate a special thanks to my fiancé Diego Fugiwara for his encouragement and love during the past few years. His support was in the end what made this thesis possible.

TABLE OF CONTENTS

LIST OF TABLES

LIST OF FIGURES

LIST OF ABBREVIATIONS

β	- Cutting time factor (dimensionless)
C	- Curd
CC	- Calcium Chloride addition level (mM)
CCD	- Central composite design
CCP	- Colloidal Calcium Phosphate
CFR	- Curd fat retention (%)
Ch	- Cheese
ChY	- Cheese Yield (%)
CM	- Curd Moisture before pressing (%)
CMP	- Curd Moisture after pressing (%)
CY	- Curd Yield (%)
FIW	- Fat in whey (%)
FP	- Ratio between fat and protein (dimensionless)
M	- Milk
MF	- Milk fat content (%)
RR	- Reflectance Ratio (dimensionless)
T	- Temperature (°C)
t_{cut}	- Cutting time of the coagulum (min)

t_{max} - time from enzyme addition to the inflection point of the light backscatter ratio (min)

TS - Total solid (%)

W - Whey

WF - Whey fat content (%)

WFL - Whey fat losses (%)

Chapter 1 : INTRODUCTION

Cheese manufacture represents a very important segment of the US economy. According to United States Department of Agriculture (USDA) the total U.S. cheese production in 2009, excluding cottage cheese, was 10.1 billion pounds which was 2% above 2008 production. Cheese quality has a large economic impact in the cheese industry and is significantly affected by curd moisture content, a critical ripening factor that affects cheese texture and flavor.

The rate and extent of syneresis influences the moisture, mineral, and lactose content of curd; affects protein and fat losses in whey; and impact cheese texture, color, flavor, safety and yield. The syneresis step is affected by milk composition and process conditions with the effect not clearly understood. The control of syneresis is really important in terms of cheese optimization process.

Unfortunately, there are currently no process control technologies available for curd syneresis. As a result, the control of the syneresis process is empirical with each plant using process conditions that have historically produced an acceptable product. Castillo et al. (2005) and Fagan (2007c) showed that light backscatter at 980 nm offered a potential method for monitoring the status of syneresis in cheese vat. A sensor technology that is able to control curd moisture content would have a large impact on cheese manufacturing worldwide in terms of product quality, consistency and production efficiency since an increase in moisture content by as little as 1% would have an important effect on cheese yield, quality and profits.

This study aimed:

(i) To determine if a light backscatter technology could be used to monitor and control the coagulation and the syneresis steps in cheesemaking;

(ii) To analyze the effect of independent variables (temperature, β, pH, fat/protein ratio, and calcium chloride addition level) on different cheesemaking parameters such as pressed curd moisture, yield, and whey fat losses to evaluate the effect of those experimental factors and their interaction on process optimization;

(iii) To determine if light backscatter can be used to predict the moisture content of pressed curd over a wide range of coagulation and syneresis conditions normally encountered in cheesemaking.

Chapter 2 : LITERATURE REVIEW

2.1. Cheese manufacture

Cheese is the generic name for a group of fermented milk-based food products produced throughout the world in a great diversity of flavors, texture, and forms (Fox, 2000).

Cheesemaking involves a number of main stages which are common to most types of cheese. There are also different stages required to produce specifics varieties. Although the manufacturing protocols can differ for individual varieties, cheese processing can be basically divided into the following steps: milk pre-treatment, coagulation, syneresis, whey drainage, molding, pressing, salting, and ripening or maturation (Figure 2.1).

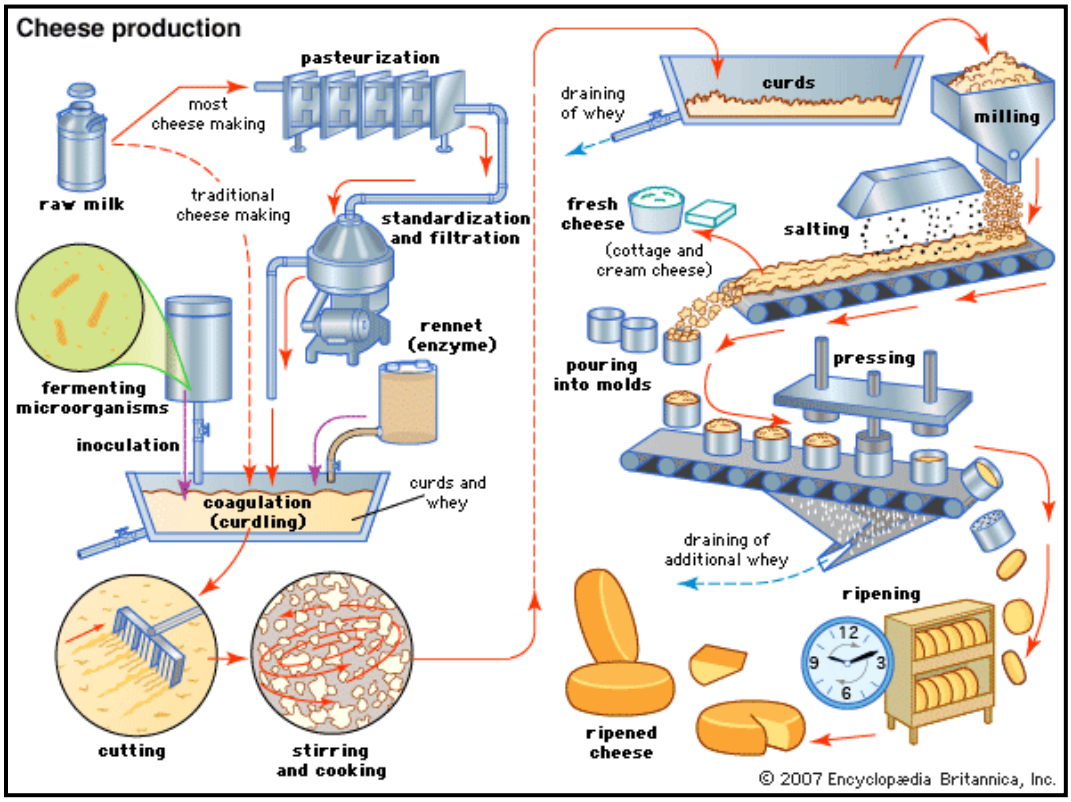

Figure 2.1 - Technological steps in cheese manufacturing (Encyccheese, 2011).

After pre-treatment, milk is coagulated by enzymatic and/or acid action, which transforms the milk into a gel. Casein gels consist of a three-dimensional, porous and viscoelastic matrix of casein micelles saturated with an interstitial, viscous fluid called whey. Once the gel reaches an adequate firmness, the gel is cut into curd grains, which induces syneresis and the expulsion of whey. After a certain stirring period, the physical separation of the whey and curd follows. Thus, curd is further processed into cheese by molding, pressing, salting, and ripening.

2.1.1. Milk pre-treatment

The cheese quality is strongly influenced by the milk quality. The treatments to be applied to the milk before cheesemaking depend on the composition and the properties of the milk; and the type of cheese to be produced. Milk pre-treatment processes include: pasteurization, milk fat content standardization, and homogenization. The addition of calcium chloride ($CaCl_2$) is also conducted prior to curd making depending on the severity and type of milk pre-treatment.

The pasteurization has both positive and negative effects on cheese. While the process does make a safer product by reducing the bacteria level, cheese loses flavor and character. According to Fox 1993, although raw milk is still used in commercial and farmhouse cheesemaking, most cheese milk is now pasteurized. Since 1949, the US government has forbidden the sale of cheeses made from unpasteurized milk unless the cheese is aged at least 60 days to ensure that the cheese is free from pathogenic bacteria.

Fat standardization is the adjustment of the fat composition to a specified fat to protein ratio. It is important because the level of fat influences several aspects of cheese, including composition, biochemistry, microstructure, yield,

rheological and textural properties, cooking properties, and ripening (Guinee and McSweeney 2006). Scott et al. (1998) listed the following reasons for standardization of cheese milks:

- Compensate for seasonal variation in the raw milk composition to produce a consistent cheese;
- Fulfill the different fat standards requirements: 'full fat', 'half fat', and 'quarter fat'; which have been normal for some semi-hard cheeses (e.g. Edam) and soft cheeses (e.g. Camembert);
- Satisfy a growing market demand for reduced and low fat cheeses.

Milk for cheesemaking is not normally homogenized, because homogenized milk forms a rennet coagulum (gel) with a lower tendency to undergo syneresis upon cutting or stirring than that from nonhomogenized milk. The homogenization results in cheese with higher moisture content. The homogenization results in a reduction fat globule size and an increase in the interfacial fat surface by a factor of 5-6. Simultaneously the fat globules become coated with a protein layer consisting of casein micelles, spread casein micelles, micelle subunits, and whey proteins; casein is preferentially absorbed over whey proteins at the fat-water interface (Guinee et al., 1997). It may be advantageous to homogenize milk for low-fat cheese so as to obtain higher moisture content and thus softer cheese texture. Besides the higher moisture content, homogenization of milk produces cheese with altered texture (e.g., lower elasticity and firmness), altered flavor (e.g., hydrolytic rancidity), and altered functionality (e.g., reduced flow) (Fox et al 2000).

Calcium chloride is often added to cheese milk because it stimulates coagulation, curd firming, and whey separation. This is probably due to Ca^{2+} binding to the casein micelles in such a way that it reduces the repulsive forces

between them, perhaps by promoting hydrophobic interactions and hence the aggregation reaction of enzymatic coagulation (Green et al., 1977). Other salts like phosphate can be added with the same propose.

Once the milk is ready to process, the coagulation is induced either by acidification or enzyme addition. Sometimes a combination process is applied.

2.1.2. Coagulation

The essential step in the manufacture of all cheese varieties involves coagulation of the casein fraction of the milk protein to form a gel that entraps the fat, if present (Fox et al 2000).

Two types of coagulation are applied at industrial scale: acid coagulation and rennet coagulation. Sometimes a combination of those is used. Rennet coagulation is faster (minutes) compared to the slower rate of acid development (hours) required by cultures to coagulate milk for cheeses such as cottage cheese. In contrast, milk coagulates very rapidly using the addition of acid directly. Rennet milk gels also undergo much greater syneresis than acid milk gels, which helps to produce cheeses with lower moisture levels (Lucey 2002). Coagulation of milk by rennet probably occurred initially by accident, as warm milk was stored in sacks made from the stomachs of ruminant animals which contained some residual proteinase.

Lucey 2002 stated that coagulation of milk by rennet may be divided into primary (enzymatic hydrolysis) and secondary (casein micelle aggregation) stages, although these stages overlap to some extent during cheesemaking. During the primary stage, κ-casein is cleaved by rennet at the Phe_{105}-Met_{106} bond to yield two peptides with markedly different properties. The casein macropeptide moiety (CPM) or glycomacropeptide (GMP) (residues 106 to 169)

is hydrophilic and soluble and diffuses away from the micelle after hydrolysis, whereas the *para*- κ-casein moiety (residues 1 to 105) is strongly hydrophobic and remains attached to the micelle. The progressive hydrolysis of κ-casein during the primary stage destabilizes the casein micelles that become susceptible to aggregation and after a lag phase, a three-dimensional gel network (called a 'coagulum') is formed (Figure 2.2) (Lucey and Fox, 1993).

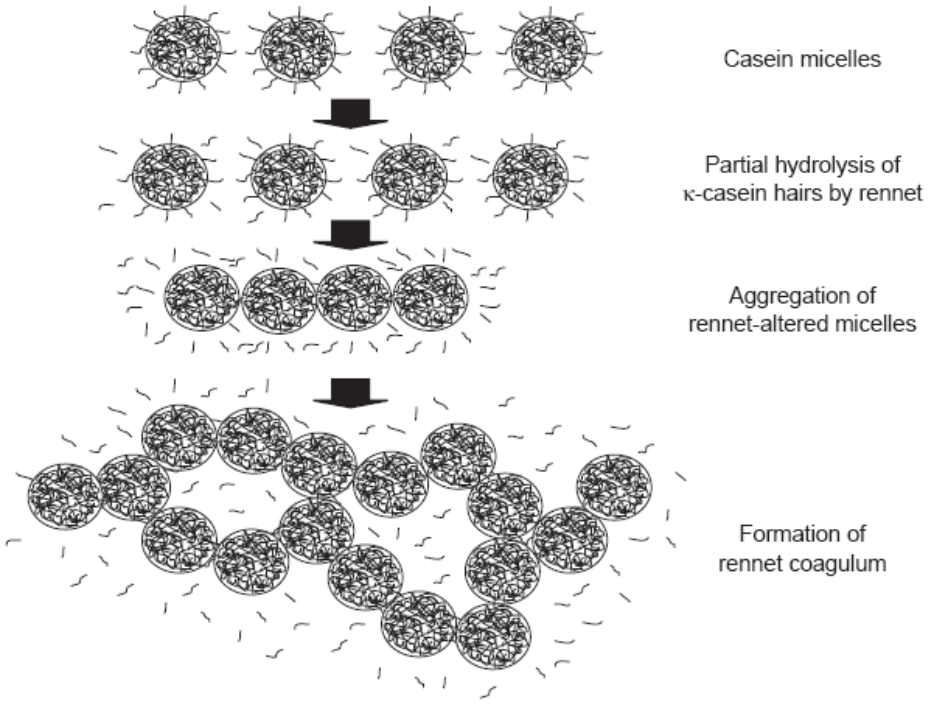

Figure 2.2 - Schematic drawing of the various processes occurring during the rennet coagulation of milk (Lucey, 2002).

According to Green and Gradison (1993) the increase in curd firmness is due to increases in both number and strength of linkage between micelles.

The rheological properties of the gel vary according to the conditions of coagulation (quantity of milk-clotting enzyme, pH, temperature, rate of acidification), and the original characteristics of the milk (Brulé and Lenoir, 1987).

In practice cutting time is a visually determined parameter (Berridge clotting time), which corresponds to the apparition of the first clots on the walls of a rotating glass tube. Once the gel reaches an adequate firmness, the gel is cut into curd grains, which induces syneresis and the expulsion of whey.

2.1.3. Syneresis

Syneresis can be described as the course by which the coagulum is concentrated by the elimination of water and soluble constituents (Weber, 1987). Syneresis is one of the most important processes in cheesemaking because it directly affects cheese yield and quality through its effect on moisture, mineral and lactose content of curd (Weber, 1987). Surprisingly, syneresis is one of the less understood processes in cheese manufacturing. This process can occur spontaneously but it is very limited with enzymatic coagulation. Thus usually two mechanisms are used to promoting syneresis: cutting and stirring.

Walstra et al. (1985) found that there are three possible causes of syneresis: change in solubility, rearrangement, and shrinkage of casein particles. The rearrangement of the *para*-κ-casein micelle network is the main cause of syneresis. The extent of rearrangement that occurs is related to the dynamics (average life-time) and relaxation of the protein-protein bonds as expressed in terms of the loss tangent which indicates the viscoelastic character of the material and to the resistance to yielding of the casein strands (Lee, 2010). Mellema et al. (2002) classified the main types of rearrangements in rennet-induced gels as follows:

a) Sub-particles or intra-particle rearrangements (size in casein gels <~0.2 μm);

b) Inter-particle rearrangement (size in casein gels ~0.2-1 μm);

c) Inter-cluster rearrangement (size in casein gels ~1-40 μm);

d) syneresis (macroscopic).

The rearrangement types are illustrated in Figure 2.3.

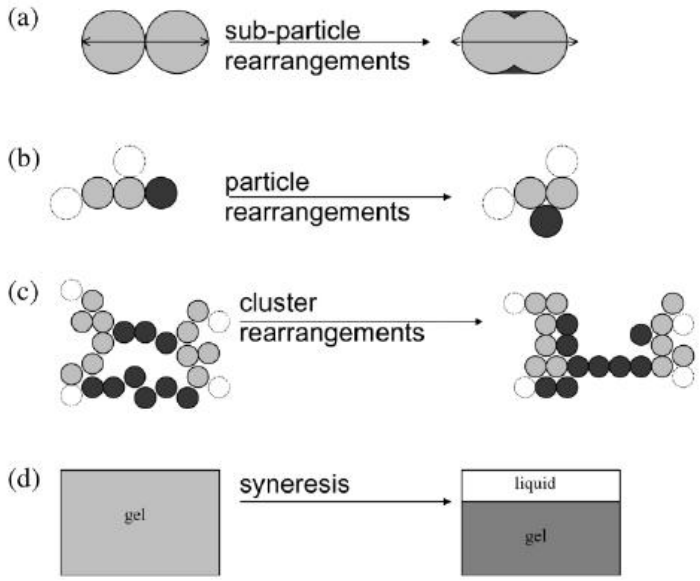

Figure 2.3 - Four different levels of structural network rearrangements on rennet-induced casein gels: (a) sub-particles; (b) inter-particles; (c) inter-cluster; and (d) the whole gel.

During syneresis, micelle rearrangement results in coarsening of the gel, which decreases the total free energy of the system by increasing the number of bonds (Lucey, 2002). In other words, after cutting, the matrix is continuously rearranging towards equilibrium, exerting a pressure on whey that escapes at the curd grains boundaries as the curd grain continues to shrink, and their permeability decreases with time.

The rate and extent of syneresis depend on a number of factors including coagulation conditions, the resulting gel properties, and cutting/stirring conditions (Fagan, 2007).

Although this project in considering only the principal whey drainage that occurs in the vat, a secondary or complementary whey drainage that takes place during molding, pressing, salting, and ripening is crucial in cheese technology as it contributes to determine the dry matter content and composition of drained curd and consequently those of the final product (Fagan 2007).

After a certain stirring period, the physical separation of the whey and curd in vat is completed. Thus, curd is further pressed into cheese.

2.1.4. Pressing

Curd is typically transferred to molds of the cheese's characteristic shape and size. The principal purpose of molding is to allow the curd to form a continuous mass; matting of high-moisture curds occurs readily under their own weight but pressing is required for low-moisture cheese (Fox et al., 2000).

Pressed cheeses are submitted to a pressing system after have been molded with the purpose of assist final whey expulsion, provide texture, shape the cheese, and provide a rind on cheeses with long ripening periods. Pressing should be gradual at first, because initial high pressure compresses the surface layer and can lock moisture into pockets in the body of the cheese (Tetra Pack, 1995). The intensity of pressure and the length of the pressing process vary with the type of cheese; it typically ranges between 0.1 and 1 kg/cm^2 (Everard et al., 2011) where the smallest pressure is usually applied to fresh cheese.

2.2. Factors affecting coagulation and syneresis

Although coagulation and syneresis are different steps in the cheesemaking processes they are not independent. Consequently, factors that affect curd formation or structure may also affect syneresis.

2.2.1. Factors affecting coagulation

Colette (2006) stated that the rate of coagulation and the resulting firmness of the gel depend on rennet concentration, coagulation temperature, milk pH, milk fat content, and addition of calcium chloride. Table 2.1, adapted from Colette (2006), outlines the effect factors on coagulation.

Table 2.1 - Factors affecting curd formation.

Factors	**Curd Formation**
Milk pre-treatment	
Refrigeration	Decrease
Pasteurization temperature increase	Decrease
Homogenization	Decrease
$CaCl_2$ addition	Increase
Milk composition	
Fat Content decrease	Increase
CCP increase	Increase
Casein concentration increase	Increase
Coagulation Condition	
Temperature increase	Increase
pH decrease	Increase
Enzyme concentration increase	Increase

The effect of enzyme concentration on the coagulation is directly related to time of reaction and gel firmness. There are many equations to describe its effect on clotting time, which are valid within certain limits of enzyme concentration, temperature, and pH. According to Lucey (2002) the most widely used is the Holter equation:

$$CT = \left(\frac{K}{[E]}\right) + A \qquad \text{Eqn.2.1}$$

where CT is the clotting time, K is a constant , [E] is the enzyme concentration and A is a constant. Clotting time is the total time required for both enzymatic and aggregation phases of coagulation, so A in this equation refers to the time need for the second phase, which is not enzyme dependent (Lucey, 2002). According to Equation 2.1 when the enzyme concentration [E] is large, clotting time tends to A and clotting time depends mostly on the aggregation.

The optimum coagulation temperature for rennet-induced gels is 30-35 ^{o}C and the typical coagulation temperature used in cheesemaking is around 31 ^{o}C (Lucey, 2002). Temperature seems to have a larger effect on the aggregation phase (second phase) than the enzymatic phase. This results because the Q_{10} of the primary reaction is of the order of 2 while that of secondary reaction is about 11-16 (Brulé and Lenoir, 1987; Lucey, 2002).

The pH effect is noticed on coagulation time and the firmness of the gel. Although changes in pH affects both the enzymatic and aggregation reactions, it is more affective on the second phase (Castillo et al., 2000b). Lowering the pH decreases time and results in a firmer gel probably due to increased rennet activity and reduced electrostatic repulsion between micelles (Mishra et al., 2005). In rennet gel there is an increase in the gel permeability with lower pH

results in the formation of large pores (Mishra et al., 2005) which increase salt losses and fat losses when whole milk is used (Patel et al., 1972). At pH above 7 the enzyme is rapidly inactivated and coagulation does not occur (Brulé and Lenoir, 1987). There is also a limit regarding lowering the pH because at pH=4.6 (casein isoeletric point) demineralization of casein micelles starts.

According to Guinee et al. (2007) it is expected that variation in fat-protein ratio of cheese milk with a fixed protein level, would affect manufacturing efficiency, composition, and quality of Cheddar cheese. As fat concentration of milk decreases, the syneresis rate increases. As fat content increases, the number of interstices within the reticulum that are occupied by fat globules also increases, thus leading to increased impedance of whey drainage (Calvo and Balcones, 2000).

By adding calcium the coagulation time reduces and the coagulum firmness increases. This is not related only to a lowering of pH. Addition of calcium reduces coagulation time even at constant pH, and flocculation occurs at a lower degree of κ-casein hydrolyses (Lucey, 2002). This is probably due to Ca^{+2} binding to the casein micelles in such a way that it reduces the repulsive force between them, perhaps by promoting hydrophobic interactions and hence the aggregation reaction of enzymatic coagulation (Colette, 2006).

2.2.2. Factors affecting syneresis

It is well known that rate and extent of syneresis depends on the equilibrium between the pressure gradient within the gel network and the resistance to whey expulsion (e.g., permeability) (Walstra, 1985). Factors affecting syneresis change the rate of whey flow by modifying this equilibrium. A large number of factors affecting the extent and rate of syneresis have been widely reported. Factors affecting syneresis were reviewed by Walstra et al. (1985),

Weber (1987), and Pearse and Mackinlay (1989). Weber classified the factors affecting syneresis into three groups: "direct", "indirect" and "pre-coagulation" factors as summarized by Figure 2.4.

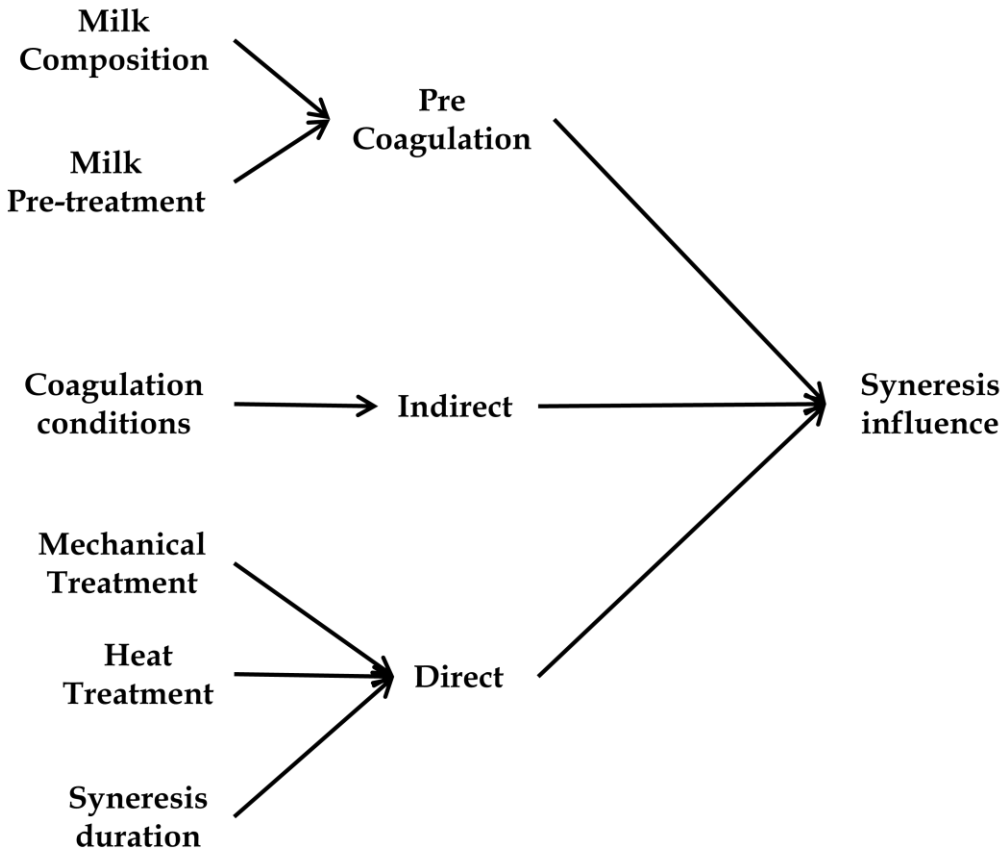

Figure 2.4 - Factors affecting the rate and extent of syneresis process during cheesemaking.

Pre-coagulation factors are related to the native milk composition characteristics such as fat and protein concentration or are compositional changes induced during the pre-treatment applied to the milk. More soluble milk proteins (especially if denatured) decreases syneresis. When fat content increases, drainage is slowed because it results in spatial impedance. Thermal treatment and refrigeration of milk also diminish syneresis as a result of modification of the native casein micelle composition and/or structure.

Indirect factors represent those related with coagulation effects. Coagulation factors determine the gel characteristics and indirectly influence the syneresis process. The higher the coagulation temperature, the higher the permeability, the larger the pores, the faster the syneresis reaction and the larger the amount of whey separation. Lowering the pH of enzymatic gels enhances the syneresis. The decrease of pH diminishes the micelle hydration and brings about a partial release of Ca from the curd (CCP demineralization). Some curd reactive sites become available allowing bond rearrangement and increasing the syneresis.

Direct factors affect syneresis after the gel is formed and are physical in nature such as mechanical treatments (cutting procedure and time, stirring procedure and speed), heat treatment (cooking), the pre-draining of whey (with water addition), and the duration of the process. Cutting the curd facilitates whey expulsion by increasing the solid/liquid interface area. Delaying cutting time reduces the capability of rearrangement of the casein network decreasing whey drainage. Stirring promotes whey drainage by increasing external pressure and prevents curd grains from fusion and sedimentation. Heating promotes protein matrix contraction (i.e., higher rearrangement capability, permeability, and endogenous syneresis pressure) and the rate of lactose fermentation. The increased acidity contributes to the curd shrinkage. Some cheese varieties include a curd washing which increases the moisture content of curd, reduces its lactose content, final acidity and firmness, and increases the openness of texture.

2.3. Syneresis control and cheese quality parameters

The cheese process is evaluated by the final yield of the product which is directly related with the final moisture content. Although yield is a very

important parameter it cannot be analyzed by itself once the cheese quality depends on fat content, mineral contents, texture, and flavor, among others.

Syneresis is considered to be one of the most important steps in cheesemaking (Walstra, 1993) as a result of its effect on moisture, mineral and lactose content of curd (Weber, 1989). Syneresis control influences cheese homogeneity, quality and yield and also has an impact on protein and fat losses in whey. In essence, the flow of whey must be controlled during cheese manufacturing to minimize losses of solids in whey and to obtain the desired cheese moisture content in order to decrease the production of downgraded cheese. Thus better control of the syneresis process would result in an improvement of the homogeneity and quality of dairy products.

Syneresis is empirically controlled worldwide by modifying vat temperature, milk pH, stirring speed and process duration, but there does not exist any precise system capable of predicting the course of drainage accurately.

Different empirical techniques have been developed to study the kinetics of syneresis as reviewed by Walstra, et al. (1985) and Walstra (1993). Experimental methods used to collect syneresis data (Patel et al., 1972; Marshall, 1982; Renault et al., 1997; Castillo et al. 2005) for modeling the process include:

a) Measuring curd shrinkage by the changes in height, area, volume or mass;

b) Measuring amount of whey expulsion or the degree of dilution of either an added tracer or a natural tracer such as milk fat globules;

c) Determining dry matter content of the curd pieces;

d) Determining curd grain density.

Unfortunately, most of these methods are based on off line measurements. As a result, the experimental conditions applied are generally so distant from industrial practice that the results are not easily extrapolated to industrial conditions. Indeed, according to Zviedrans and Graham (1981), most of the proposed methods are often short of precision and accuracy.

The LFV syneresis sensor prototype used by Fagan et al., 2006 was found to monitor milk coagulation and curd syneresis. The sensor response during syneresis allowed the modeling of whey fat concentration, curd yield and curd moisture content under a wide range of coagulation and syneresis conditions (Fagan et al., 2006).

2.4. Application of optical sensor technologies in cheesemaking automation

The relatively low cost, small size, and sensitivity of fiber optic sensors has made them applicable for various monitoring technologies (Lamb, 2010). Optical techniques are also very suitable for inline measurement and can be continuous and nondestructive (Payne, 2007) which is crucial for implementation in a cheese plant.

Optical sensor technologies have been successfully applied for cheese processing monitoring (Castillo et al., 2000; O'Callaghan et al., 1999; Payne et al, 1993). The CoAguLite™ sensor (Model 5, Reflectronics Inc., Lexington, KY, USA) is an optical fiber light backscatter sensor that has been used to monitor milk coagulation and predict both clotting and cutting times (Payne and Castillo, 2007). This sensor used near infrared light at 880 nm and consisted of two 600 μm diameter fibers. One fibre transmitted infrared radiation into the milk sample while the other fiber transmitted the radiation scattered by the milk particles present in the milk to a silicon photo-detector. Further details on the CL sensor

and data acquisition system were presented by Castillo et al. (2000) and Castillo et al. (2006b).

The CoAguLite sensor was tested by Fagan et al. (2007) for monitoring coagulation and syneresis, but the sensor output during syneresis included a high degree of scatter due to the two-phase mixture of curd pieces and whey. This problem was attributed to the optical fiber employed (0.6 mm diameter) had a small field of view in relation to a typical curd piece (5 – 10 mm diameter).

Therefore a larger field of view sensor was proposed with a design that allows light to be collected from a larger area. As expected, the LFV sensor (Univ. Kentucky, Lexington) was showed to be able to monitor both milk coagulation and curd syneresis in a stirred cheese vat (Fagan et al. 2007).

The first objective was to analyze the trend of the LFV sensor response with an extended number of process condition variables, and compare the results with Fagan et al. (2007). In addition, the second objective was carried out to study the cheese process optimization since changes in cheese processing conditions have been shown to affect moisture content, yield, and consequently quality. The last objective was a first attempt to control pressed curd moisture under a wide range of milk processing conditions, relating this parameter with the LFV sensor response.

Chapter 3 : MATERIALS AND METHODS

3.1. Experimental design

Five factors based on cheese process practice were selected for testing: coagulation temperature (˚C), cutting time factor (β), milk pH, fat/protein ratio (*FP*), and calcium chloride addition level (*CC*). The selection of factors levels as showed in Table 3.1 was based on previous research and practical considerations. A temperature range from 27 to 37ºC was selected to have a 10ºC interval for thermal coefficient calculation and avoid temperatures higher than 37ºC. Fagan et al. (2007) stated that the average melting point of milk fat is 37ºC which results in a greater level of fat being released. β was selected based on general cheesemaking practice. Typically, cheese makers select β between 1.4 and 2.2 (Payne, 2009; personal communication) as a function of the cheese variety (i.e., cutting time ranged between 1.4 and 2.2 times t_{max}). The minimum practical value for β is 1.4 as there is a lag time required after determination of t_{max}. The pH had the range between 5.9 and 6.0. By having pH<6 CCP demineralization was avoided. Protein was kept constant (3.3%) and fat was changed to obtain an interval between low fat milk (0.3% fat) and rich whole milk (3.6% fat). Based on Fagan 2007b the levels of calcium chloride addition were defined to range between 0.4 and 3.6 mM.

Table 3.1 - The factors and levels employed in the experimental design.

Factor	Coded Value				
	-2	-1	0	1	2
Coagulation Temperature (°C)	27	29.5	32	34.5	37
Cutting Time Factor (β)	1.4	1.8	2.2	2.6	3
pH	5.9	6.05	6.2	6.35	6.5
Fat/Protein Ratio	0.1	0.375	0.65	0.925	1.2
Calcium Concentration (mM)	0.4	1.2	2	2.8	3.6

To achieve the proposed objectives, a central composite design (CCD) was selected. This experimental design allowed the estimation of first order terms and quadratic terms, providing levels at which the independent variables optimized a dependent variable. The CCD consisted of a 2^{k-1} fractional factorial portion known as cube points (k = 5 factors), 2^k axial points, and seven replicated center points (i.e., 33 runs in total) as shown in Table 3.2. The 33 experimental conditions were run in three randomized blocks.

Table 3.2 - List of treatments with factors and levels according to CCD design.

Trt[1]		*T*	*β*	*pH*	*FP*	*CC*
1	Cube points	29.5	1.8	6.05	0.375	2.8
2		29.5	1.8	6.05	0.925	1.2
3		29.5	1.8	6.35	0.375	1.2
4		29.5	1.8	6.35	0.925	2.8
5		29.5	2.6	6.05	0.375	1.2
6		29.5	2.6	6.05	0.925	2.8
7		29.5	2.6	6.35	0.375	2.8
8		29.5	2.6	6.35	0.925	1.2
9		34.5	1.8	6.05	0.375	1.2
10		34.5	1.8	6.05	0.925	2.8
11		34.5	1.8	6.35	0.375	2.8
12		34.5	1.8	6.35	0.925	1.2
13		34.5	2.6	6.05	0.375	2.8
14		34.5	2.6	6.05	0.925	1.2
15		34.5	2.6	6.35	0.375	1.2
16		34.5	2.6	6.35	0.925	2.8
17	Axial points	27	2.2	6.2	0.65	2
18		37	2.2	6.2	0.65	2
19		32	1.4	6.2	0.65	2
20		32	3	6.2	0.65	2
21		32	2.2	5.9	0.65	2
22		32	2.2	6.5	0.65	2
23		32	2.2	6.2	0.1	2
24		32	2.2	6.2	1.2	2
25		32	2.2	6.2	0.65	0.4
26		32	2.2	6.2	0.65	3.6
27	Central points	32	2.2	6.2	0.65	2
28		32	2.2	6.2	0.65	2
29		32	2.2	6.2	0.65	2
30		32	2.2	6.2	0.65	2
31		32	2.2	6.2	0.65	2
32		32	2.2	6.2	0.65	2
33		32	2.2	6.2	0.65	2

[1]*trt* = treatment; *T* = temperature; *β* = cutting time factor; *FP* = fat/protein ratio; *CC* = calcium chloride addition level.

3.2. Milk preparation and compositional analysis

3.2.1. Skim milk powder analysis

In order to determine the protein content of SMP, two 200 mL solutions, solution 1 (10% w/w) and solution 2 (12% w/w), were prepared using an extra grade low temperature sprayed-dried skim milk powder (SMP) (Dairy America, Inc. Fresno, CA, USA) and deionized water. SMP was brought into solution by stirring for 30 min at 48 rpm and at 38°C. After which three 60 mL samples of each solution were taken for analysis. Two drops of a preservative (Bronolab-W, D&F Control Systems, Dublin CA, USA) were added to the samples which were stored at 2°C prior to protein analysis using a MilkoScan FT120 (Foss Electric, Denmark). The SMP protein content (P_{SMP}) was calculated using the protein content of each solution (P_1 and P_2) (Equation 3.1). The SMP fat content (F_{SMP}) was provided by the supplier (certificate of analysis) and it was considered to be the same for all SMP bags (F_{SMP}=0.87%) with no interferences because this concentration is too small if compared to the fat concentration of the reconstituted milk.

$$P_{SMP}(\%) = \frac{(P_1 \times 0.10 + P_2 \times 0.12)}{2} \qquad \text{Eqn. 3.1}$$

3.2.2. Cream analysis

Unpasteurized and unhomogenized cream was obtained from a local milk process plant (Winchester Farms Dairy, Winchester, KY, USA) and the measurement of its pH was determined as soon it was received which was used as a reference to ensure quality. A decrease in the cream pH can be an indication of microorganism contamination. The milk reconstitution procedure

(section 3.2.3) was applied using m_{SMP} = 29 g, m_{cream} = 16 g, and m_{water} = 255 g. Three 60 mL samples of the solution were taken for compositional analysis. Two drops of Bronolab were added to the samples which were stored at 2°C prior to protein analysis using a MilkoScan FT120. The cream protein content (P_{cream}) was calculated using the protein content of the reconstituted milk (P_{milk}) and the SMP (P_{SMP}) as shown in Equation 3.2. The cream fat content (F_{cream}) was provided by Winchester Dairy for each batch.

$$P_{cream}(\%) = \left(\frac{(P_{milk} \times m_{milk} - P_{SMP} \times m_{SMP})}{m_{cream}}\right) \times 100 \qquad \text{Eqn. 3.2}$$

3.2.3. Milk reconstitution

A cheese vat (Type CAL 11L, Pierre Guerin Technologies, S.A.S., Mauze, France) was used to prepare milk. It was connected to a Lauda Ecoline water bath with ±0.01°C of accuracy (E200, Brinkman Instruments, Inc. NY, USA) which supplied temperature controlled water to the vat jacket.

A batch of milk was prepared to achieve a selected fat/protein ratio. Mass of skim milk powder, cream, and deionized water were defined according to equations 3.6, 3.7, and 3.8 and those were weighed. Cream pH was measured as a quality check.

A mass balance was carried out for protein, fat, and total mass as described by Equation 3.3, 3.4, and 3.5, respectively.

$$m_{SMP} \times P_{SMP} + m_{cream} \times P_{cream} = m_{milk} \times P_{milk} \qquad \text{Eqn. 3.3}$$

$$m_{SMP} \times F_{SMP} + m_{cream} \times F_{cream} = m_{milk} \times \left(\frac{F}{P}\right)_{milk} \times P_{milk} \quad \text{Eqn. 3.4}$$

$$m_{SMP} + m_{cream} + m_{water} = m_{milk} \quad \text{Eqn. 3.5}$$

The amount of skin milk powder, cream, and deionized water for each experiment were calculated using Equation 3.6, 3.7, and 3.8, respectively for a quantity of milk (m_{milk}) of 10400 g,. The amount of protein in milk was constant and equal to 3.3%.

$$m_{SMP} = \frac{(F_{cream} \times P_{milk} \times m_{milk} - (F/P)_{milk} \times P_{milk} \times P_{cream} \times m_{milk})}{(F_{cream} \times P_{SMP} - P_{cream} \times F_{SMP})} \quad \text{Eqn. 3.6}$$

$$m_{cream} = \frac{(P_{milk} \times m_{milk} - P_{SMP} \times m_{SMP})}{P_{cream}} \quad \text{Eqn. 3.7}$$

$$m_{water} = m_{milk} - m_{SMP} - m_{cream} \quad \text{Eqn. 3.8}$$

The mass of water (m_{water}) was heated to 38˚C in the cheese vat and 2000 g was withheld for washing SMP and cream beakers. Calcium chloride ($CaCl_2$) at the required level (Table 3.1) was added (m_{CaCl_2}). The SMP was added into the vat and the mixture was remained stirring for 30 min at 48 rpm. Then, the cream was added into the vat with stirring for an additional 10 min at the same speed. A sample of milk (200g) was taken for compositional analysis and divided in three portions. Two drops of Bronolab were added to the samples which were stored at 2°C prior to fat, protein and total solids analysis using MilkoScan FT120.

The pH was measured (pH_{milk}) at the experimental target temperature. The milk pH was adjusted using 1.0 M hydrochloric acid (HCl). The amount of

acid required to change the pH was determined by testing and a linear regression to be described by the following equation:

$$\frac{m_{HCl}}{1kg\ milk} = -17.533 \times pH + 114.49 \quad \text{Eqn. 3.9}$$

The amount of acid added was determined by calculating the difference between the test target pH and the measured pH multiplied by 95% and using equation 3.10. This procedure guaranteed that the pH would require additional acid adjustment.

$$m_{HCl} = 0.95\ \left(m_{milk} \times 17.533\ \left(pH_{milk} - pH_{exp}\right)\right) \quad \text{Eqn. 3.10}$$

To keep constant milk dilution rate while adding different amounts of acid for pH adjustment and $CaCl_2$, the amount of liquid added was fixed at 100g. The HCl was mixed with an amount of water (m_{water}) calculated using Equation 3.11. The mixture, HCl + water + $CaCl_2$, was added to the milk and it was stirred for 3 minutes at 48 rpm. The pH-adjusted milk was storage in the cold room at ~ 2°C overnight.

$$m_{water} = 100g - m_{CaCl_2} - m_{HCl} \quad \text{Eqn. 3.11}$$

3.3. Test procedure

3.3.1. The large field of view sensor

Inline, continuous monitoring of milk coagulation and curd syneresis was performed using two different light backscatter sensor technologies, the CoAguLite (CL) (Model 5, Reflectronics, Inc., Lexington, KY) and the prototype

Large Field of View (LFV) sensors which was designed and built at the University of Kentucky. Those sensors were installed in the wall of the same cheese vat described in the milk reconstitution section. A black lid was placed on top of the vat to prevent outside light from interfering on the sensor's response.

Light backscatter response from the two sensors was continuously monitored from the time of rennet addition (t_{c_0}) to the end of syneresis ($t_{S_{85}}$). The CL sensor gave the experimental value of t_{max}.

A schematic for the LFV sensor prototype is shown in Figure 3.1.

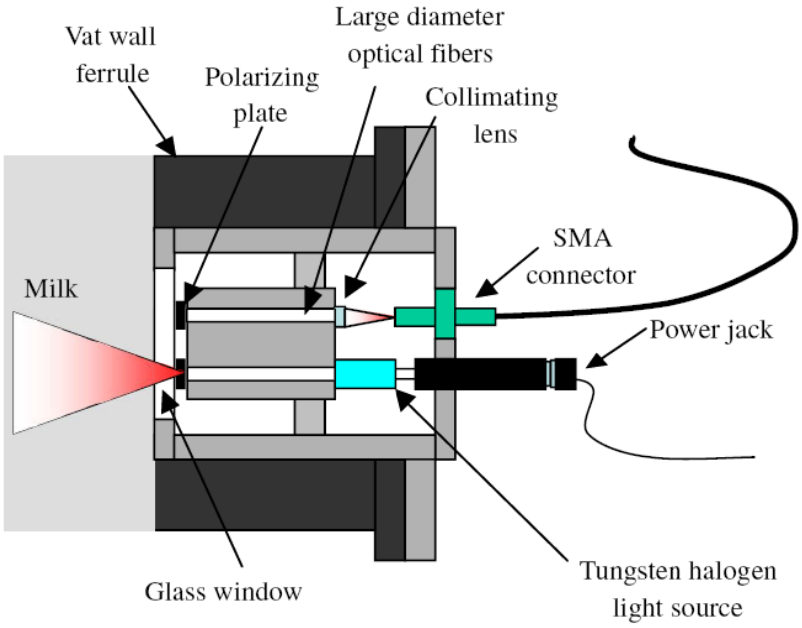

Figure 3.1 - Schematic of the large field view sensor configuration.

Light from a tungsten halogen light source (model LS1B, Ocean Optics, Inc., Dunedin, FL, USA; spectral range of 360– 2000 nm) was transmitted through a large diameter (5 mm) optical fiber (model FTICR19733, Fiberoptics Technology, Inc., Pomfret, CT, USA), a vertical polarizer (model 43-782, Edmund Optics, Inc., Barrington, NJ, USA) and a glass window (model 02 WBK 224,

Melles Griot Inc., Rochester, NY, USA) to the sample. The large-diameter (20 mm) glass window allows scattered light to be collected from a large area. Another polarizing plate allows for the selective detection of horizontally polarized light. Reflected light is transmitted through another optical fiber and a collimating lens (Edmund Optics Inc.) that focuses the scattered light onto a 800 μm diameter fiber optic cable (Spectran Specialty Optics, Avon, CT, USA) to the master unit of a miniature fibre optic spectrometer (model HR2000CG-UV-NIR, Ocean Optics B.V., Duiven, Netherlands). Spectra were collected over the range 300 nm to 1100 nm with a resolution of 0.7 μm. The integration time was set to 6 s by the computer software (OOIBase, Version 1.5, Ocean Optics, Inc.) and the scans to average was set to 1. Each spectral scan was automatically processed by subtracting the dark spectral scan. Each spectral scan was reduced to 41 averages by dividing them into 20 nm wavebands with mid-wavelengths of 280 + 20·n ($1 \leq n \leq 40$) and averaging the optical response for the wavelengths constituting each waveband. The 41 wavebands obtained were in the range (300-1100 nm). The voltage (sensor output) for the first min of data were averaged within each waveband (w) to calculated the initial voltage response, $V_o(w)$. The voltage intensity at every waveband, $V(w)$ was divided by its corresponding $V_o(w)$ to obtain the light backscatter ratio (R). The first derivative (R') of the light backscatter ratio profile was calculated by conducting linear least-squares regression typically with the most recently collected 4 min of data. The calculated slope was assigned to the midpoint of the data subset used.

3.3.2. Milk coagulation

The milk that was prepared a day before was weighed (m'_{milk}) and transferred to the cheese vat. Once thermal equilibrium was achieved the pH was measured (pH'_{milk}) and pH adjustment was fine-tuned to the target pH with

1.0M HCl (m'_{HCl}). To keep constant milk dilution rate while adding different amounts of acid for pH readjustment the amount of liquid added was fixed at 100g. The mass of HCL and water were calculated using Equation 3.12 and 3.13, respectively.

$$m'_{HCl} = \left(m'_{milk} \times 17.533 \left(pH'_{milk} - pH_{exp}\right)\right) \quad \text{Eqn. 3.12}$$

$$m'_{water} = 100g \times \frac{m'_{milk}}{m_{milk}} - m'_{HCl} \quad \text{Eqn. 3.13}$$

Milk pH readjustment after some hours of $CaCl_2$ and HCl addition ensured that any observed effect of independent variables on dependent variables was not due to an indirect effect of $CaCl_2$ on milk pH. The pH adjustment of milk systems must take into consideration that pH rises approximately 0.15 pH units during 18 h of storage. Cold storage reportedly causes calcium, magnesium, and phosphorous to dissociate from the micelle and consequently increases [Ca^{+2}] and pH (McMahon et al, 1984).

After pH adjustment the milk was sampled for compositional analysis. The sample mass (m_r) was determined such that 10kg of milk was left into the cheese vat (Equation 3.14). The milk removed was divided in three samples. Two drops of a preservative (Bronolab-W, D&F Control Systems, Dublin CA, USA) were added to the samples which were stored at 2°C prior to analysis for fat, protein and total solids content using a Milkoscan FT120.

$$m_r = m'_{milk} + m'_{HCl} + m'_{water} - 10000g \quad \text{Eqn. 3.14}$$

The enzyme used for milk coagulation was chymosin (CHY-MAX® Extra; Chr. Hansen Inc., Milwaukee, WI, USA), which is a 100% pure chymosin (EC 3.4.23.4 isozyme B) produced by submerged fermentation on a vegetable substrate with *Aspergillus niger* var. *awamori*. It had a relative milk-clotting activity test (REMCAT) strength of 642.90 IMCU mL^{-1}. Chymosin was added to the milk in the vat at a level of 0.03 mL kg^{-1} milk. At the starting time for each experiment 0.3264 g of enzyme (d=1.088 g/mL) was weighed and diluted in 15 mg of deionized water.

The coagulation step began by adding the enzyme solution to the vat and simultaneously initiating data acquisition. After enzyme addition, milk was stirred for 3 min at 48 rpm after which the stirrers were removed and replaced with cutters (Figure 3.2). Each cutter had 6 vertical knives and 1 horizontal knife that connected the vertical knives near the bottom of the vat.

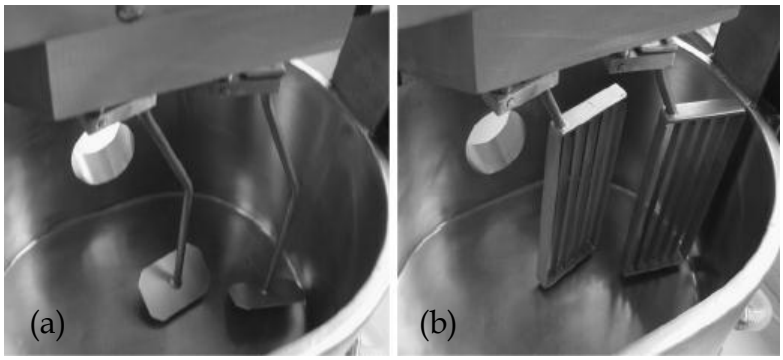

Figure 3.2 - (a) The double-O cheese vat with twin counter-rotating stirrers, also showing the sampler ferrule situated at approximately mid-height on the vat wall; (b) The vat with counter-rotating cutter (Everard et al., 2008).

3.3.3. Cutting time selection and gel cutting procedure

The CL sensor determined an experimental t_{max} for each test. The output voltage was zeroed by excluding light from the sensor and adjusting the output voltage to 1 V. The sensor gain was calibrated to give a 2 V signal response when placed in skim milk sample. Response data were collected every 6 s.

Parameters in the text or tables presented with an asterisk denote that they where calculated from the CL sensor as distinct from those obtained from the LFV sensor. The initial voltage response (V^*_0) was calculated by averaging the first ten data points corrected for the 1 V offset. A light backscatter ratio (R*) was calculated by dividing the sensor output voltage (less the 1 V output) by V^*_0. The first derivative (R´*) of the light backscatter ratio profile was calculated by conducting linear least-squares regression on the most recently collected 4 min of data.

Therefore, based on t_{max} and a constant β selected for each experiment, the experimental cutting time (t_{cut}) was calculated using the following prediction Equation 3.15 proposed by Payne et al. (1993):

$$t^*_{cut} = \beta \times t^*_{max} \qquad \text{Eqn. 3.15}$$

When t^*_{cut} was achieved the gel was cut. The last recorded time point prior to cutting was designated $t_{c_{cut}}$, with the next time point defined as the start of the syneresis process (t_{S_0}). The cutting process was divided in three consecutive stages. The first stage consisted of 20s agitation at 12 rpm and a 40s rest period, the second stage consisted of 20s of agitation at 22rpm and a 40s rest period, and the third stage consisted of 20s of agitation at 22rpm and a 40s rest period. During the first rest period both sensors were cleaned with a soft brush. The cutters were removed and they were replaced with stirrers again. The curd

was left to heal for 4 min before stirring at 17 rpm. The stirring process continued at this speed up to 85 min ($t_{s_{85}}$).

3.3.4. Curd and whey sampling procedure

A homogeneous sample of curd and whey was removed from the cheese vat at 5 min from cutting (t_{s_5}) and every 10 minutes thereafter up to $t_{s_{85}}$ (i.e. 9 samples). Samples of ~180 mL were removed at each time point using a specially designed sampler, manufactured at the University of Kentucky in collaboration with Teagasc and University College Dublin, which gives a more homogeneous sample. The sampler had a chamber that was filled when a plunger was pushed into the vat's interior and withdrawn (Figure 3.3). The sample was immediately poured into a previously weighed set (sieve + pan). The sieve was a number 200 stainless steel standard test sieve (Fisher Scientific, NH, USA) with a 75 μm absolute pore size in order to separate the curd and whey. The sieve characteristics were selected to ensure that, whey fat globules were not retained by the sieve. The set (sieve + pan) with sample was weighed then the pan with whey was also weighed, both using an analytical balance having a resolution of 0.1g ± 0.2g (Adventure Pro AV-8101, Ohaus, NY, USA).

Figure 3.3 – The specially designed sampler for sampling curd and whey from the vat (Everard et al., 2008).

3.3.5. Compositional analysis of curd and whey

(i) Total solid

The total solids content of curd and whey was determined by drying samples in a convection oven at 108°C until they reached a constant weight (~15 h). The curd and whey samples were approximately 3 g and 5 g respectively. The samples were weighed into pre-weighed aluminum dishes using an analytical balance having a resolution of 0.1 mg ± 0.2 mg (AE260, Mettler-Toledo, Inc., OH, USA). Each sample was analyzed in triplicate.

(ii) Whey composition

The fat, protein, and total solid content of whey was determined by near infrared spectroscopy (NIR) using the MilkoScan FT120, which was calibrated using 10 certified raw cow whey samples supplied by DQCI Services, (Mounds View, MN, USA). Filtered whey samples of 60 mL to which two drops of

preservative (Bromolab-W) were added were stored for this purpose at 2°C prior to analysis. Each filtered whey sample was analyzed in triplicate.

3.3.6. Pressure procedure for curd moisture and cheese yield

Approximately 21 g of curd was weighed into a weighing plastic dish using an analytical balance having a resolution of 0.1g ± 0.2g (Adventure Pro AV-8101, Ohaus, NY, USA). The curd sample was transferred into the drainage vessel (Figure 3.4a) and a metal weight (Figure 3.4b) was placed on top of the curd.

Different drainage vessel materials were tested and different hole sizes were also tested. A curd drainage vessel designed to give consistent samples was fabricated using a 50 mL graduated cylinder with 128 holes (2.8 mm in diameter) made along the sides 30 holes in the bottom. The metal weight consisting of a stainless steel cylinder 1.15 cm in diameter, 17 cm long, and weight of 400g ± 2g; which give a pressure of ~96g/cm^2.

The drainage vessel and the metal weight were previously weighed. The pressure set (drainage vessel, weight, and curd sample) was weighed and placed on a grid to allow whey to drain from the drainage vessel (Figure 3.4c).

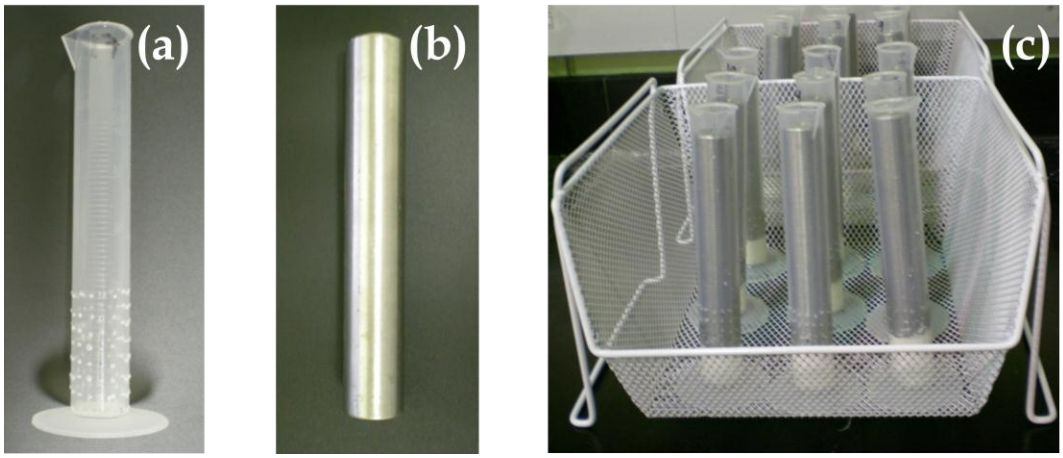

Figure 3.4 - Pressure system components. (a) curd drainage vessel; (b) metal weight; and (c) grid where the pressure set was placed.

After 3 hours, the pressure set was weighed and the pressed curd was cut in three similar size pieces and each piece was weighed into pre-weighed aluminum dishes using an analytical balance having a resolution of 0.1 mg ± 0.2 mg (AE260, Mettler-Toledo, Inc., OH, USA). The pressed curd samples were dried in a convection oven at 108°C, until they reached a constant weight (~15 h). Each sample was analyzed in triplicate and the pressed curd moisture content calculated.

3.3.7. Curd and whey measurement at end of syneresis

The curd and whey remaining in the vat were measured to be part of curd yield calculation. The vat was empted through a sieve and into a previously weighed 5 L container. The vat was washed with 2 kg of deionized water. The set (sieve + curd + container + whey) was weighed and the container with whey was also weighed, both using an analytical balance having a resolution of 0.1 g ± 0.2g (Adventure Pro AV-8101, Ohaus, NY, USA).

3.4. Statistical analysis

The goal of the statistical regression analysis was the determination of a relationship between different responses and the experimental conditions. The select data were processed and analyzed using ADX Interface for the Design and Analysis of Experiments (ADX Interface) on Statistical Analysis System (SAS® 9.2). The ADX Interface can be accessed from the main SAS menu by selecting "Solutions", "Analysis", and "Design of Experiments". The analyses of variance were carried out at a 5% level of significance.

The dependent variables experimentally obtained and a number of estimated parameters were calculated using experimental data and following the procedures describe below.

3.4.1. Curd moisture

Based on total solid analysis of curd before and after, curd moisture wet basis was calculated using the following equation:

$$\boldsymbol{CM_t \ or \ CMP_t}(\%) = \left(\frac{m_i - m_f}{m_i}\right) \times 100 \qquad \text{Eqn. 3.16}$$

where CM_t was the curd moisture before pressing at each sampling time (5, 15, 25…85 min after cutting), CMP_t was the curd moisture after pressing at the respective times (5, 15, 25…85 min after cutting), m_i was the average of the triplicate measurements of initial curd weight, and m_f was the average of the triplicate measurements of final curd weight.

3.4.2. Fat

Four fat parameters were calculated: whey fat content, whey fat losses, fat in whey, and curd fat retention.

(i) Whey fat content

Whey fat content of samples was measured using the MilkoScan to give percent by weight of fat in the whey sample for each time sampling .

(ii) Fat in whey, whey fat losses and curd fat retention

Fat in whey (*FIW*, % by weight) for each experiment was calculated as shown in Equation 3.17 where m_t is the whey mass for each sampling time (5, 15, 25…85 min) and WF_t is the whey fat content of the respective samples.

$$\boldsymbol{FIW}(\%) = \left(\frac{fat\ in\ whey\ (g)}{whey\ (g)}\right) \times 100 =$$

$$\left(\frac{\sum(m_t * WF_t)}{\sum(m_t)} \times 100\right), t = 5{,}15{,}25 \ldots 85 \qquad \text{Eqn. 3.17}$$

Whey fat losses (*WFL*, % by weight) and curd fat retention (*CFR*, % by weight) for each experiment were calculated as described by in Equation 3.18 and 3.19 respectively, where m is the beginning milk mass (m=10kg), and *MF* is the milk fat content.

$$\boldsymbol{WFL}(\%) = \left(\frac{fat\ in\ whey\ (g)}{fat\ in\ milk\ (g)}\right) \times 100 =$$

$$\left(\frac{\sum(W_t * WF_t)}{(m * MF)} \times 100\right), t = 5{,}15{,}25 \ldots 85 \qquad \text{Eqn. 3.18}$$

$$\boldsymbol{CFR}(\%) = \left(\frac{fat\ in\ curd\ (g)}{fat\ in\ milk\ (g)}\right) \times 100 =$$

$$\left(\frac{\sum[(m * MF) - (m_t * WF_t)]}{(m * MF)} \times 100\right), t = 5{,}15{,}25 \ldots 85 \qquad \text{Eqn. 3.19}$$

3.4.3. Curd yield

Curd yield for each experiment was computed as wet basis (CY_{wb}), and dry basis (CY_{db}). There are two different approaches to calculate those parameters. The first one considered that total solid of curd was constant during syneresis and with that all sampling curd data could be used and curd yield, wet basis, was calculated using the sum of curd collected each sampling time (C_i, where i=5, 15, 25…85) divide by the milk mass used at the begging (m=10kg) as showed in Equation 3.20. For the same approach curd yield, dry basis, was calculated taking CY_{wb} and multiplying that by the ratio between curd total solid (TS_c) and milk total solid (TS_M) as showed in Equation 3.21. The second approach calculated curd yield using only the final data (at 85 min) where mass of milk could be considered as a sum of mass of whey plus mass of curd at that time. In this case, curd yield, wet basis, was calculate using the mass of curd at 85 min (C_{85}) divide by the sum of mass of curd at 85min (C_{85}) and mass of whey at the same time (W_{85}) as showed in Equation 3.22. So, curd yield, dry basis, was calculated taking C_{85} and multiplying that by total solid of curd (TS_C) and divide by a sum as showed in Equation 3.23.

$$\boldsymbol{CY_{wb}} = \left(\frac{C_5 + C_{15} + C_{25} + C_{35} + C_{45} + C_{55} + C_{65} + C_{75} + C_{85}}{M}\right) \times 100 \qquad \text{Eqn. 3.20}$$

$$\boldsymbol{CY_{db}} = \frac{C}{M} \times \frac{TS_C}{TS_M} \times 100 = CY_{wb} \times \frac{TS_C}{TS_M} \times 100 \qquad \text{Eqn. 3.21}$$

$$\boldsymbol{CY85_{wb}} = \left(\frac{C_{85}}{C_{85} + W_{85}}\right) \times 100 \qquad \text{Eqn. 3.22}$$

$$\boldsymbol{CY85_{db}} = \left(\frac{C_{85} \times TS_c}{(C_{85} \times TS_c) + (W_{85} \times TS_w)}\right) \times 100 \qquad \text{Eqn. 3.23}$$

3.4.4. Cheese yield

Cheese yield for each experiment was computed on a wet basis (ChY_{wb}) and dry basis (ChY_{db}) based on curd yield using all data (first approach as described above for curd yield) and pressed cheese yield (PY), and was calculated as showed in Equation 3.24 and 3.25 respectively. Mass of curd (C), mass of milk (M), mass of cheese (Ch), total solid of curd (T_c), total solid of milk (TS_M) and total solid of cheese (T_{ch}) were used in the calculation of cheese yield as shoed by the following equations:

$$\boldsymbol{ChY_{wb}} = CY_{wb} \times PY_{wb} = \frac{C}{M} \times \frac{Ch}{C} \qquad \text{Eqn. 3.24}$$

$$\boldsymbol{ChY_{db}} = CY_{db} \times PY_{db} = \left(\frac{C}{M} \times \frac{TS_c}{TS_M}\right) \times \left(\frac{Ch}{C} \times \frac{TS_{ch}}{TS_c}\right) \qquad \text{Eqn. 3.25}$$

Chapter 4 : RESULTS AND DISCUSSION

A total of 99 coagulation tests were performed from June 2008 to June 2009 according to the central composite design as described in the Material and Methods section. The design included three replications. The statistical analysis of the data was performed using the Statistical Analysis System (SAS®, version 9.2).

A preliminary statistical analysis showed that the first replication was significant different at the 0.05 level of significance, so the main analysis were conducted using the data in replications 2 and 3 which contained 66 tests.

The independent variable β in this project called "cutting time factor" is a constant used to predict the experimental cutting time as showed in Equation 3.15, so an increase in β represents a delay in cutting and a firmer gel. In that way, the term "cutting time" (t_{cut}) instead of the symbol β will be used during the discussion.

4.1. The LFV light backscatter response

As stated by Fagan et al. (2007c), Figure 4.1 shows that during coagulation, the LFV reflectance ratio increased sigmoidly, and the response was greatest at 980 nm as indicated by the peak at this wavelength observed throughout coagulation. With the onset of syneresis following cutting of the gel, the signal decreased exponentially over time. Thus, the LFV sensor response during syneresis is further characterized by a valley at 980nm. Further, it is observed that generally LFV sensor also incorporated less noise at 980 nm that at the other wavelengths. So, 980 nm wavelength was selected for further analysis.

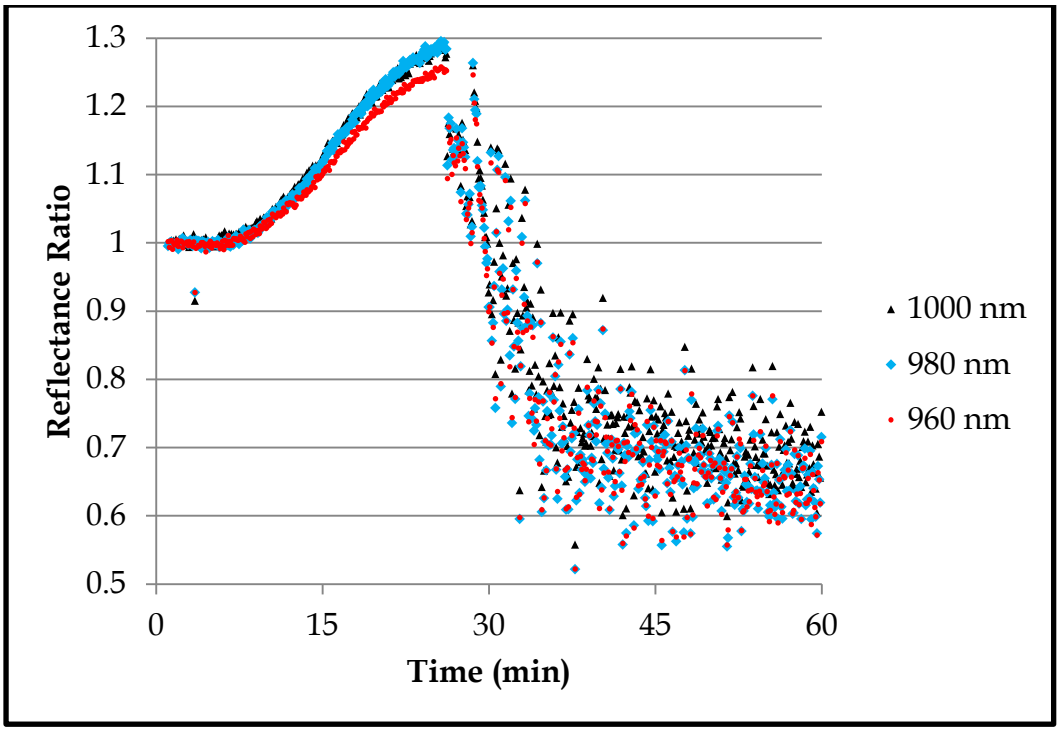

Figure 4.1 - Profile of the large field view (LFV) sensor at 960, 980, and 1000 nm during coagulation and syneresis (T=32°C; β=2.2; pH=6.2; FP=0.65; CC=2mM).

A typical light backscatter ratio profile obtained in the cheese vat during the coagulation and syneresis process using the large field view sensor (LFV) at 980nm is shown in Figure 4.2.

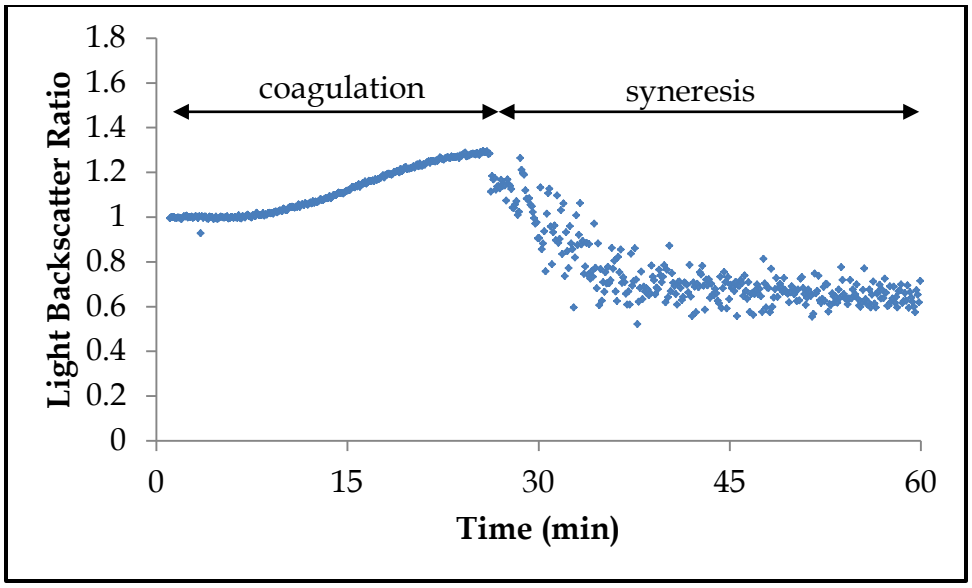

Figure 4.2 - Typical sensor profile of the large field view (LFV) sensor at 980 nm during coagulation and syneresis (T = 32°C; β = 2.2; pH = 6.2; FP = 0.65; CC = 2mM).

4.2. The effect of experimental factors on optical and chemical dependent variables.

Curd moisture, fat concentration, and yield are important parameters for quality control in cheese manufacturing. Syneresis step affects all those parameters, so it is important to understand this process and its effects.

Table 4.1, adapted from Fagan (2006), summarizes the effect of temperature, cutting time, pH, fat/protein ratio, and calcium chloride addition level on syneresis rate and their consequences on cheese quality.

Table 4.1 - Proposed consequence of the effect of temperature, cutting time, pH, fat/protein ratio, and calcium chloride addition level on cheese quality.

Parameter	**Proposed Mechanisms**	**Consequence**	**Reference**
Temperature			
Increasing; T < ~32°C	Increased fusion of casein micelles→ increased strength or number of bonds	↑ whey expelled ↓TS released	Mishra et al. (2005) Lagoueyte et al. (1994)
Increasing; 37 > T > 32°C	Network susceptible to rearrangement and to spontaneous breaking of bonds	↑whey expelled ↑TS released	Mishra et al. (2005) Lucey (2002) Lagoueyte et al. (1994)
t_{cut}			
Late cut; t_{cut} > optimum	Increased strength or number of bonds →increased network rigidity	↓ whey expelled ↑Curd Moisture	Mishra et al. (2005)
Early cut; t_{cut} < optimum	Decreased firmness	↑fat and TS released	Mishra et al. (2005)
pH			
Increasing *pH* pH < 6.0	Increased the electrostatic repulsion → reduces aggregation of casein	↓ whey expelled	Mishra et al. (2005) Lucey (2002)
Increasing *pH* pH > 6.0	Increase pH above optimum chymosin pH → Decreased firmness	↑ fat release	Lucey (2002)

Table 4.1 (continued)

FP			
Increasing	Increased interstices occupied by fat globules Increased gel rigidity	↓ whey expelled	Guinee (1997) Calvo& Balcone (2000)
CC			
Increasing; *CC* < ~10mM	Electrostatic attraction → more linkages and increased firmness	↑ whey expelled	McMahon et al. (1984) Lucey & Fox (1993)
Increasing; *CC* > ~10mM	Ionic strength → decreased firmness, weak gel	↓ whey expelled	McMahon et al. (1984) Lucey & Fox (1993)

The effect of independents variables temperature (*T*), cutting time factor (*β*), pH, milk fat/protein ratio (*FP*), and calcium chloride addition level (*CC*) on light backscatter parameters and on cheesemaking indexes were investigated using the ADX tool in SAS. The general model used is showed in Equation 4.1 where Y is the dependent variable which will be defined for each analysis, α_0 is the intercept, α_j represent the regression coefficient (j=0, 1…20), and ε is the random error. For each parameter the analysis of variance was conducted and the coefficients were tested using F-test at 5% level of significance to check whether they were significantly different from zero (H_0: $\alpha_j=0$). Outliers were removed considering statistics based on residuals ($P<0.05$) and influential observations were kept.

$$Y = \alpha_0 + \alpha_1 T + \alpha_2 \beta + \alpha_3 pH + \alpha_4 FP + \alpha_5 CC + \alpha_6 T^2 + \alpha_7 T\,\beta + \alpha_8 T\,pH$$
$$+\alpha_9 T\,FP + \alpha_{10} T\,CC + \alpha_{11}\beta^2 + \alpha_{12}\beta\,pH + \alpha_{13}\beta\,FP + \alpha_{14}\beta\,CC + \alpha_{15} pH^2$$
$$+ \alpha_{16} pH\,FP + \alpha_{17} pH\,CC + \alpha_{18} FP^2 + \alpha_{19} FP\,CC + \alpha_{20} CC^2 + \epsilon \qquad \text{Eqn. 4.1}$$

Table 4.2 is an example of ANOVA generated for curd moisture before pressing at 5 min after cutting where one point was removed as outlier. For each group of parameters analyzed a simplified table was constructed showing only the column Pr > F.

Table 4.2 - Analysis of variance for curd moisture before pressing at 5 min after cutting.

	Master Model				
Source[1]	**DF**	**SS**	**MS**	**F**	**Pr>F**
T	1	0.717852	0.717852	1.318011	0.2572
β	1	0.423752	0.423752	0.778029	0.3825
pH	1	3.825052	3.825052	7.022981	0.0111
FP	1	92.65742	92.65742	170.1235	<.0001
CC	1	0.004219	0.004219	0.007746	0.9303
T x *T*	1	0.656641	0.656641	1.205625	0.2782
T x *β*	1	0.181503	0.181503	0.333249	0.5667
T x pH	1	0.128778	0.128778	0.236443	0.6292
T x *FP*	1	1.407003	1.407003	2.583326	0.1151
T x *CC*	1	0.306153	0.306153	0.562112	0.4574
β x *β*	1	0.013488	0.013488	0.024765	0.8757
β x pH	1	0.229503	0.229503	0.421379	0.5196
β x *FP*	1	0.002278	0.002278	0.004183	0.9487
β x *CC*	1	0.564453	0.564453	1.036363	0.3142
pH x pH	1	0.218773	0.218773	0.401678	0.5295
pH x *FP*	1	0.275653	0.275653	0.506112	0.4806
pH x *CC*	1	0.149878	0.149878	0.275183	0.6025
FP x *FP*	1	0.078144	0.078144	0.143476	0.7067
FP x *CC*	1	0.050403	0.050403	0.092543	0.7624
CC x *CC*	1	0.721816	0.721816	1.325289	0.2559
Model	20	102.717	5.135848	9.429665	<.0001
(Linear)	5	97.62829	19.52566	35.85005	<.0001
(Quadratic)	5	1.793052	0.35861	0.658426	0.6568
(Cross Product)	10	3.295606	0.329561	0.605089	0.8009
Error	44	23.96451	0.544648		
(Lack of fit)	6	1.759679	0.29328	0.501901	0.8029
(Pure Error)	38	22.20483	0.584338		
Total	64	126.6815			

Table 4.2 (continued)

	Predictive Model				
Source[1]	**DF**	**SS**	**MS**	**F**	**Pr>F**
pH	1	3.825052	3.825052	7.8530	0.0068
FP	1	92.65742	92.65742	190.23	<.0001
Model	2	96.48247	48.24124	99.042	<.0001
Error	62	30.19899	0.48708		
(Lack of fit)	6	1.087732	0.181289	0.3487	0.9077
(Pure Error)	56	29.11126	0.519844		
Total	64	126.6815			

[1]*T* = temperature; β = cutting time factor; *FP* = fat/protein ratio; *CC* = calcium chloride addition level; x denotes interaction of experimental factors.

The master model (Equation 4.1) includes all factors and their interactions. The predictive model includes only the factors currently designated as significant and significant interactions ($\alpha_j \neq 0$; $P<0.05$). When an interaction effect has been selected but the corresponding lower-order main effects haven't, those were added to the predictive model to preserve hierarchy.

Prediction profiler graphs were generated by displaying the predict response as one variable is changed while the others are held constant at central point (*T* = 32°C; β = 2.2; pH = 6.2; *FP* = 0.65; *CC* = 2mM) and for each significant interaction a surface plot was generated by predicting response as two variables are changed while the others are held constant at central point.

4.2.1. The parameter t_{max} for LFV light backscatter

The most significant time-based parameter determined from the light backscatter profile is t_{max} as it is a measure of the enzymatic reaction rate (Tabayehnejad, 2010). It is determined as the time between enzyme addition and

the infection point of the sigmoidal section (coagulation step) of the light backscatter ratio profile as shown in Figure 4.3.

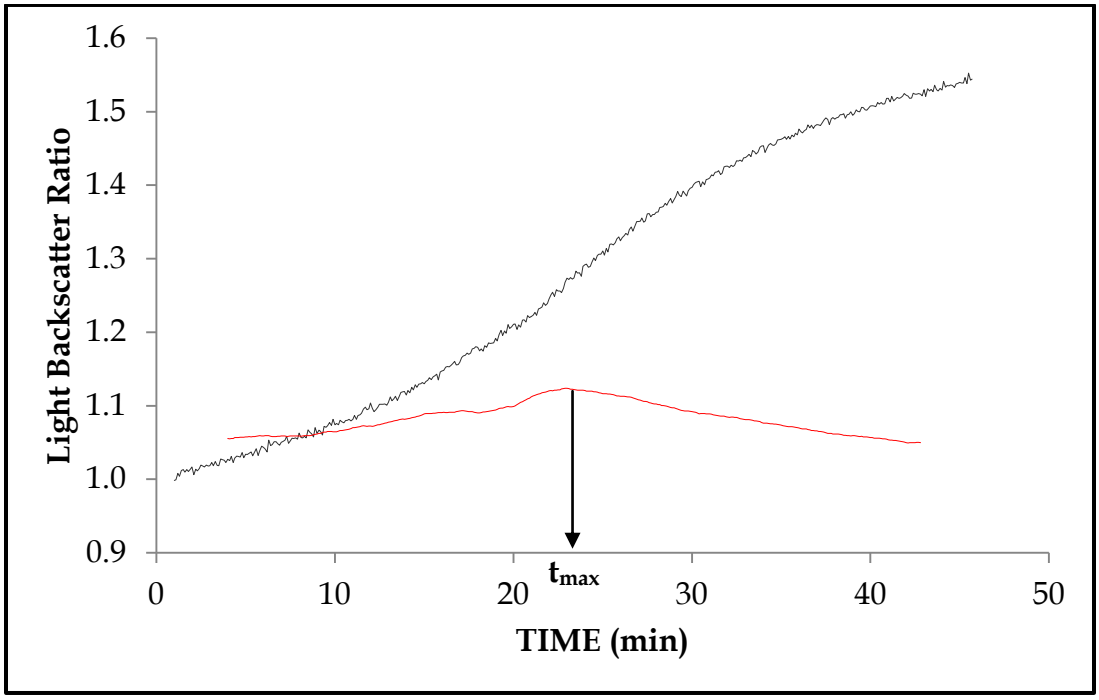

Figure 4.3 - Light backscatter ratio profile (R) and its characteristic first derivative (R') versus time for LFV sensor during coagulation phase (T = 32°C; β = 2.2; pH = 6.2; FP = 0.65; CC = 2mM).

Table 4.3 shows the p-values from the analysis of variance for t_{max}. The R-squared for master model and predictive model are also included in Table 4.3. The t_{max} predictive model was highly significant in their fit ($P < 0.001$).

Table 4.3 - P-value for t_{max}.

Factors[1]	t_{max}
T	<.0001*
β	0.2585[ns]
pH	<.0001*
FP	0.4364[ns]
CC	0.0241*
T x *T*	0.0043*
T x β	0.8913[ns]
T x pH	0.0352*
T x *FP*	0.0903[ns]
T x *CC*	0.4297[ns]
β x β	0.1613[ns]
β x pH	0.7638[ns]
β x *FP*	0.2226[ns]
β x *CC*	0.3147[ns]
pH x pH	<.0001*
pH x *FP*	0.9782[ns]
pH x *CC*	0.8058[ns]
FP x *FP*	0.2374[ns]
FP x *CC*	0.7226[ns]
CC x *CC*	0.5814[ns]
R^2 - Master Model	94.22
R^2 - Predictive Model	92.69

[1]*T* = temperature; β = a constant as defined by the experimental design and used to establish the experimental cutting time; *FP* = fat/protein ratio; *CC* = calcium chloride addition level; x denotes interaction of experimental factors.

*significant ($P < 0.05$); [ns]not significant ($P > 0.05$).

The t_{max} model was significantly affected by *T*, pH, *CC*, *T*-squared, *T* x pH, and pH-squared as showed in its predictive models (Equation 4.2)

$$\boldsymbol{t_{max}} = 1546.86 - 13.76\,T - 448.19\,pH - 0.54\,CC + 0.0755\,T^2 + 1.32\,(T \times pH) + 35.14\,pH^2 \quad \text{Eqn. 4.2}$$

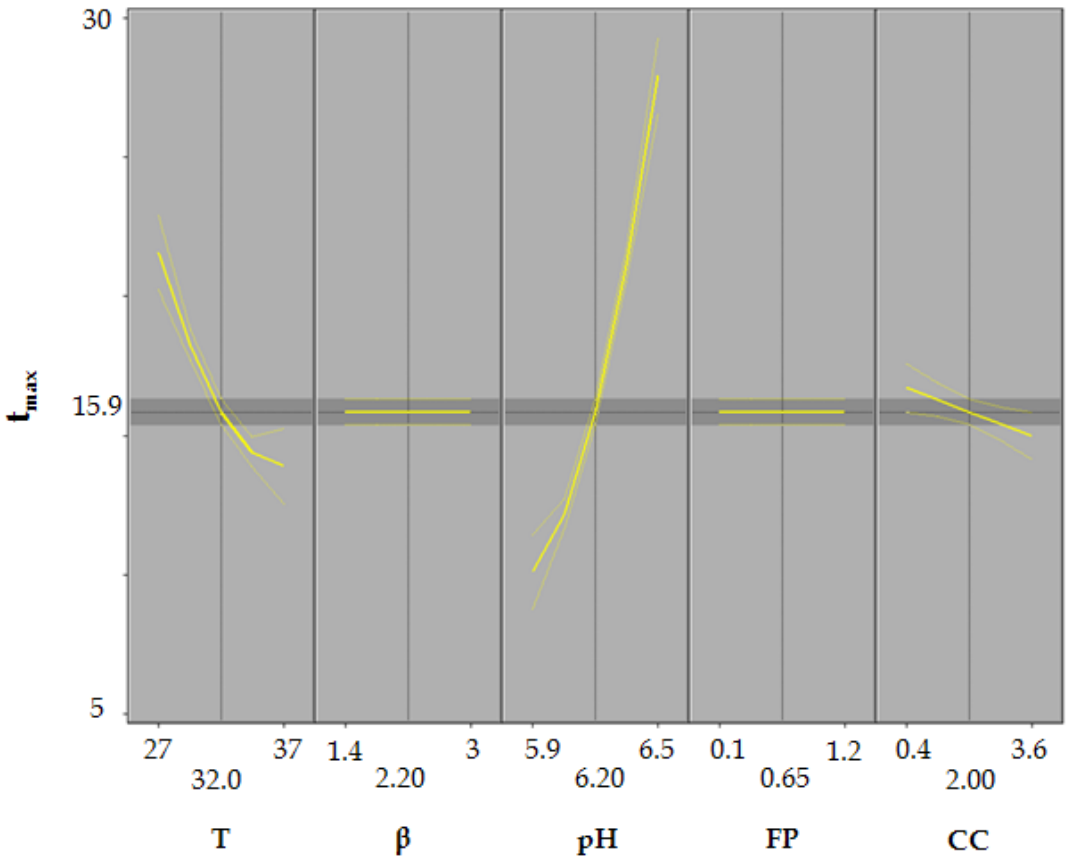

Figure 4.4 - Prediction profiler for the independents variables temperature (*T*), cutting time factor (β), pH, fat/protein ratio (*FP*), and calcium chloride addition level (*CC*) on t_{max}.

The prediction profiler graph for t_{max} as a function of the independent variables is shown in Figure 4.4. Increasing temperature was shown to decrease t_{max}. This results from the increased reaction rate activity of enzymes with

temperature. Increasing temperature also increases the aggregation and gel firmness reaction. The enzymatic reaction follows an Arrhenius model and thus is not linear with temperature as observed in Figure 4.3. Increasing pH was shown to increase t_{max}. Lowering the pH of milk reduces electrostatic repulsion between micelles what results in a reduction in the coagulation time. Increasing *CC* was shown to decreasing t_{max}. Since pH was adjusted after at least 12 hours of $CaCl_2$ addition, the observed effect of *CC* wasn't due to reduce milk pH but to $CaCl_2$ aggregation effect. Lucey (2002) stated that addition of calcium reduces the rennet coagulation time, even at constant milk pH, and flocculation occurs at lower degree of k-casein hydrolysis. Cutting time and fat/protein ratio had no effect on t_{max}. β was not expected to have any effect on t_{max} because it was used to calculate t_{cut} which takes places after t_{max}.

The response surface graph (Figure 4.5) for t_{max} shows the significant interaction between temperature and pH. The temperature effect is more accentuated at lower pH and the pH effect is more accentuate at higher temperature. As low pH contributes to the coagulation reaction, temperature effect is clearer.

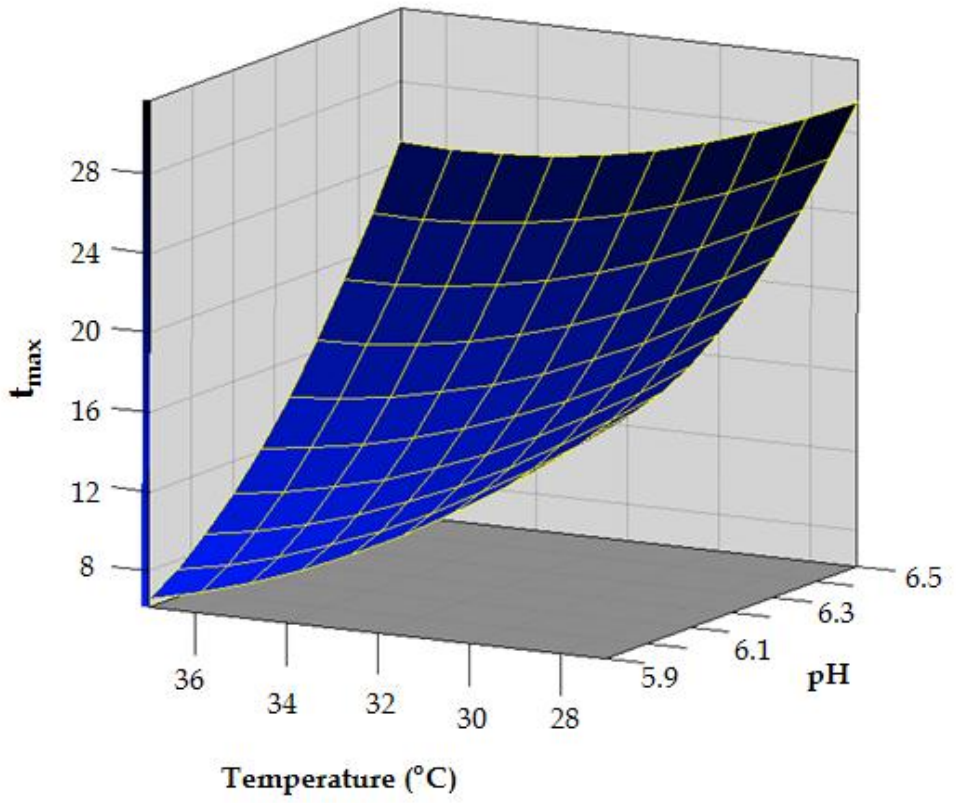

Figure 4.5 - Response surface plot for the effect of T and pH on t_{max}.

4.2.2. Curd moisture

During the syneresis process at each sampling time, curd moisture was measured before pressing was applied and after pressing was applied to curd.

(i) Curd moisture before pressing

Table 4.4 shows the p-value results from the analysis of variance for curd moisture before pressing (CM_t) at each sampling time (5, 15, 25…85 min after cutting). The coefficients of determination, R^2, for both master and predictive

models are also included in Table 4.4. All curd moisture before pressing predictive models were highly significant in their fit (P < 0.001).

Table 4.4 - P-value for curd moisture before pressing.

	Curd Moisture Before Pressing (CM_t)[2]				
Factors[1]	CM_5	CM_{15}	CM_{25}	CM_{35}	CM_{45}
T	0.2572[ns]	0.5854[ns]	0.0148*	0.024*	0.0004*
β	0.3825[ns]	0.015*	<.0001*	0.0013*	<.0001*
pH	0.0111*	0.0771[ns]	0.0011*	0.0212*	0.0004*
FP	<.0001*	<.0001*	<.0001*	<.0001*	<.0001*
CC	0.9303[ns]	0.593[ns]	0.7939[ns]	0.5536[a]	0.5623[ns]
T x *T*	0.2782[ns]	0.0538[ns]	0.1905[ns]	0.1485[ns]	0.1981[ns]
T x *β*	0.5667[ns]	0.9449[ns]	0.434[ns]	0.1856[ns]	0.7701[ns]
T x pH	0.6292[ns]	0.1945[ns]	0.4767[ns]	0.8349[ns]	0.0278*
T x *FP*	0.1151[ns]	0.0638[ns]	0.8393[ns]	0.3704[ns]	0.527[ns]
T x *CC*	0.4574[ns]	0.3267[ns]	0.8617[ns]	0.9689[ns]	0.4232[ns]
β x *β*	0.8757[ns]	0.457[ns]	0.5316[ns]	0.2157[ns]	0.0167*
β x pH	0.5196[ns]	0.4854[ns]	0.6768[ns]	0.143[ns]	0.4252[ns]
β x *FP*	0.9487[ns]	0.8941[ns]	0.0445*	0.4727[ns]	0.2431[ns]
β x *CC*	0.3142[ns]	0.2119[ns]	0.8421[ns]	0.0354*	0.9343[ns]
pH x pH	0.5295[ns]	0.6403[ns]	0.982[ns]	0.8592[ns]	0.179[ns]
pH x *FP*	0.4806[ns]	0.4134[ns]	0.3307[ns]	0.5416[ns]	0.3832[ns]
pH x *CC*	0.6025[ns]	0.1867[ns]	0.7757[ns]	0.1129[ns]	0.8922[ns]
FP x *FP*	0.7067[ns]	0.2166[ns]	0.5282[ns]	0.3987[ns]	0.2768[ns]
FP x *CC*	0.7624[ns]	0.996[ns]	0.4196[ns]	0.6833[ns]	0.722[ns]
CC x *CC*	0.2559[ns]	0.7562[ns]	0.631[ns]	0.5893[ns]	0.1806[ns]
R^2 - Master Model	81.08	72.73	81.13	75.17	82.66
R^2 - Predictive Model	76.16	59.89	78.77	67.64	78.03

[1]*T* = temperature; *β* = cutting time factor; *FP* = fat/protein ratio; *CC* = calcium chloride addition level; x denotes interaction of experimental factors.

[2]CM_t; t = sampling time (minutes after cutting time).

*significant (P < 0.05); [ns]not significant (P > 0.05); [a] not significant but factor was added to model to preserve hierarchy.

Table 4.4 (continued)

Factors[1]	CM_{55}	CM_{65}	CM_{75}	CM_{85}
T	0.1077[a]	0.0937[a]	0.0186*	0.0017*
β	0.0003*	0.0024*	0.0024*	0.4967[ns]
pH	0.1237[ns]	0.0162*	0.0199*	0.0057*
FP	<.0001*	<.0001*	<.0001*	<.0001*
CC	0.4029[ns]	0.5451[ns]	0.3552[ns]	0.1371[ns]
T x *T*	0.0073*	0.0265*	0.0353*	0.0181*
T x *β*	0.7184[ns]	0.6183[ns]	0.6265[ns]	0.784[ns]
T x pH	0.1308[ns]	0.9432[ns]	0.8609[ns]	0.1758[ns]
T x *FP*	0.2579[ns]	0.359[ns]	0.1197[ns]	0.1254[ns]
T x *CC*	0.499[ns]	0.4285[ns]	0.4501[ns]	0.3023[ns]
β x *β*	0.1028[ns]	0.6001[ns]	0.5028[ns]	0.2077[ns]
β x pH	0.5054[ns]	0.3564[ns]	0.5106[ns]	0.0787[ns]
β x *FP*	0.7463[ns]	0.5666[ns]	0.8214[ns]	0.6795[ns]
β x *CC*	0.9597[ns]	0.4079[ns]	0.5144[ns]	0.798[ns]
pH x pH	0.6016[ns]	0.6839[ns]	0.2796[ns]	0.5324[ns]
pH x *FP*	0.8213[ns]	0.3879[ns]	0.5163[ns]	0.2121[ns]
pH x *CC*	0.0802[ns]	0.4653[ns]	0.7552[ns]	0.9843[ns]
FP x *FP*	0.6464[ns]	0.2985[ns]	0.0243*	0.222[ns]
FP x *CC*	0.3827[ns]	0.7101[ns]	0.3027[ns]	0.9432[ns]
CC x *CC*	0.2183[ns]	0.3577[ns]	0.1204[ns]	0.4444[ns]
R^2 - Master Model	77.66	73.5	75.93	79.2
R^2 - Predictive Model	68.83	68.79	70.26	71.05

The master model explained a 72.73-82.66% of the experimental variation for *CM* depending on the sampling point. Predictive models were developed for curd moisture before pressing at each sample time after cutting as detailed in equations containing significant factors ($P < 0.05$) and factors added to preserve hierarchy with their respective estimated coefficient α_j as shown in Table 4.5. The predictive models explained 59.89-78.77% of observed variability.

Table 4.5 - List of predictive models for curd moisture before pressing (CM_t[1]).

$$\boldsymbol{CM_5} = 77.19 + 1.88\,pH - 5.05\,FP$$

$$\boldsymbol{CM_{15}} = 84.98 + 0.95\,\beta - 5.26\,FP$$

$$\boldsymbol{CM_{25}} = 72.44 - 0.13\,T - 0.49\,\beta + 3.16\,pH - 12.92\,FP + 3.0\,(\beta \times FP)$$

$$\boldsymbol{CM_{35}} = 66.56 - 0.14\,T + 3.77\,\beta + 2.39\,pH - 5.3\,FP + 2.85\,CC - 1.24\,(\beta \times CC)$$

$$\boldsymbol{CM_{45}} = 268.3 - 6.84\,T + 10.45\beta - 30.55\,pH - 6.04\,FP + 1.07(T \times pH) - 1.93\beta^2$$

$$\boldsymbol{CM_{55}} = 148.46 - 4.10\,T + 1.5\,\beta - 5.7\,FP + 0.06\,T^2$$

$$\boldsymbol{CM_{65}} = 132.07 - 4.30\,T + 1.58\,\beta + 3.26\,pH - 6.82\,FP + 0.06\,T^2$$

$$\boldsymbol{CM_{75}} = 129.42 - 3.81\,T + 1.38\,\beta + 2.75\,pH - 12.68\,FP + 0.056\,T^2 + 5.03\,FP^2$$

$$\boldsymbol{CM_{85}} = 132.48 - 4.08\,T + 3.24\,pH - 6.88\,FP + 0.06\,T^2$$

[1]CM_t; t = sampling time (minutes after cutting time).

T = temperature; β = cutting time factor; FP = fat/protein ratio; CC = calcium chloride addition level.

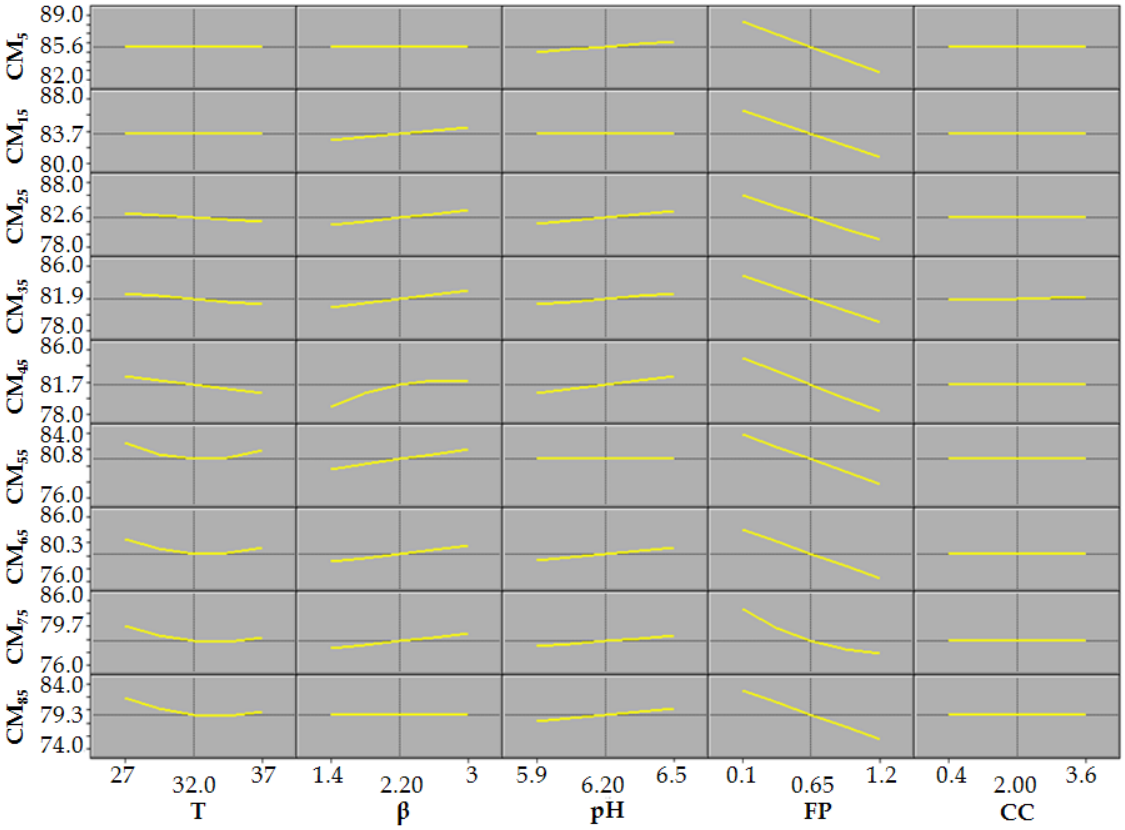

Figure 4.6 - Prediction profiler for the independents variables temperature (*T*), cutting time factor (β), pH, fat/protein ratio (*FP*), and calcium chloride addition level (*CC*) on curd moisture before pressing at each sampling time (CM_t).

The prediction profiler graph for CM_t as a function of the independent variables is shown in Figure 4.6. It shows that curd moisture trend response changed depending on the sampling point. Increasing the temperature was shown to decrease CM_{25}, CM_{35}, and CM_{45}, and to minimize CM_{55}, CM_{65}, CM_{75}, and CM_{85} at ~32˚C. Although not all models showed the same result, increasing temperature below 32˚C decreased curd moisture because gels formed at higher temperatures have increased rearrangement capability (larger tan δ) and greater permeability, which results in a faster rate of syneresis and larger amount of whey separation (Castillo et al., 2006; Mishara et al.,2005; Lagoueyte et al., 1994). Other side, increasing temperature above 32˚C increased curd moisture because

higher temperatures increase gel permeability accompanied with increased loss of solid (Mishara et al.,2005; Lagoueyte et al., 1994; Lucey, 2002).

Increasing β was shown to increase CM_{15}, CM_{25}, CM_{35}, CM_{45}, CM_{55}, CM_{65}, and CM_{75}. The effect of increasing t_{cut} on increasing curd moisture is in agreement with previous studies (Johnson et al., 2001). If gel is cut too soon a softer gel is produced which can easily break during stirring process releasing more whey. Delaying cutting time results in a firmer gel which has a reduced ability rearrange and, subsequently, a limited capability to shrink and expel whey.

Increasing the pH was shown to increase CM_5, CM_{25}, CM_{35}, CM_{45}, CM_{65}, CM_{75}, and CM_{85}. Decreasing pH decreased curd moisture because the higher aggregating tendency of fully converted micelles at lower pH (van den Bijgaart, 1988) results in a faster syneresis rate.

Increasing the fat/protein ratio was shown to decrease curd moisture for all samples. This result is in agreement with Guinee 2007 and Mateo 2009. It has been suggested that as fat content increases, the number of interstices within the reticulum that are occupied by fat globules also increases, thus leading to increased impedance of whey drainage (Calvo & Balcones, 2000; Pearse & Mackinlay, 1989; Marshall, 1982) which results in a increase curd moisture.

The unexpected negative effect of *FP* can be explained according to Mateo at al. (2009) by the variation in total solids of milk in the selected design. Data analysis showed that increasing *FP* increased total solid (Figure 4.7). Thus, at the initial stage of syneresis the curd has less water at higher fat concentration which can explain the lower curd moisture.

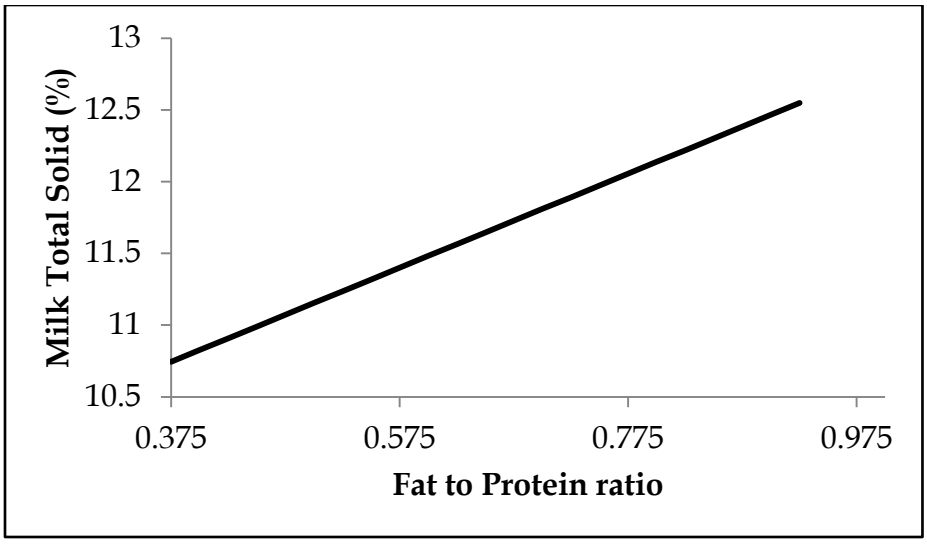

Figure 4.7 - Prediction profiler fat/protein ratio (*FP*) on milk total solid (% by weight).

Changes in calcium did not have an effect on curd moisture. Van den Bijgaart (1988) stated that the rate of the enzymatic reaction is not significantly affected by added $CaCl_2$ if a pH correction is made. The same result was found by Fagan et al. (2007b).

(ii) After pressing

Table 4.6 shows the p-value results from the analysis of variance for curd moisture after pressing (CMP_t) at each sampling time (5, 15, 25…85 min after cutting). The coefficients of determination, R^2, for both master and predictive models are also included in Table 4.6Table 4.4. All curd moisture after pressing predictive models were highly significant in their fit ($P < 0.001$).

Table 4.6 - P-value for curd moisture after pressing.

	Curd Moisture After Pressing (CMP_t)[2]				
Factors[1]	CMP_5	CMP_{15}	CMP_{25}	CMP_{35}	CMP_{45}
T	0.0004*	<.0001*	<.0001*	<.0001*	<.0001*
β	0.8768[ns]	<.0001*	<.0001*	<.0001*	<.0001*
pH	0.0013*	<.0001*	<.0001*	<.0001*	<.0001*
FP	<.0001*	<.0001*	<.0001*	<.0001*	<.0001*
CC	0.1632[ns]	0.1397[a]	0.2066[ns]	0.6336[ns]	0.2387[ns]
T x *T*	0.1539[ns]	0.1088[ns]	0.2028[ns]	0.3031[ns]	0.3020[ns]
T x *β*	0.9261[ns]	0.2955[ns]	0.9472[ns]	0.3542[ns]	0.0111*
T x pH	0.2078[ns]	0.0593[ns]	0.0706[ns]	0.0061*	0.0034*
T x *FP*	0.7076[ns]	0.1422[ns]	0.7108[ns]	0.2191[ns]	0.2219[ns]
T x *CC*	0.0618[ns]	0.4464[ns]	0.2074[ns]	0.1011[ns]	0.8193[ns]
β x *β*	0.7905[ns]	0.5375[ns]	0.6548[ns]	0.0473*	0.3657[ns]
β x pH	0.0654[ns]	0.7259[ns]	0.5943[ns]	0.7972[ns]	0.0244*
β x *FP*	0.1000[ns]	0.2973[ns]	0.0826[ns]	0.2801[ns]	0.1490[ns]
β x *CC*	0.8925[ns]	0.4102[ns]	0.4495[ns]	0.6018[ns]	0.7432[ns]
pH x pH	0.6555[ns]	0.8154[ns]	0.2556[ns]	0.7847[ns]	0.7182[ns]
pH x *FP*	0.8342[ns]	0.3270[ns]	0.3181[ns]	0.7793[ns]	0.3801[ns]
pH x *CC*	0.7836[ns]	0.0328*	0.1146[ns]	0.1654[ns]	0.3897[ns]
FP x *FP*	0.0831[ns]	0.0108*	0.1225[ns]	0.0414[ns]	0.0050*
FP x *CC*	0.2918[ns]	0.6166[ns]	0.6361[ns]	0.3026[ns]	0.1319[ns]
CC x *CC*	0.6195[ns]	0.8577[ns]	0.1565[ns]	0.9641[ns]	0.1597[ns]
R^2 - Master Model	68.78	93.55	91.00	92.38	94.62
R^2 - Predictive Model	54.44	91.47	86.20	90.33	93.04

[1]*T* = temperature; *β* = cutting time factor; *FP* = fat/protein ratio; *CC* = calcium chloride addition level; x denotes interaction of experimental factors.

[2]CMP_t; t = sampling time (minutes after cutting time).

*significant (P < 0.05); [ns]not significant (P > 0.05); [a] not significant but factor was added to model to preserve hierarchy.

Table 4.6 (continued)

	Curd Moisture After Pressing (CMP_t)[2]			
Factors[1]	CMP_{55}	CMP_{65}	CMP_{75}	CMP_{85}
T	<.0001*	<.0001*	<.0001*	<.0001*
β	<.0001*	<.0001*	<.0001*	<.0001*
pH	<.0001*	<.0001*	<.0001*	<.0001*
FP	<.0001*	<.0001*	<.0001*	<.0001*
CC	0.6953^{ns}	0.0687^{a}	0.8838^{ns}	0.6467^{a}
T x *T*	0.3590^{ns}	0.4634^{ns}	0.0564^{ns}	0.0204*
T x *β*	0.2157^{ns}	0.005*	0.9557^{ns}	0.0734^{ns}
T x pH	0.0024*	0.3096^{ns}	0.4236^{ns}	0.0186*
T x *FP*	0.1483^{ns}	0.7589^{ns}	0.2847^{ns}	0.5148^{ns}
T x *CC*	0.4278^{ns}	0.4055^{ns}	0.3559^{ns}	0.8385^{ns}
β x *β*	0.0286*	0.2838^{ns}	0.3367^{ns}	0.1999^{ns}
β x pH	0.7027^{ns}	0.1304^{ns}	0.7341^{ns}	0.6579^{ns}
β x *FP*	0.9030^{ns}	0.7755^{ns}	0.5728^{ns}	0.2891^{ns}
β x *CC*	0.3335^{ns}	0.2620^{ns}	0.3614^{ns}	0.6407^{ns}
pH x pH	0.3790^{ns}	0.6418^{ns}	0.3918^{ns}	0.6130^{ns}
pH x *FP*	0.6751^{ns}	0.5432^{ns}	0.2823^{ns}	0.5220^{ns}
pH x *CC*	0.4695^{ns}	0.0036*	0.2752^{ns}	0.3039^{ns}
FP x *FP*	0.0116*	0.001*	0.0026*	<.0001*
FP x *CC*	0.8688^{ns}	0.1621^{ns}	0.7503^{ns}	0.7409^{ns}
CC x *CC*	0.0799^{ns}	0.2235^{ns}	0.4030^{ns}	0.0018*
R^2 - Master Model	95.28	92.85	88.49	96.16
R^2 - Predictive Model	93.69	91.01	85.08	95.30

The master model explained a 68.78-96.16% of the experimental variation for *CMP* depending on the sampling point. Predictive models were developed for curd moisture after pressing at each sampling time after cutting as detailed on equations containing significant factors ($P < 0.05$) and factor that was added to preserve hierarchy with their respective estimated coefficient α_j as shown in Table 4.7. The predictive models explained 54.44-95.3% of observed variability.

Table 4.7 - List of predictive models for curd moisture before pressing (CMP_t[1]).

$$\boldsymbol{CMP_5} = 49.99 - 0.44\,T + 6.58\,pH - 7.39\,FP$$

$$\boldsymbol{CMP_{15}} = -12.66 - 0.35\,T + 1.32\,\beta + 15.37\,pH - 14.02\,FP + 17.98\,CC - 2.94(pH \times CC) + 3.69\,FP^2$$

$$\boldsymbol{CMP_{25}} = 17.87 - 0.36\,T + 1.75\,\beta + 9.73\,pH - 9.35\,FP$$

$$\boldsymbol{CMP_{35}} = 298.74 - 9.40\,T + 9.97\,\beta - 36.61\,pH - 14.95\,FP + 1.45\,(T \times pH) - 1.75\,\beta^2 + 3.57\,FP^2$$

$$\boldsymbol{CMP_{45}} = 222.11 - 9.24\,T + 24.08\,\beta - 19.09\,pH - 15.38\,FP + 0.37\,(T \times \beta) + 1.28\,(T \times pH) - 5.28\,(\beta \times pH) + 4.39\,FP^2$$

$$\boldsymbol{CMP_{55}} = 284.66 - 9.49\,T + 9.37\,\beta - 34.21\,pH - 15.15\,FP + 1.45\,(T \times pH) - 1.43\,\beta^2 + 4.00\,FP^2$$

$$\boldsymbol{CMP_{65}} = 98.38 - 1.6\,T - 13.16\,\beta + 2.50\,pH - 17.97\,FP - 27.82\,CC + 0.51\,(T \times \beta) + 4.44(pH \times CC) + 6.35\,FP^2$$

$$\boldsymbol{CMP_{75}} = 19.18 - 0.48\,T + 2.64\,\beta + 9.39\,pH - 17.83\,FP + 6.71\,FP^2$$

$$\boldsymbol{CMP_{85}} = 273.11 - 10.20\,T + 2.90\,\beta - 25.09\,pH - 17.74\,FP + 2.22\,CC + 0.038\,T^2 + 1.15(T \times pH) + 5.82\,FP^2 - 0.52\,CC^2$$

[1]CMP_t; t = sampling time (minutes after cutting time).

T = temperature; β = cutting time factor; FP = fat/protein ratio; CC = calcium chloride addition level.

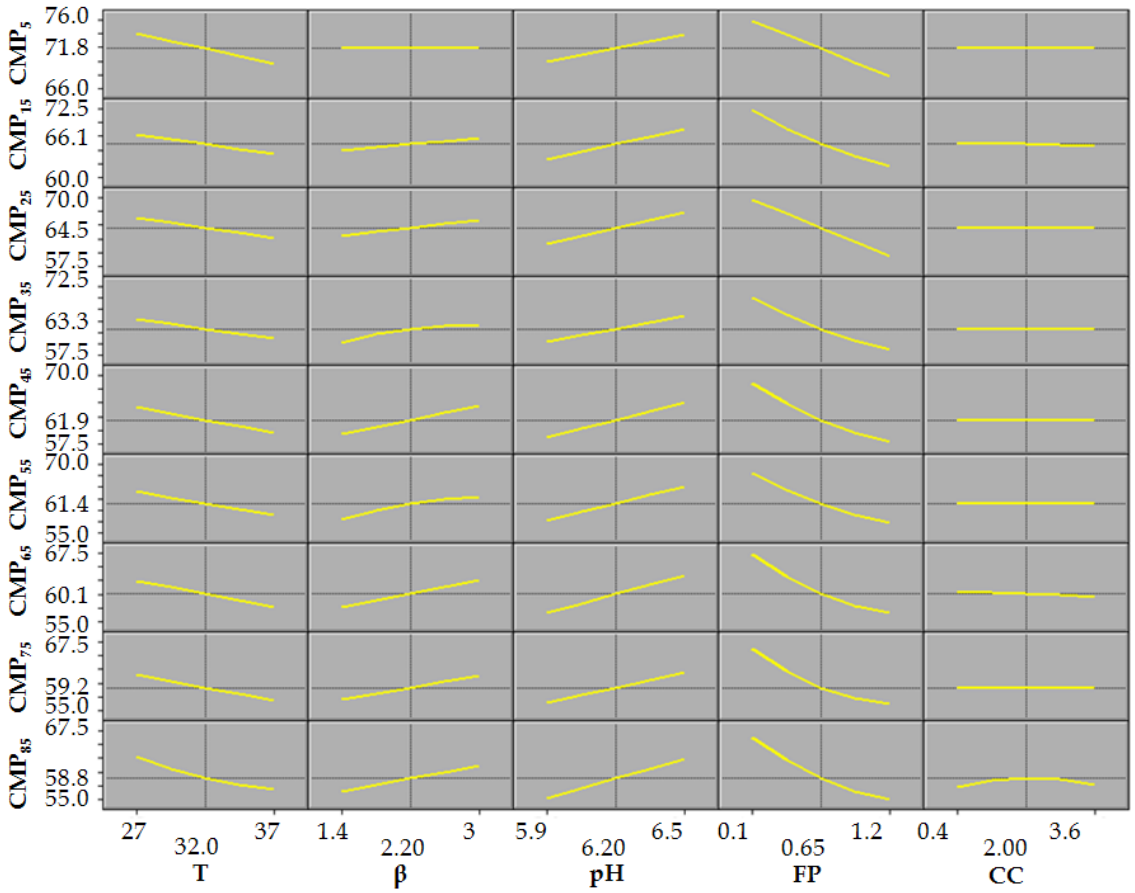

Figure 4.8 - Prediction profiler for the independents variables temperature (*T*), cutting time factor (β), pH, fat/protein ratio (*FP*), and calcium chloride addition level (*CC*) on curd moisture after pressing at each sampling time (CMP_t).

The prediction profiler graph for CMP_t as a function of the independent variables is shown in Figure 4.8. Increasing the temperature was shown to decrease curd moisture after pressing. Increasing β was shown to increase CMP_t except at 5 min after cutting time. Increasing the pH was shown to increase CMP_t. Increasing the fat/protein ratio was shown to decrease curd moisture after pressing for all samples.

Curd moisture after pressing shows similar results as curd moisture before pressing but the trend observed with the prediction profiler for curd moisture after pressing looked more consistent between samples for different

times. This was expected since after pressing moisture samples were more uniform than those for before pressing. This suggests that LFV sensor technology is not only able to assist with curd moisture content control in the vat but also with pressed curd control. Table 4.8, adapted from Fagan (2006) summarizes the effect of temperature, cutting time, pH and fat content on syneresis and consequently on curd moisture.

Table 4.8 - Factors affecting curd moisture.

Factors	**Syneresis**	**Curd Moisture**
Increased Temperature	Increase	Decrease
Earlier t_{cut}	Increase	Decrease
Lower pH	Increase	Decrease
Increased Fat Content*	Increase	Decrease

*different from result

Figure 4.9 shows the response surface graph for curd moisture after pressing as a function of *CC* and pH which clearly show the significant interaction between those two factors. The effect of *CC* differs depending on pH and on sampling time. Decreasing the *CC* at an early stage of syneresis (from 5 to 35 min), decreased *CMP* at low pH but increased *CMP* at higher pH values. After 45 min of syneresis decreasing the *CC* increased *CMP* at low pH but decreased *CMP* at higher pH values. Those graphs show the importance of combining the correct amount of $CaCl_2$ and pH to reach the desirable cheese moisture and the influence of syneresis duration on this parameter.

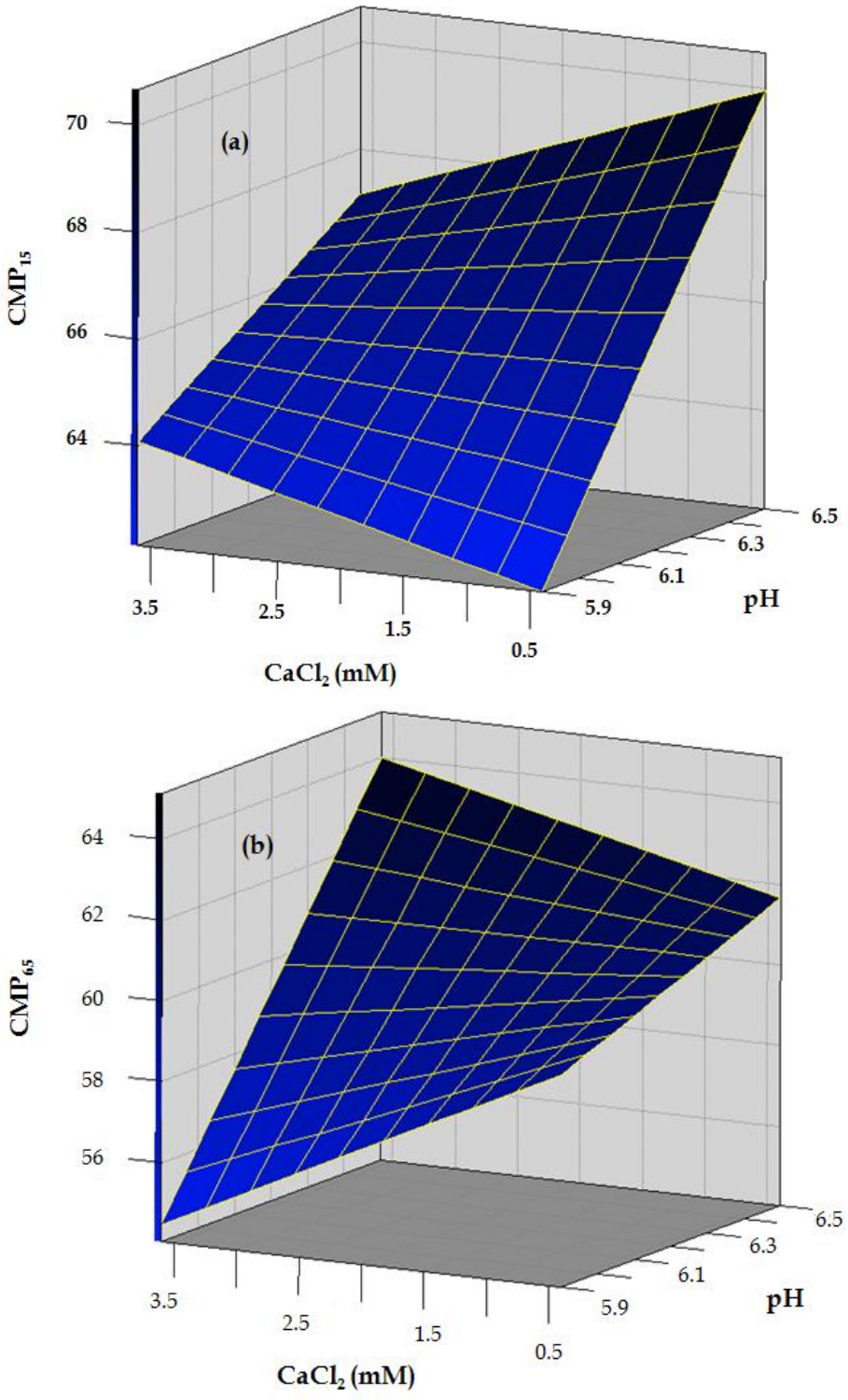

Figure 4.9 - Response surface plot for the effect of *CC* and pH on curd moisture after pressing: a) sample collected 15 min after cutting (CMP_{15}) and b) sample collected 65 min after cutting (CMP_{65}).

The response surface graph (Figure 4.10) for curd moisture after pressing shows the significant interaction between temperature and the cutting time factor, β. The temperature effect is more accentuate at smaller β and the β effect is more accentuated at higher temperature. A short cutting time results in a gel excessively soft and them compensation effect of temperature is more intense. Increasing temperature increases the rearrangement capability, permeability and endogenous pressure, which in a soft gel becomes quite important for successful syneresis. However a long cutting time, the gel is excessively firm and temperature cannot increase the rearrangement tendency too much. In the same way at high temperature the gel can rearrange quite well and syneresis is high, but increasing the cutting time makes the gel firmer and syneresis reduces. Similarly, at low temperature the gel rearrangement tendency is already small and the gel tends to retain a lot of moisture, thus increasing cutting time does not show much effect.

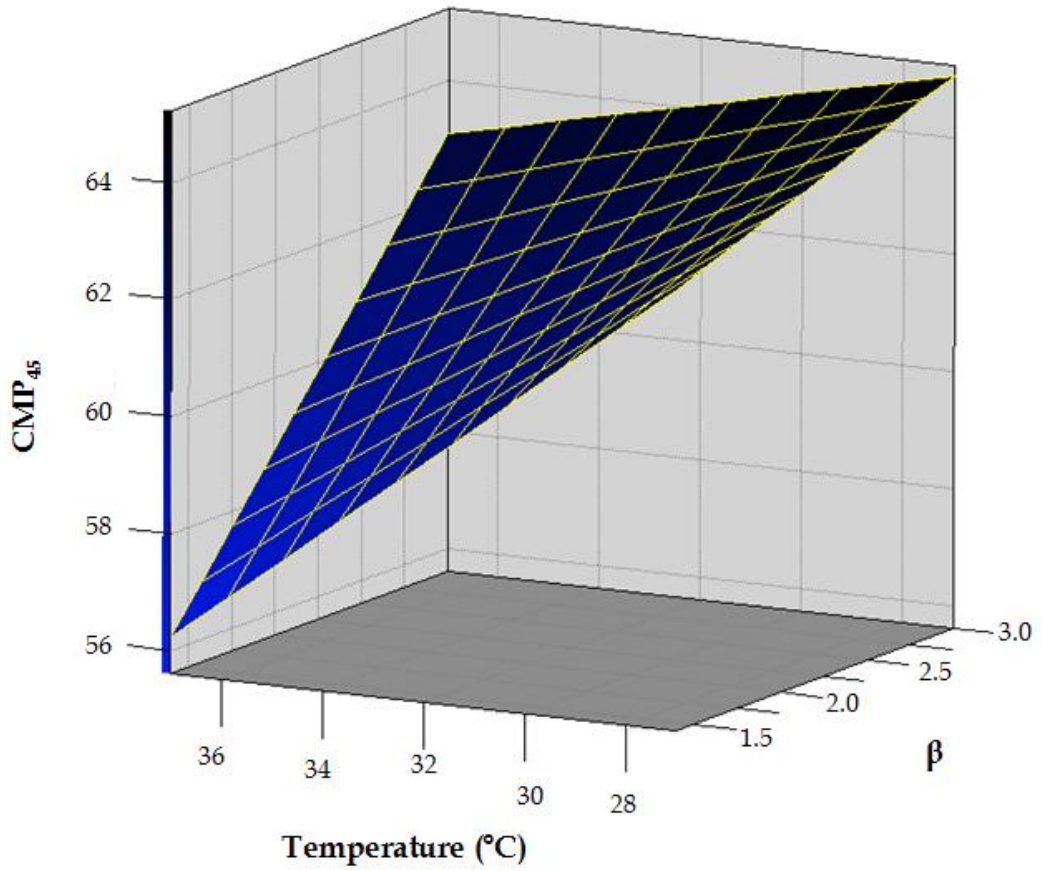

Figure 4.10 - Response surface plot for the effect of T and β on curd moisture after pressing for 45 min after cutting sample (CMP_{45}).

According to the curd moisture model sowed in Table 4.7 and illustrated in Figure 4.10, at 32˚C, regular coagulation temperature, changing β from 1.5 to 3 results in a change in moisture content in the pressed cheese close to 7% (from 62.7 to 67.4%). This difference can change the sensory attributes of the cheese and it is considerable economically.

The response surface graph (Figure 4.11) for curd moisture after pressing shows the significant interaction between temperature and pH. The temperature effect is more accentuated at lower pH and the pH effect is more accentuate at higher temperature. At lower pH a softer gel is produced and the effect of temperature is more intense. Increasing pH reduces the amount of H^+, which

increases the net negative charge on the casein micelles, increasing eletrostatic repulsion (Lucey, 2004). Likely, this would negatively affect rearrangement capability producing a firmer gel which is less affected by temperature changes.

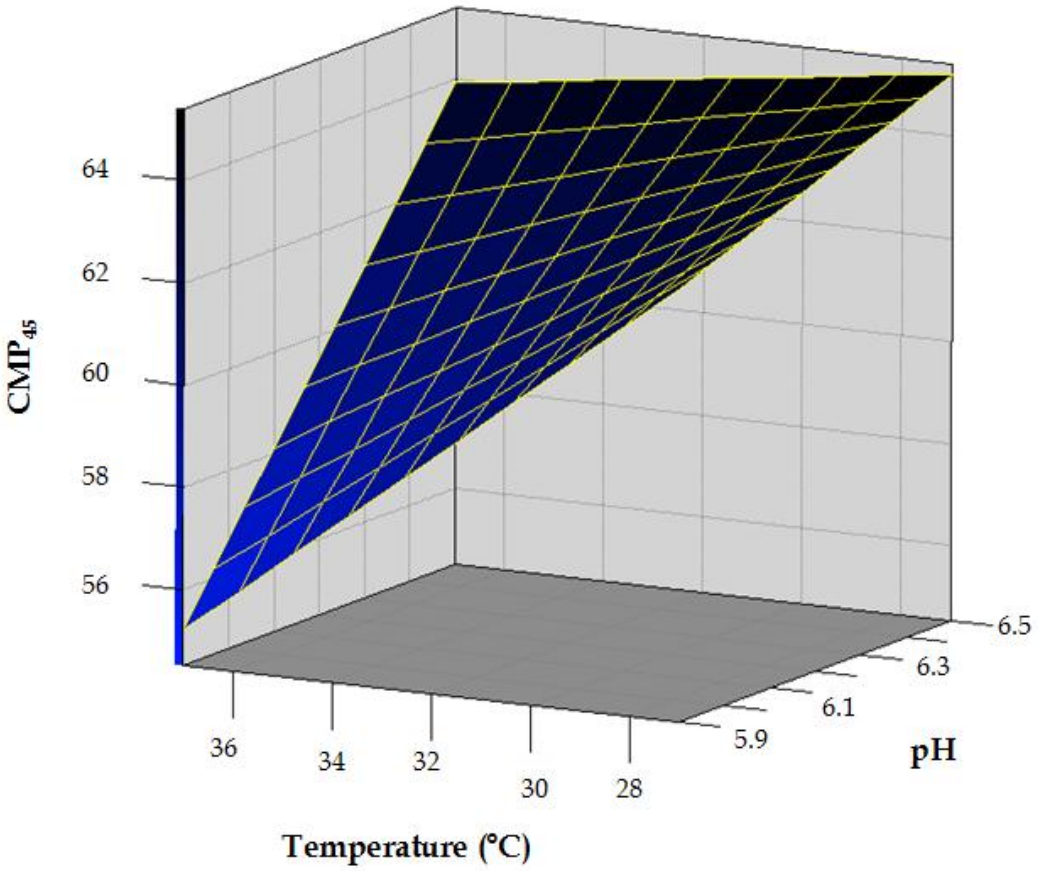

Figure 4.11 - Response surface plot for the effect of *T* and pH on curd moisture after pressing for 45 min after cutting sample (CMP_{45}).

4.2.3. Fat

The following four fat parameters were analyzed: whey fat content, fat in whey, whey fat losses, and curd fat retention.

(i) Whey fat content (%)

Whey fat content (WF_t) represents a percentage of fat in whey at each sampling time. Table 4.9 shows the p-value results from the analysis of variance for this parameter at each sampling time (5, 15, 25…85 min after cutting). The coefficients of determination, R^2, for both master and predictive models are also included in Table 4.9. All whey fat content predictive models were highly significant in their fit ($P < 0.001$).

Table 4.9 - P-value for whey fat content.

	Whey Fat Content (WF_t)				
Factors[1]	WF_5	WF_{15}	WF_{25}	WF_{35}	WF_{45}
T	<.0001*	0.0161*	0.0074*	0.0444*	0.0101*
β	0.7545^{ns}	0.3984^{ns}	0.8058^{ns}	0.5193^{ns}	0.9257^{ns}
pH	<.0001*	<.0001*	<.0001*	<.0001*	<.0001*
FP	<.0001*	<.0001*	<.0001*	<.0001*	<.0001*
CC	0.0625^{ns}	0.0284*	0.0264*	0.0332*	0.0434*
T x *T*	<.0001*	0.0005*	<.0001*	0.0006*	0.0002*
T x β	0.4685^{ns}	0.4013^{ns}	0.3113^{ns}	0.3008^{ns}	0.1651^{ns}
T x pH	0.6514^{ns}	0.4013^{ns}	0.4700^{ns}	0.4577^{ns}	0.3969^{ns}
T x *FP*	0.0085*	0.1034^{ns}	0.1134^{ns}	0.1076^{ns}	0.0368*
T x *CC*	0.1758^{ns}	0.2160^{ns}	0.2474^{ns}	0.3740^{ns}	0.3036^{ns}
β x β	0.4147^{ns}	0.4182^{ns}	0.4034^{ns}	0.3484^{ns}	0.3219^{ns}
β x pH	0.0882^{ns}	0.1339^{ns}	0.1134^{ns}	0.3008^{ns}	0.1651^{ns}
β x *FP*	0.3649^{ns}	0.8677^{ns}	0.6521^{ns}	0.8858^{ns}	0.5334^{ns}
β x *CC*	0.3192^{ns}	0.1034^{ns}	0.2474^{ns}	0.1424^{ns}	0.0554^{ns}
pH x pH	<.0001*	0.0206*	0.0038*	0.0053*	0.0136*
pH x *FP*	0.0003*	0.0122*	0.0162*	0.0304*	0.0153*
pH x *CC*	0.9956^{ns}	0.8111^{ns}	0.9917^{ns}	0.7706^{ns}	0.6604^{ns}
FP x *FP*	0.6082^{ns}	0.4182^{ns}	0.2816^{ns}	0.3484^{ns}	0.3219^{ns}
FP x *CC*	0.2398^{ns}	0.1711^{ns}	0.3855^{ns}	0.3740^{ns}	0.3969^{ns}
CC x *CC*	0.5064^{ns}	0.3022^{ns}	0.2816^{ns}	0.4878^{ns}	0.2132^{ns}
R^2 - Master Model	95.72	95.83	95.81	95.36	95.34
R^2 - Predictive Model	94.75	94.70	94.65	94.29	93.90

[1]*T* = temperature; β = cutting time factor; *FP* = fat/protein ratio; *CC* = calcium chloride addition level; x denotes interaction of experimental factors.

[2]WF_t; t = sampling time (minutes after cutting time).

*significant ($P < 0.05$); [ns]not significant ($P > 0.05$).

Table 4.9 (continued)

	Whey Fat Content (WF_t)			
Factors[1]	WF_{55}	WF_{65}	WF_{75}	WF_{85}
T	0.0042*	0.0350*	0.0076*	0.009*
β	0.8181^{ns}	0.9309^{ns}	0.9221^{ns}	0.9581^{ns}
pH	<.0001*	0.0003*	0.0003*	0.0004*
FP	<.0001*	<.0001*	<.0001*	<.0001*
CC	0.0380*	0.0350*	0.0209*	0.0449*
T x *T*	<.0001*	0.0004*	0.0004*	0.0002*
T x *β*	0.2716^{ns}	0.2929^{ns}	0.2347^{ns}	0.2589^{ns}
T x pH	0.5480^{ns}	0.3710^{ns}	0.4649^{ns}	0.4085^{ns}
T x *FP*	0.0390*	0.1292^{ns}	0.0535^{ns}	0.1151^{ns}
T x *CC*	0.2716^{ns}	0.2929^{ns}	0.1805^{ns}	0.3280^{ns}
β x *β*	0.3225^{ns}	0.3900^{ns}	0.1501^{ns}	0.1533^{ns}
β x pH	0.2716^{ns}	0.5631^{ns}	0.2347^{ns}	0.4085^{ns}
β x *FP*	0.6834^{ns}	0.9524^{ns}	0.9663^{ns}	0.8049^{ns}
β x *CC*	0.1122^{ns}	0.1728^{ns}	0.1365^{ns}	0.3280^{ns}
pH x pH	0.0048*	0.0088*	0.0083*	0.0169*
pH x *FP*	0.0176*	0.0234*	0.0265*	0.1151^{ns}
pH x *CC*	0.8105^{ns}	0.4859^{ns}	0.6123^{ns}	0.8049^{ns}
FP x *FP*	0.2064^{ns}	0.3900^{ns}	0.3498^{ns}	0.3535^{ns}
FP x *CC*	0.3503^{ns}	0.3710^{ns}	0.4649^{ns}	0.6021^{ns}
CC x *CC*	0.4763^{ns}	0.5513^{ns}	0.3498^{ns}	0.3535^{ns}
R^2 - Master Model	96.01	95.55	95.00	94.86
R^2 - Predictive Model	95.03	94.49	93.28	93.36

The master model explained ~95% of the experimental variation for *WF* depending on the sampling point. Predictive models were developed for whey fat content at each sample time after cutting as detailed on equations containing significant factors (P<0.05) and factor that was added to preserve hierarchy with their respective estimated coefficient α_j as shown in

Table 4.10. The predictive models explained ~94% of observed variability.

Table 4.10 - List of predictive models for whey fat content (WF_t[1]).

$$\boldsymbol{WF_5} = 34.31 - 0.18\,T - 10.05\,pH - 2.16\,FP + 0.003\,T^2 - 0.02\,(T \times FP) + 0.80\,pH^2 + 0.52\,(pH \times FP)$$

$$\boldsymbol{WF_{15}} = 13.6 - 0.11\,T - 3.76\,pH - 0.92\,FP - 0.007\,CC + 0.0017\,T^2 + 0.30\,pH^2 + 0.20\,(pH \times FP)$$

$$\boldsymbol{WF_{25}} = 15.39 - 0.11\,T - 4.31\,pH - 0.88\,FP - 0.007\,CC + 0.0017\,T^2 + 0.35\,pH^2 + 0.19\,(pH \times FP)$$

$$\boldsymbol{WF_{35}} = 14.53 - 0.097\,T - 4.13\,pH - 0.72\,FP - 0.0067\,CC + 0.0015\,T^2 + 0.33\,pH^2 + 0.16\,(pH \times FP)$$

$$\boldsymbol{WF_{45}} = 11.77 - 0.095\,T - 3.26\,pH - 0.58\,FP - 0.006\,CC + 0.0015\,T^2 - 0.009\,(T \times FP) + 0.26\,pH^2 + 0.19\,(pH \times FP)$$

$$\boldsymbol{WF_{55}} = 12.96 - 0.096\,T - 3.64\,pH - 0.53\,FP - 0.006\,CC + 0.0015\,T^2 - 0.0087\,(T \times FP) + 0.29\,pH^2 + 0.17\,(pH \times FP)$$

$$\boldsymbol{WF_{65}} = 12.87 - 0.094\,T - 3.59\,pH - 0.78\,FP - 0.006\,CC + 0.0014\,T^2 + 0.28\,pH^2 + 0.17\,(pH \times FP)$$

$$\boldsymbol{WF_{75}} = 13.22 - 0.096\,T - 3.69\,pH - 0.72\,FP - 0.007\,CC + 0.0014\,T^2 + 0.29\,pH^2 + 0.16\,(pH \times FP)$$

$$\boldsymbol{WF_{85}} = 11.54 - 0.10\,T - 3.22\,pH + 0.27\,FP - 0.006\,CC + 0.0016\,T^2 + 0.26\,pH^2$$

[1]*WF*$_t$; t = sampling time (minutes after cutting time). *T* = temperature; β = cutting time factor; *FP* = fat/protein ratio; *CC* = calcium chloride addition level.

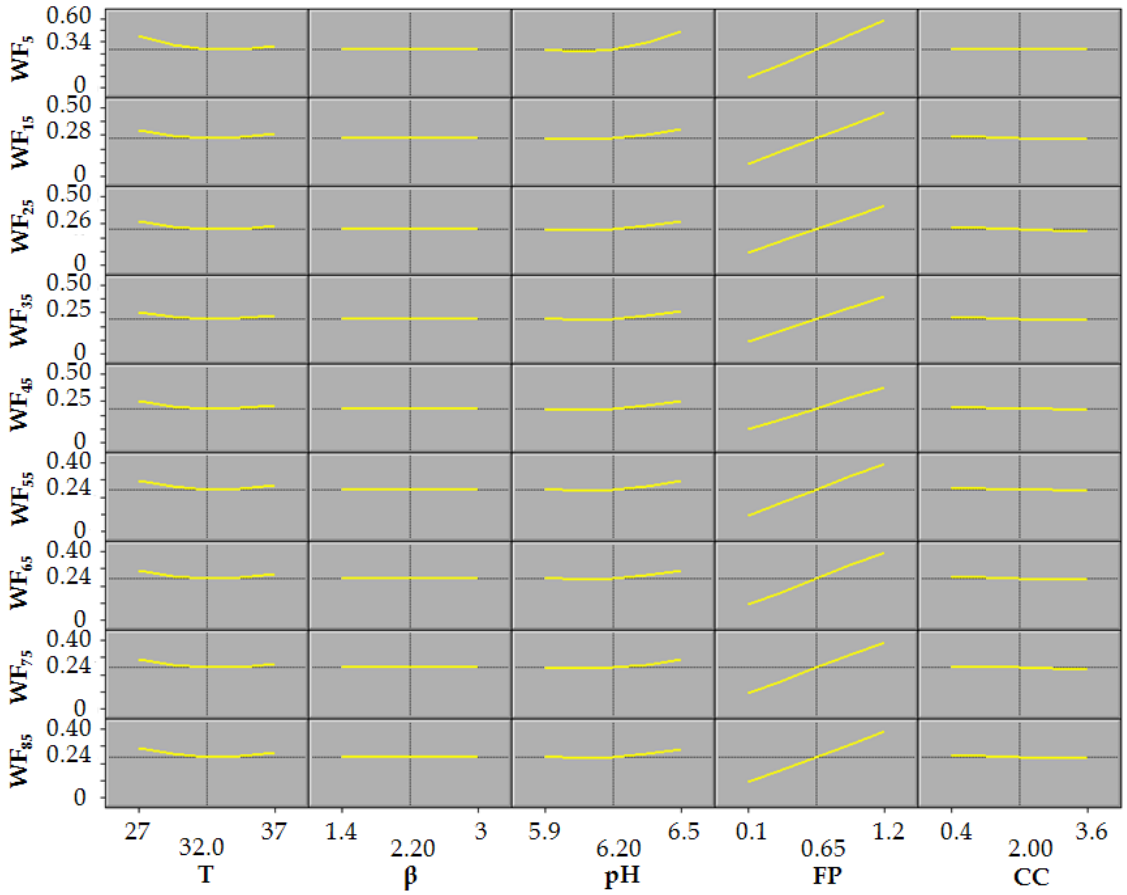

Figure 4.12 - Prediction profiler for the independents variables temperature (*T*), cutting time factor (β), pH, fat/protein ratio (*FP*), and calcium chloride addition level (*CC*) on whey fat content (WF_t).

The prediction profiler graph for WF_t as a function of the independent variables is shown in Figure 4.12. WF_t is shown to be a minimum at ~32˚C. As stated by Fagan 2006 and showed on Table 4.1 decreasing temperature below 32˚C increased the total solid release including fat because at this temperature range gel is fragil. Increasing temperature above 32˚C increase total solid release as increase syneresis ratio because the network becomes more rigid, rapid coarsening occurs, and the gel has a greater porosity.

Cutting time had no effect on whey fat content. WF_t was nearly constant with increasing pH to a pH of 6.2 above which WF_t increased. Although

syneresis rate decreases as pH increases, the gel firmness decreases resulting in an increased fat release. Increasing the fat/protein ratio was shown to increase WF_t. This is just a simple relation, more percentage of fat in milk results in more percentage of fat in whey. WF_t was shown to slowly decrease with increasing CC. According to Lucey (1993) addition of Ca increase the aggregation due to neutralization of negatively charged residues on casein.

The response surface graphs for WF_{45} as a function of *FP* and *T* and for WF_5 as a function of *FP* and pH are shown in Figure 4.13. WF_{45} was minimized at between 32 ˚C and 34.5˚C depending on *FP*. WF_5 was minimized at between pH 5.9 and 6.2 depending on *FP*. It can be explained considering optimum curd firming. Milk with higher fat content results in a soft gel. To compensate that it is necessary a bigger temperature and a smaller pH to reach the same firmness as for milk with lower *FP*.

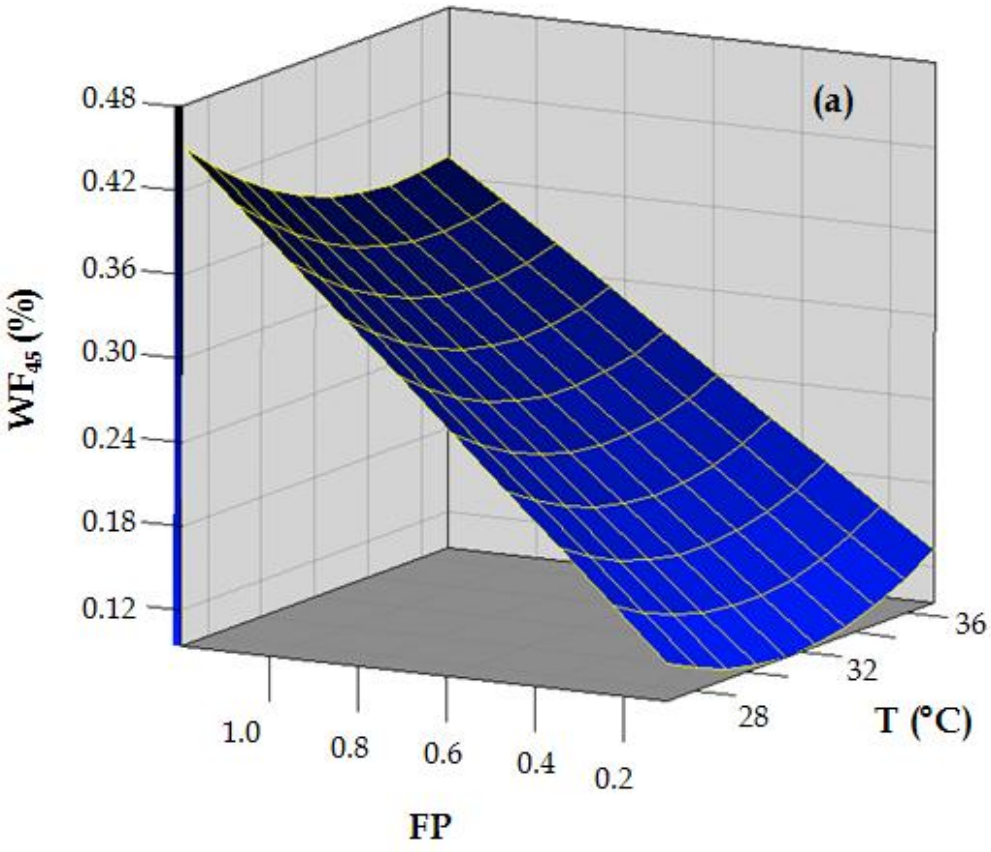

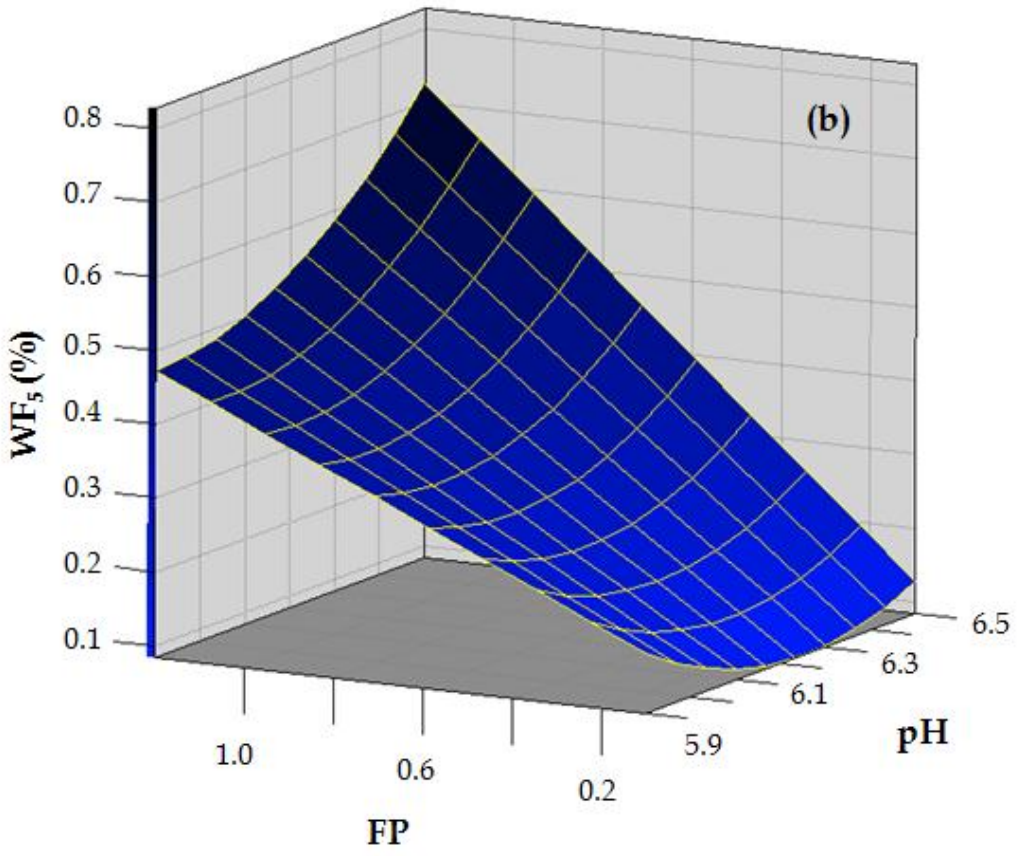

Figure 4.13 - Response surface plot for the effect of FP, T, and pH on whey fat content: a - 45 min after cutting sample (WF_{45}) and b - 5 min after cutting sample (WF_5).

(ii) Fat in whey, whey fat losses and curd fat retention

Fat in whey (*FIW*, %) represents the percentage of fat in whey for the whole syneresis process (85 min). Whey fat losses (*WFL*, %) is the percentage of milk's fat that migrates from milk to whey and curd fat retention (*CFR*, %) as its complementary is the percentage of milk's fat that stays in the curd.

In Table 4.11 the p-values from the analysis of variance for *FIW*, *WFL*, and *CFR* is shown. The coefficients of determination, R^2, for both master and

predictive models are also included in Table 4.11. Those three predictive models were highly significant in their fit ($P < 0.001$).

Table 4.11 - P-value for whey fat losses, fat in whey, and curd fat retention.

Factors[1]	*FIW*	*WFL*	*CFR*
T	0.0083*	0.8765[a]	0.8765[a]
β	0.9397[ns]	0.1629[ns]	0.1629[ns]
pH	0.0003*	0.4771[ns]	0.4771[ns]
FP	<.0001*	<.0001*	<.0001*
CC	0.0408*	0.3087[ns]	0.3087[ns]
T x *T*	0.0002*	0.0276*	0.0276*
T x *β*	0.2334[ns]	0.3494[ns]	0.3494[ns]
T x pH	0.4095[ns]	0.8229[ns]	0.8229[ns]
T x *FP*	0.1001[ns]	0.9940[ns]	0.9940[ns]
T x *CC*	0.3226[ns]	0.9494[ns]	0.9494[ns]
β x *β*	0.1653[ns]	0.7718[ns]	0.7718[ns]
β x pH	0.3857[ns]	0.3007[ns]	0.3007[ns]
β x *FP*	0.8345[ns]	0.4911[ns]	0.4911[ns]
β x *CC*	0.2925[ns]	0.9109[ns]	0.9109[ns]
pH x pH	0.0143*	0.1960[ns]	0.1960[ns]
pH x *FP*	0.0869[ns]	0.6466[ns]	0.6466[ns]
pH x *CC*	0.8441[ns]	0.2509[ns]	0.2509[ns]
FP x *FP*	0.3790[ns]	<.0001*	<.0001*
FP x *CC*	0.5455[ns]	0.5712[ns]	0.5712[ns]
CC x *CC*	0.3708[ns]	0.8829[ns]	0.8829[ns]
R^2 - Master Model	95.06	77.38	77.38
R^2 - Predictive Model	93.57	72.34	72.34

[1]*T* = temperature; *β* = cutting time factor; *FP* = fat/protein ratio; *CC* = calcium chloride addition level; x denotes interaction of experimental factors.

*significant ($P < 0.05$); [ns]not significant ($P > 0.05$); [a] not significant but factor was added to model to preserve hierarchy.

The master model explained 95.06% of the experimental variation for *FIW* and 77.38% for *WFL* and *CFR*. The predictive models developed for fat in whey, whey fat losses, and curd fat retention contain significant factors ($P<0.05$) and factor that was added to preserve hierarchy with their respective estimated coefficient α_j as shown in Table 4.12. The predictive models explained 93.57% of observed variability for *FIW* and 72.34% for *WFL* and *CFR*.

Table 4.12 - List of predictive models for fat in whey (*FIW*), whey fat losses (*WFL*), and curd fat retention (*CFR*).

$\boldsymbol{FIW} = 11.87 - 0.104\,T - 3.32\,pH + 0.27\,FP - 0.006\,CC + 0.0016\,T^2 + 0.27\,pH^2$
$\boldsymbol{WFL} = 58.997 - 2.71\,T - 19.7\,FP + 0.042\,T^2 + 10.88\,FP^2$
$\boldsymbol{CFR} = 41.003 + 2.71\,T + 19.7\,FP - 0.042\,T^2 - 10.88\,FP^2$

T = temperature; β = cutting time factor; FP = fat/protein ratio; CC = calcium chloride addition level.

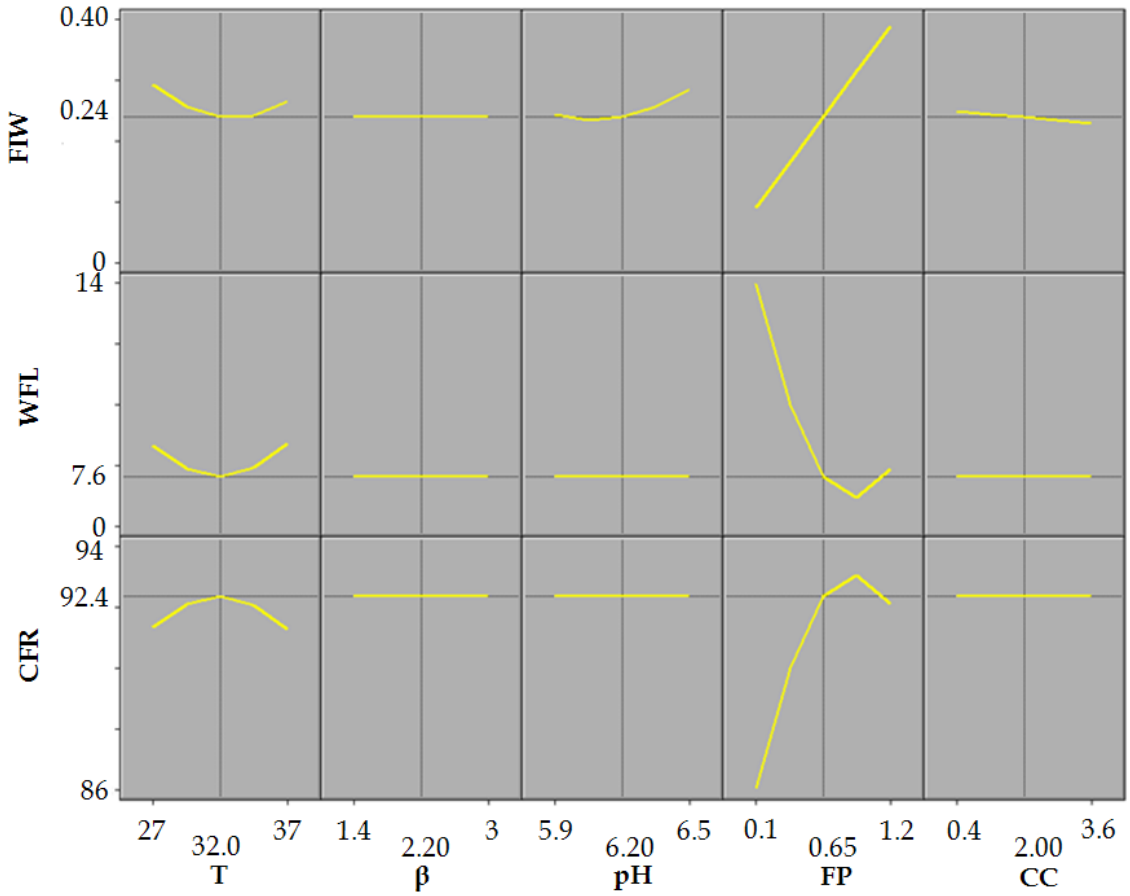

Figure 4.14 - Prediction profiler for the independents variables temperature (*T*), cutting time factor (β), pH, fat/protein ratio (*FP*), and calcium chloride addition level (*CC*) on fat in whey (*FIW*), whey fat losses (*WFL*), and curd fat retention (*CFR*).

The prediction profiler graphs for *FIW*, *WFL*, and *CFR* as a function of the independent variables are shown in Figure 4.14. As expected, *FIW* follows similar trend as WF_t. Increasing the temperature was shown to minimize *FIW* at ~32˚C. β had no effect on *FIW*. *FIW* was almost constant with increasing pH to 6.2 but it increased above that pH value. Increasing the *FP* was shown to increase *FIW*. And increasing *CC* was shown to slowly decrease *FIW*. For *WFL* and *CFR* increasing temperature was shown to minimize *WFL* and to maximize *CFR* at ~32˚C for the same reason presented for WF_t. And increasing fat/protein ratio

was shown to minimize *WFL* and to maximize *CFR* at ~0.925. This result can be explained by the result of changing *FP* on curd firmness. β, pH, and *CC* had no effect on *WFL* and *CFR*.

4.2.4. Curd yield

Curd yield is the percentage of curd produced based on the initial mass of milk utilized. It can be calculate in wet basis or dry basis and two different approaches were considered as described in Material and Methods. One had considered the whole experimental data and the other only the last data (at 85 min after cutting).

Table 4.13 shows the p-values from the analysis of variance for curd yield (wet and dry basis) using the two different approaches. The coefficients of determination, R^2, for both master and predictive models are also included in Table 4.13. All the curd yield predictive models were highly significant in their fit ($P < 0.001$).

Table 4.13 - P-value for curd yield.

	All curd data		Only 85min data	
Factors[1]	CY_{wb}	CY_{db}	$CY85_{wb}$	$CY85_{db}$
T	<.0001*	0.0323*	<.0001*	0.0128*
β	<.0001*	0.0297*	<.0001*	0.0008*
pH	<.0001*	0.0214*	<.0001*	0.0003*
FP	<.0001*	<.0001*	<.0001*	<.0001*
CC	0.6156^{ns}	0.4164^{ns}	0.3645^{ns}	0.5891^{ns}
T x *T*	0.7212^{ns}	0.0894^{ns}	0.0256*	0.7312^{ns}
T x *β*	0.5736^{ns}	0.4401^{ns}	0.5219^{ns}	0.2234^{ns}
T x pH	0.2485^{ns}	0.5022^{ns}	0.8986^{ns}	0.2059^{ns}
T x *FP*	0.8533^{ns}	0.5725^{ns}	0.5036^{ns}	0.5310^{ns}
T x *CC*	0.8271^{ns}	0.9797^{ns}	0.6902^{ns}	0.5199^{ns}
β x *β*	0.6479^{ns}	0.1341^{ns}	0.8942^{ns}	0.4435^{ns}
β x pH	0.7358^{ns}	0.4060^{ns}	0.9421^{ns}	0.7987^{ns}
β x *FP*	0.7129^{ns}	0.9961^{ns}	0.7597^{ns}	0.7154^{ns}
β x *CC*	0.2497^{ns}	0.6700^{ns}	0.9194^{ns}	0.4726^{ns}
pH x pH	0.0746^{ns}	0.7190^{ns}	0.4800^{ns}	0.7831^{ns}
pH x *FP*	0.1412^{ns}	0.0647^{ns}	0.5484^{ns}	0.6412^{ns}
pH x *CC*	0.2510^{ns}	0.7082^{ns}	0.5869^{ns}	0.3306^{ns}
FP x *FP*	0.2246^{ns}	0.8902^{ns}	0.1260^{ns}	0.7213^{ns}
FP x *CC*	0.9695^{ns}	0.6582^{ns}	0.8443^{ns}	0.5396^{ns}
CC x *CC*	0.8959^{ns}	0.3685^{ns}	0.9729^{ns}	0.5440^{ns}
R^2 - Master Model	85.31	61.79	75.84	76.49
R^2 - Predictive Model	81.02	50.27	72.73	73.09

[1]*T* = temperature; *β* = cutting time factor; *FP* = fat/protein ratio; *CC* = calcium chloride addition level; x denotes interaction of experimental factors.

[2]CY_{wb}; wb = wet basis and CY_{db}; db = dry basis.

*significant (P < 0.05); ^{ns}not significant (P > 0.05).

The master model explained 61.79-85.31% of the experimental variation for *CY* depending on the approach. The predictive models developed for curd yield (CY_{wb}, CY_{db}, $CY85_{wb}$, and $CY85_{db}$) contain significant factors (P < 0.05) and factor that was added to preserve hierarchy with their respective estimated

coefficient α_j as shown in Table 4.14. The predictive models explained 50.7-81.02% of observed variability. As expected, better result was found for curd yield dry basis using the second approach because it depends on total solid which was considered constant during the whole syneresis process when the whole experimental data was used.

Table 4.14 - List of predictive models for curd yield[1] (CY_{wb}, CY_{db}, $CY85_{wb}$, and $CY85_{db}$).

$\boldsymbol{CY_{wb}} = -22.17 - 0.60\,T + 2.13\,\beta + 10.26\,pH + 4.20\,FP$
$\boldsymbol{CY_{db}} = 5.84 - 0.41\,T + 2.63\,\beta + 7.44\,pH + 11.24\,FP$
$\boldsymbol{CY85_{wb}} = 38.58 - 4.87\,T + 2.52\,\beta + 10.54\,pH + 3.69\,FP + 0.069\,T^2$
$\boldsymbol{CY85_{db}} = -4.71 - 0.31\,T + 2.85\,\beta + 8.35\,pH + 11.22\,FP$

[1]CY_{wb}; wb = wet basis and CY_{db}; db = dry basis; two different approaches.
T=temperature; β = cutting time factor; FP = fat/protein ratio; CC = calcium chloride addition level.

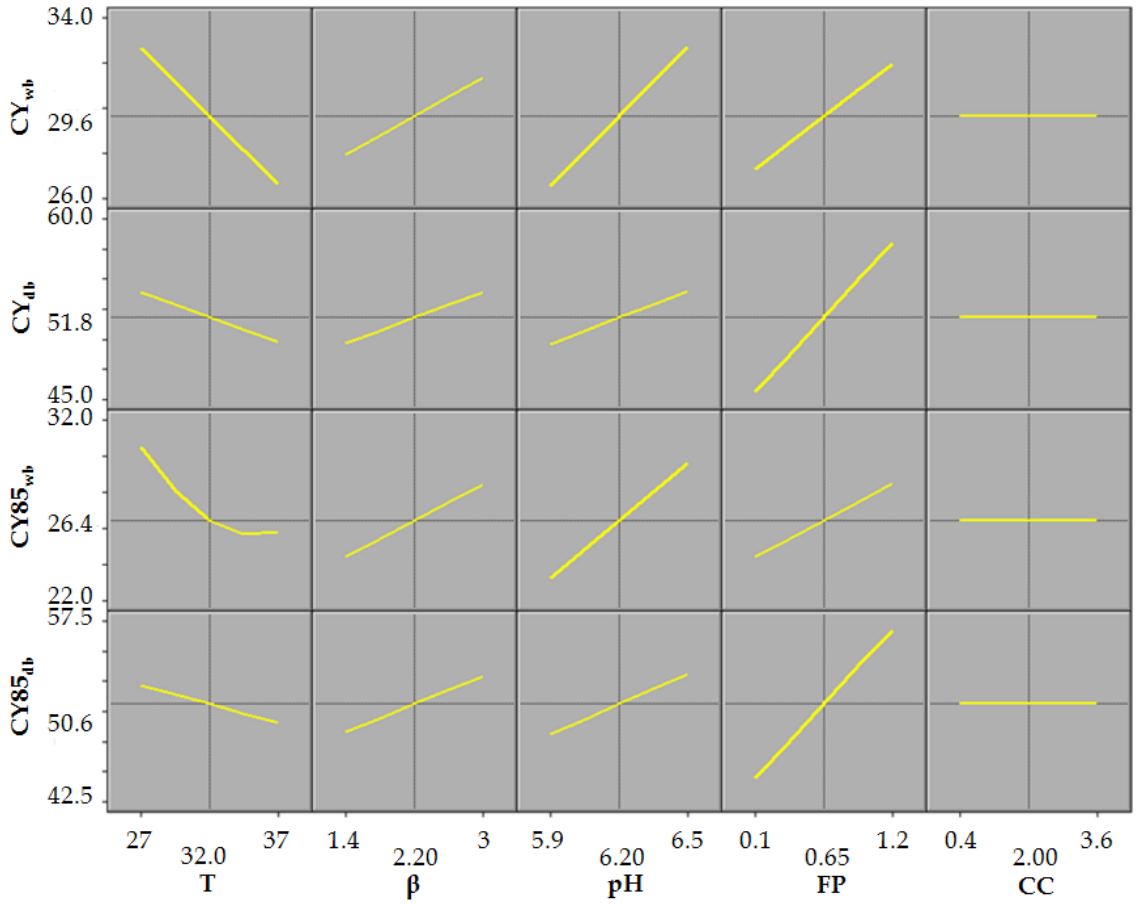

Figure 4.15 - Prediction profiler for the independents variables temperature (T), cutting time factor (β), pH, fat/protein ratio (FP), and calcium chloride addition level (CC) on curd yield wet basis (CY_{wb}) and curd yield dry basis (CY_{db}) for two different approaches.

The prediction profiler graphs for curd yield as a function of the independent variables are shown in Figure 4.15. The two approaches displayed a similar trend except for curd yield wet basis as a function of temperature. Increasing the temperature was shown to decrease curd yield. Increasing cutting time was shown to increase curd yield. Increasing the pH was shown to increase curd yield. Increasing the fat/protein ratio was shown to increase curd yield. CC had no effect on curd yield. The effects of T and pH are more pronounced for wet basis. This is result of moisture content effect on curd yield wet basis. On the

other hand the effect of *FP* is more pronounced for dry basis because an increase in *FP* increases the amount of solids.

At constant protein concentration but changing *FP*, curd yield should be for the most part discussed as a combination between moisture content and curd fat retention but surprisingly T, β, pH, and CC are just following the same trend as CM. Although increasing *FP* was shown to decrease *CM*, it was showing to increase *CY*. This is consistent because total solids were increased with increasing fat content and it is one more proof that the reduction in water at the begging of syneresis in a high fat content sample is the cause of reduced curd moisture.

4.2.5. Cheese yield

Cheese yield is the percentage of pressed curd produced based on the initial mass of milk utilized. It can be calculate either in wet basis or in dry basis.

Table 4.15 shows the p-values from the analysis of variance for cheese yield (wet and dry basis) using the two different approaches. The coefficients of determination, R^2, for both master and predictive models are also included in Table 4.15. The two cheese yield predictive models were highly significant in their fit ($P<0.001$).

Table 4.15 - P-value for cheese yield.

	Cheese Yield (*ChY*)	
Factors[1]	ChY_{wb}	ChY_{db}
T	<.0001*	0.2931
β	0.0005*	0.4866
pH	<.0001*	0.1782
FP	<.0001*	<.0001*
CC	0.6895	0.3343
T x *T*	0.2258	0.051
T x *β*	0.9018	0.9361
T x pH	0.6482	0.7257
T x *FP*	0.9901	0.2397
T x *CC*	0.5542	0.5553
β x *β*	0.3034	0.3054
β x pH	0.5379	0.5131
β x *FP*	0.9869	0.6716
β x *CC*	0.4146	0.4234
pH x pH	0.6475	0.4244
pH x *FP*	0.0263	0.0727
pH x *CC*	0.394	0.2958
FP x *FP*	0.2905	0.7006
FP x *CC*	0.4602	0.5545
CC x *CC*	0.8478	0.386
R^2 - Master Model	79.94	67.59
R^2 - Predictive Model	74.33	53.59

[1]*T* = temperature; *β* = cutting time factor; *FP* = fat/protein ratio; *CC* = calcium chloride addition level; x denotes interaction of experimental factors.

[2]ChY_{wb}; wb = wet basis and ChY_{db}; db = dry basis.

*significant (P < 0.05); [ns]not significant (P > 0.05).

The predictive model explained 74.33% of the experimental variation for ChY_{wb} and only 53.59% for ChY_{db}. The predictive models developed for cheese yield (ChY_{wb} and ChY_{db}) contain significant factors (P<0.05) and factor that was

added to preserve hierarchy with their respective estimated coefficient α_j as shown in Table 4.16.

Table 4.16 - List of predictive models for cheese yield[1] (ChY_{wb} and ChY_{db}).

$\boldsymbol{ChY_{wb}} = 16.04 - 0.253\,T + 1.15\,\beta + 0.12\,pH - 48.12\,FP + 8.41\,(pH \times FP)$
$\boldsymbol{ChY_{db}} = 40.19 + 12.81\,FP$

[1]ChY_{wb}; wb = wet basis and ChY_{db}; db = dry basis.

T = temperature; β = cutting time factor; FP = fat/protein ratio; CC = calcium chloride addition level.

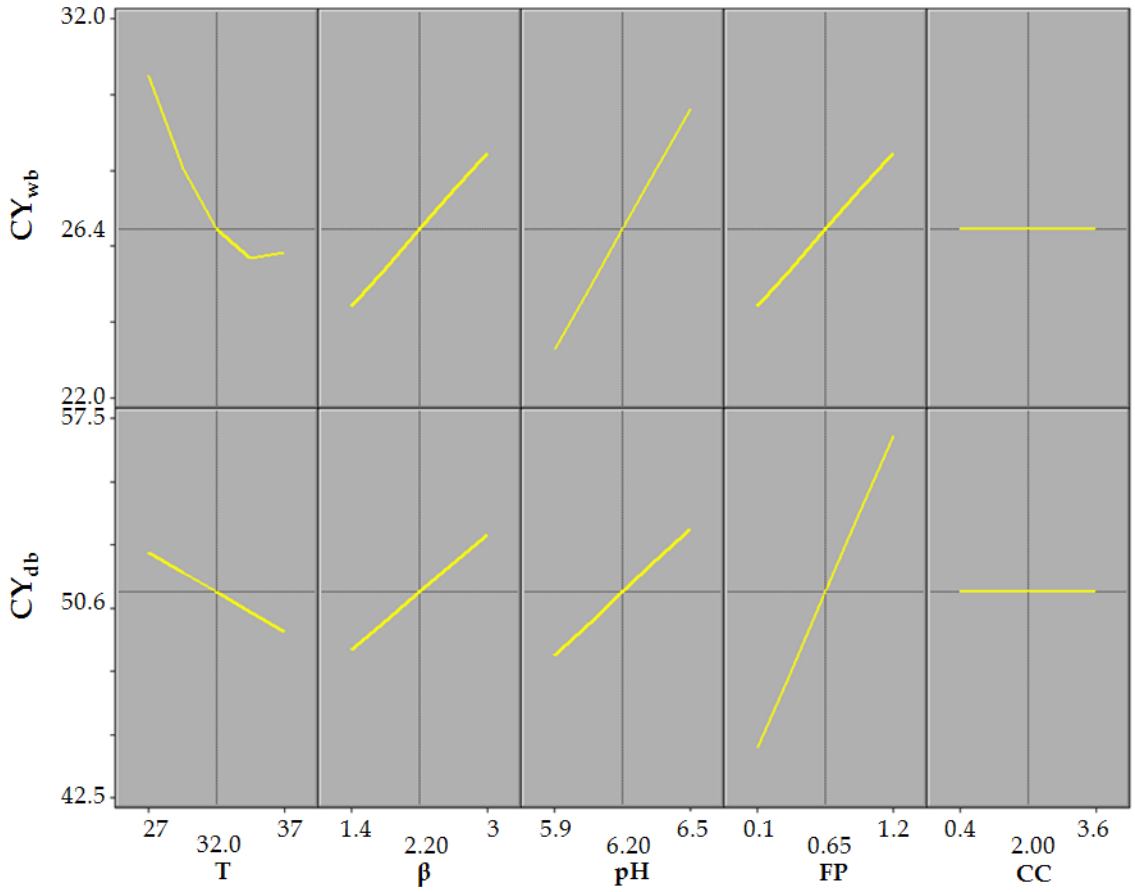

Figure 4.16 - Prediction profiler for the independents variables temperature (*T*), cutting time factor (β), pH, fat/protein ratio (*FP*), and calcium chloride addition level (*CC*) on cheese yield wet basis (ChY_{wb}) and cheese yield dry basis (ChY_{db}).

The prediction profiler graphs for cheese yield as a function of the independent variables are shown in Figure 4.16. Cheese yield wet basis followed the same trend than curd yield. Increasing the temperature was shown to decrease cheese yield, increasing β was shown to increase cheese yield, increasing the pH was shown to increase cheese yield, increasing the *FP* was shown to increase cheese yield, and *CC* had no effect on cheese yield. Cheese yield dry basis increased only with increasing *FP* and was not affected by *T*, β, pH, and *CC*. The unexpected result for cheese yield dry basis could be explained by the number of assumptions made to calculate this parameter.

4.3. Prediction of curd moisture

Based on the first order response of the light backscatter ratio observed in the syneresis data with time after curd cutting (Figure 4.2) and the observation that moisture content also observed a first order response with time then a new equation was developed relating reflectance ratio as a function of curd moisture with no time dependence. This relationship may permit better control of moisture on the final pressed cheese product.

4.3.1. Reflectance ratio equation

Considering that the reflectance response from the LFV sensor during syneresis appeared to follow a first order it was fitted to the following equation:

$$R_t = R_\infty + (R_0 - R_\infty)e^{-k_{LFV}*t} \qquad \text{Eqn. 4.3}$$

where R_t was the light backscatter ratio during syneresis at time t(min), R_∞ was the light backscatter ratio during syneresis at an infinite time, R_0 was the light backscatter ratio during syneresis at t_0, and k_{LFV} was the kinetic rate constant (min^{-1}) for the LFV sensor response during syneresis.

A MatLab® (Mathwork R2010a) program (Appendix A) was developed to predict the parameters R_0, R_∞ and k_{LFV}. Because of interferences (curd aggregation into clumps, settling to the bottom of vat, etc.) that can show up on sensor response at the end stage of syneresis, the data used to fit the curve was selected visually from the beginning of syneresis (t = 0) until the interference (t = Tv) as showed in Figure 4.17.

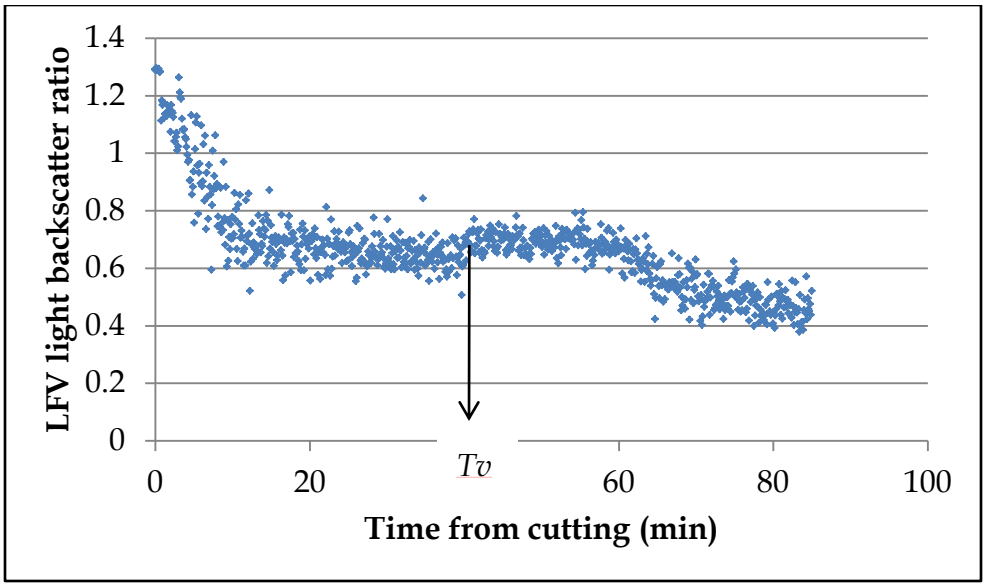

Figure 4.17 - Time selected visually (Tv) in a LFV sensor profile at 980 nm during syneresis (T = 32˚C; β = 2.2; pH = 6.2; FP = 0.65; CC = 2mM).

Figure 4.18 illustrates the fitting of Equation 4.3 to experimental data for a central point condition (T = 32°C; β = 2.2; pH = 6.2; FP = 0.65; CC = 2mM) for which Tv = 40 min, R_0 = 1.3276, R_∞ = 0.6416, k_{LFV} = 0.1634, and R^2=0.8537. The fit of this equation had a range of R^2 between 0.58-0.94, but most were bigger than 0.8 as shown in Table 4.17. Table 4.17 also shows Tv, R_0, R_∞ and k_{LFV} for each experiment of the two replications.

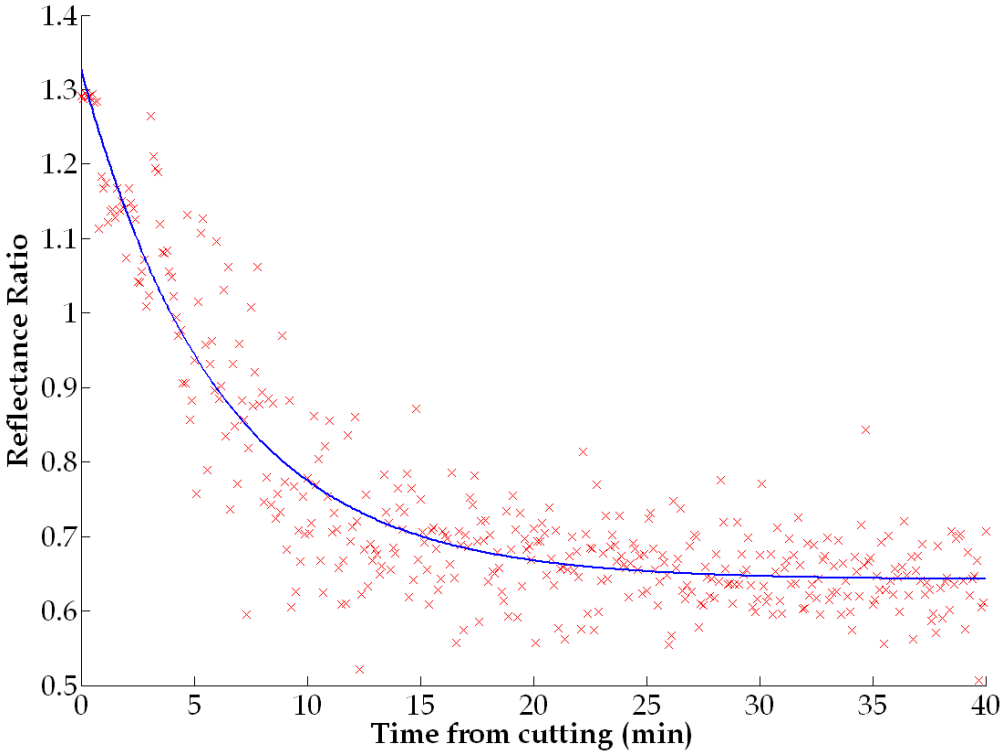

Figure 4.18 - Kinetics of LFV light backscatter ratio as a function of time during syneresis at central point (T=32°C; β=2.2; pH=6.2; FP=0.65; CC=2mM). Time zero corresponds to the cutting time and theoretical curve (—) was fitted assuming first-order kinetics (Equation 4.3). (x) Experimental data.

Table 4.17 - Results for reflectance ratio fitting to Equation 4.3**.**

	[2]Rep 2					Rep 3				
***Trt*[1]**	***Tv***	R_0	R_∞	k_{LFV}	R^2	***Tv***	R_0	R_∞	k_{LFV}	R^2
1	30.6	1.1854	0.7023	0.1553	0.64	60	1.1295	0.4707	0.0624	0.84
2	75.1	1.2133	0.7461	0.2031	0.68	45.1	1.3134	0.6958	0.3481	0.81
3	20.1	1.0817	0.5232	0.0488	0.67	85	1.1806	0.565	0.0333	0.93
4	85.1	1.093	0.6927	0.1021	0.68	35.9	1.204	0.776	0.1437	0.82
5	45.1	1.1949	0.7258	0.0844	0.73	85	1.1711	0.5057	0.0374	0.89
6	36	1.269	0.675	0.2159	0.80	66.8	1.1638	0.5792	0.1646	0.80
7	35.1	1.4772	0.9672	0.0965	0.75	29.2	1.3003	0.8464	0.1443	0.74
8	46	1.1638	0.6245	0.1989	0.76	46	1.2682	0.7434	0.1368	0.79
9	41.1	1.2052	0.6631	0.2687	0.76	35.1	1.2566	0.6392	0.1748	0.88
10	47.3	1.285	0.6676	0.1555	0.74	31.2	1.2169	0.641	0.1935	0.81
11	45.1	1.3357	0.6013	0.1246	0.87	48.4	1.2956	0.7669	0.1	0.84
12	48.2	1.2684	0.6977	0.2447	0.85	49.2	1.3343	0.6293	0.2099	0.85
13	45.1	1.3044	0.5388	0.1248	0.84	38.2	1.5062	0.5454	0.2322	0.85
14	35.8	1.2213	0.5397	0.1579	0.86	45.1	1.0901	0.6116	0.1192	0.60
15	45.1	1.1672	0.5413	0.1103	0.74	60	1.4191	0.6674	0.1028	0.86
16	48	1.2444	0.6184	0.1647	0.78	37.4	1.2726	0.7121	0.1564	0.79
17	35.4	1.1874	0.524	0.041	0.82	18.1	1.2404	0.7961	0.1183	0.80
18	85	1.0683	0.3671	0.0572	0.88	45.1	1.2777	0.5635	0.1766	0.80
19	39.3	1.1902	0.4742	0.0861	0.87	45.1	1.2667	0.6649	0.1495	0.78
20	46.5	1.5522	0.8641	0.1398	0.81	29.3	1.3146	0.6397	0.1411	0.76
21	45.1	1.3628	0.6245	0.426	0.80	46.3	1.3461	0.6433	0.2323	0.82
22	37.7	1.2537	0.7304	0.1048	0.79	37.3	1.2874	0.712	0.16	0.77
23	53.1	1.336	0.234	0.07	0.94	58.9	1.2062	0.5723	0.0507	0.87
24	57.5	1.1845	0.6346	0.1798	0.82	58	1.1766	0.7014	0.1743	0.58
25	60.5	1.2618	0.6095	0.149	0.81	45.9	1.353	0.817	0.184	0.74
26	39.7	1.1261	0.4498	0.2155	0.82	57.2	1.1974	0.5701	0.1874	0.86
27	75.2	1.2714	0.5758	0.1459	0.79	19.5	1.1555	0.674	0.2366	0.77
28	45.3	1.1366	0.5341	0.104	0.79	85	1.2093	0.5549	0.0816	0.83
29	50.6	1.1806	0.5973	0.1701	0.75	53.3	1.4611	0.7466	0.1128	0.84
30	40	1.3276	0.6416	0.1634	0.85	38.1	1.2996	0.7383	0.1522	0.71
31	26	1.4647	0.6791	0.1708	0.88	50.8	1.18	0.6279	0.2448	0.71
32	25.1	1.5007	1.0095	0.2529	0.69	60	1.2143	0.5716	0.1163	0.80
33	41	1.1968	0.5762	0.2101	0.76	29.3	1.3782	0.787	0.2735	0.75

[1]Trt=treatment number;

[2]Rep = replication; *Tv* = visually time selected; R_0 = light backscatter ratio at t_0, R_∞ = light backscatter ratio during syneresis at an infinite time, k_{LFV}= kinetic rate constant (min^{-1}) for the LFV sensor response during syneresis

The variability observed between each replication (Rep2 and Rep3) presented in Table 4.17 for the parameters estimated can be explained by the scatter data obtained by the LFV sensor, possible agglomeration of curd into clumps, and a non homogeneous mixture of curd and whey.

4.3.2. Curd moisture (dry basis) equation.

A number of authors have observed that the expulsion of whey from rennet induced milk gels follows first kinetics (Marshall, 1982; Peri et al., 1985; Weber, 1989; Castillo et al., 2000; Fagan et al.,2008). Therefore the following first order equation was fitted to the curd moisture experimental data.

$$CM_t = CM_\infty + (CM_0 - CM_\infty)e^{-k_{CM}*t} \qquad \text{Eqn. 4.4}$$

where CM_t was the curd moisture (%) during syneresis at time t(min), CM_∞ was the curd moisture (%) during syneresis at an infinite time, CM_0 was the curd moisture content (%) at t_0 i.e. the milk moisture content, and k_{CM} was the kinetic rate constant (min^{-1}) for curd moisture content changes during syneresis. A MatLab program (Appendix A) was developed to predict the parameters CM_0, CM_∞ and k_{CM}. The data points selected to fit this equation was the curd moisture content values between t = 5 min after cutting and *Tv*. The data above *Tv* was truncated because there was no corresponding reflectance data.

Figure 4.19 illustrates the regression fit for curd moisture content (dry basis) according to Equation 4.4 for a central point condition (T=32°C; β=2.2; pH=6.2; *FP*=0.65; *CC*=2mM) for which CM_0=758.59, CM_∞=183.14, k_{CM}=0.463, and R^2=0.9989. The regression had an R^2 ~0.99 for all experiments as shown in Table 4.18. Table 4.18 shows also CM_0, CM_∞ and k_{CM} for each experiment of the two replications.

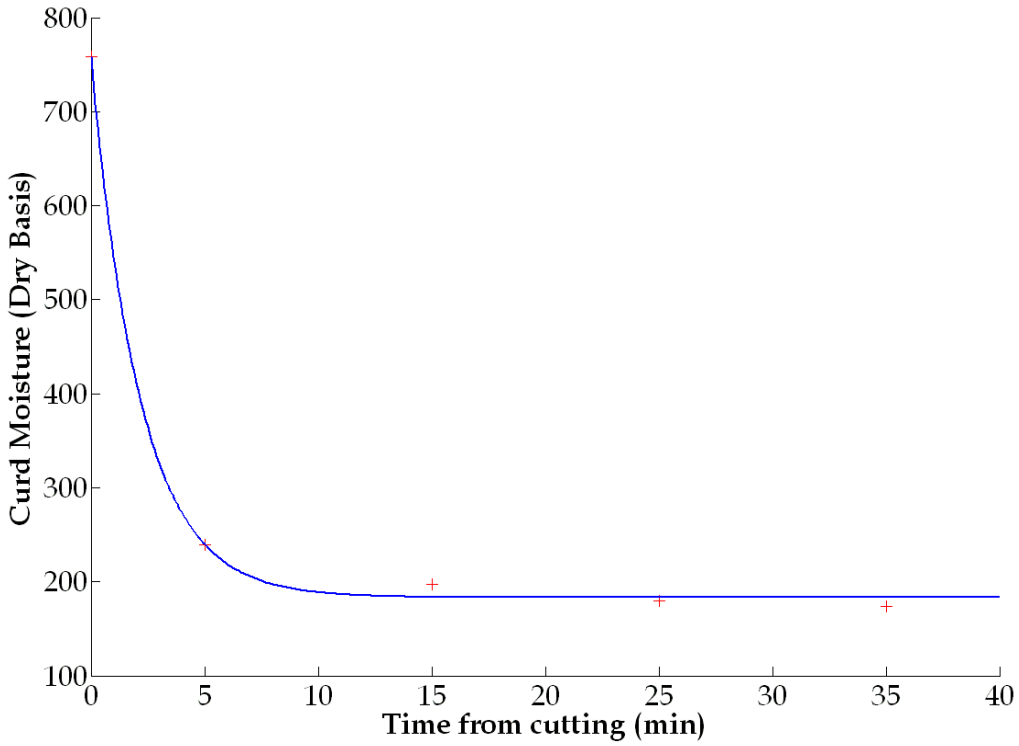

Figure 4.19 - Kinetics of curd moisture content (dry basis) as a function of time during syneresis at central point (T=32°C; β=2.2; pH=6.2; FP=0.65; CC=2mM). Time zero corresponds to the cutting time and theoretical curve (—) was fitted assuming first-order kinetics (Equation 4.4). (+) Experimental data.

Table 4.18 - Results for reflectance ratio fitting to Equation 4.4.

Trt[1]	CM_0	CM_∞	k_{CM}	R^2	CM_0	CM_∞	k_{CM}	R^2
1	831.714	197.292	0.307	0.9992	837.178	190.572	0.4062	0.9997
2	708.357	159.181	0.3664	0.9997	686.138	160.319	0.455	0.9986
3	821.291	217.879	0.4162	0.9973	821.527	225.992	0.3403	0.9987
4	691.108	169.337	0.4403	0.9989	685.664	174.776	0.3851	0.9979
5	831.93	204.061	0.4519	0.9985	847.425	214.99	0.2992	0.9996
6	688.002	164.584	0.477	0.9988	676.781	166.345	0.4761	0.9989
7	848.631	224.082	0.317	0.9996	816.803	231.742	0.4134	0.9984
8	684.188	190.469	0.3607	0.9980	687.03	186.698	0.3598	0.9971
9	845.147	176.154	0.4534	0.9989	817.129	171.339	0.436	0.9975
10	684.268	176.196	0.402	0.9986	708.163	141.213	0.4452	0.9990
11	807.359	205.581	0.4022	0.9983	834.845	209.207	0.4504	0.9994
12	685.508	172.015	0.4443	0.9976	705.684	170.376	0.3794	0.9972
13	814.067	192.977	0.5057	0.9995	846.648	202.663	0.4332	0.9995
14	696.172	145.57	0.5536	0.9990	714.757	157.013	0.4587	0.9994
15	812.1	219.599	0.4635	0.9983	833.953	229.693	0.4253	0.9991
16	691.122	162.177	0.4739	0.9992	721.658	181.863	0.3909	0.9997
17	775.632	193.872	0.4137	0.9996	783.789	216.352	0.3836	0.9977
18	755.616	168.637	0.4112	0.9981	747.888	172.734	0.3858	0.9995
19	752.469	164.419	0.4301	0.9985	747.376	168.064	0.4143	0.9972
20	745.267	194.138	0.4164	0.9991	766.477	192.017	0.4102	0.9973
21	771.07	164.442	0.5112	0.9993	783.102	166.584	0.4242	0.9995
22	732.573	203.885	0.3855	0.9983	777.915	205.749	0.3914	0.9992
23	897.605	238.704	0.4189	0.9985	930.856	245.901	0.4096	0.9988
24	634.18	147.797	0.433	0.9988	659.201	154.387	0.3257	0.9995
25	751.744	175.972	0.4216	0.9990	785.347	185.28	0.3269	0.9995
26	752.972	173.189	0.4627	0.9988	751.276	181.945	0.4526	0.9989
27	751.017	176.596	0.4283	0.9983	780.257	177.189	0.443	0.9995
28	768.798	173.895	0.5009	0.9990	783.123	182.118	0.4652	0.9998
29	739.59	179.421	0.4292	0.9989	774.088	192.379	0.4125	0.9993
30	758.59	183.145	0.463	0.9989	769.072	184.835	0.4064	0.9989
31	762.279	175.99	0.4416	0.9988	765.528	182.282	0.4358	0.9991
32	750.332	178.462	0.5351	0.9991	767.277	190.811	0.4348	0.9994
33	746.709	173.272	0.4586	0.9985	743.836	187.49	0.426	0.9983

[1]Trt=treatment number;

[2]Rep = replication; CM_0 = curd moisture at t_0, CM_∞ = curd moisture at an infinite time, k_{CM} = kinetic rate constant (min^{-1}) for curd moisture changes during syneresis.

4.3.3. Curd moisture prediction equation

Both the sensor response and the curd moisture content (dry basis) decreased with a first order response after cutting. Consequently, an equation can be developed relating reflectance (R_t) to curd moisture content by equating these two equations and eliminating time. The following equation was developed relating sensor reflectance (R_t) to curd moisture content (CM_t).

$$R_t = R_\infty + (R_0 - R_\infty)\left(\frac{CM_t - CM_\infty}{CM_0 - CM_\infty}\right)^{\frac{k_{LFV}}{k_{CM}}} \quad \text{Eqn.4.5}$$

where R_t was the light backscatter ratio during syneresis at time t(min), R_∞ was the light backscatter ratio during syneresis at an infinite time, R_0 was the light backscatter ratio during syneresis at t_0, CM_t was the curd moisture (%) during syneresis at time t(min), CM_∞ was the curd moisture (%) during syneresis at an infinite time, CM_0 was the curd moisture content (%) at t_0 i.e. the milk moisture content, k_{LFV} was the kinetic rate constant (min^{-1}) for the LFV sensor response during syneresis, and k_{CM} was the kinetic rate constant (min^{-1}) for curd moisture content changes during syneresis.

Initial curd moisture (CM_0) can be defined previously by doing milk composition analysis. Initial light backscatter ratio (R_0) can be read from the computer program at the beginning of the cheese process. R_∞, CM_∞, k_{LFV}, and k_{CM} must be estimated.

4.3.4. Prediction equation

(i) Effect of experimental conditions on R_∞, CM_∞, k_{LFV}, and k_{CM}.

The first attempt was to leave Equation 4.5 only as a function of experimental conditions. Thus models were developed for each parameter as a function of T, β, pH, FP, and CC. Also a ratio (k) between k_{LFV} and k_{CM} was tested.

Table 4.19 shows the p-values from the analysis of variance for curd moisture equation's parameters (CM_∞ and k_{CM}), for LFV light backscatter ratio equation's parameters (R_∞ and k_{LFV}), and for the ratio k. The R-squared for master model and predictive model are also included in Table 4.19. The predictive model was highly significant in their fit ($P < 0.001$).

Table 4.19 - P-value for curd moisture equation's parameters and LFV light backscatter ratio equation's parameters.

	LFV light backscatter parameters[3]		**Curd Moisture parameters[2]**		
Factors[1]	R_∞	k_{LFV}	CM_∞	k_{CM}	k[4]
T	0.0713[ns]	0.1079[a]	<.0001*	0.0111*	0.2903[a]
β	0.4091[ns]	0.5402[a]	<.0001*	0.3606[ns]	0.3648[a]
pH	0.1055[ns]	0.0007*	<.0001*	0.0184*	0.0067*
FP	0.0905[ns]	0.0003*	<.0001*	0.5183[ns]	<.0001*
CC	0.8756[ns]	0.9941[a]	0.1708[ns]	0.2219[ns]	0.6561[a]
T x *T*	0.3239[ns]	0.0117*	0.0529[ns]	0.1111[ns]	0.0290*
T x *β*	0.1378[ns]	0.3549[ns]	0.6135[ns]	0.3365[ns]	0.2501[ns]
T x pH	0.7149[ns]	0.6173[ns]	0.0939[ns]	0.8431[ns]	0.5552[ns]
T x *FP*	0.9156[ns]	0.0293*	0.9601[ns]	0.1408[ns]	0.0476*
T x *CC*	0.4856[ns]	0.6709[ns]	0.3187[ns]	0.2830[ns]	0.7956[ns]
β x *β*	0.5587[ns]	0.1360[ns]	0.5000[ns]	0.4185[ns]	0.2002[ns]
β x pH	0.1590[ns]	0.0902[ns]	0.3836[ns]	0.1000[ns]	0.0154*
β x *FP*	0.2182[ns]	0.4153[ns]	0.0993[ns]	0.6058[ns]	0.3403[ns]
β x *CC*	0.5948[ns]	0.0081*	0.9253[ns]	0.5248[ns]	0.0145*
pH x pH	0.3936[ns]	0.0376*	0.2758[ns]	0.7050[ns]	0.0493*
pH x *FP*	0.6094[ns]	0.5610[ns]	0.2501[ns]	0.2050[ns]	0.2622[ns]
pH x *CC*	0.0628[ns]	0.9061[ns]	0.0852[ns]	0.6876[ns]	0.9013[ns]
FP x *FP*	0.1580[ns]	0.0647[ns]	<.0001*	0.0960[ns]	0.2009[ns]
FP x *CC*	0.4357[ns]	0.1072[ns]	0.3145[ns]	0.5342[ns]	0.0269*
CC x *CC*	0.8379[ns]	0.6496[ns]	0.3930[ns]	0.3769[ns]	0.3491[ns]
R^2 - Master Model	36.23	61.2	95.36	41.62	60.48
R^2 - Predictive Model	no[5]	49.1	92.96	16.86	53.11

[1] *T* = temperature; *β* = a constant as defined by the experimental design and used to establish the experimental cutting time; *FP* = fat/protein ratio; *CC* = calcium chloride addition level; x denotes interaction of experimental factors.

[2] R_∞ = light backscatter ratio during syneresis at an infinite time; k_{LFV} = kinetic rate constant (min^{-1}) for the LFV sensor response during syneresis.

[3] CM_∞ = curd moisture (%) during syneresis at an infinite time; k_{CM} = kinetic rate constant (min^{-1}) for curd moisture content changes during syneresis.

[4] k = ratio between k_{LFV} and k_{CM}.

[5] A predict model wasn't generated for R_∞ because no effect was significant.

*significant ($P < 0.05$); [ns]not significant ($P > 0.05$); [a] not significant but factor was added to model to preserve hierarchy.

The predictive models developed for CM_∞, k_{LFV}, k_{CM}, and k contain significant factors ($P < 0.05$) and factor that was added to preserve hierarchy with their respective estimated coefficient α_j as shown in Table 4.20. R_∞ doesn't have a predictive model because no effect was significant for this parameters. The only parameter well explained by the predictive model was CM_∞ with 92.96%.

Table 4.20 - List of predictive models for k_{LFV}, CM_∞, k_{CM}, and k[1].

$$\boldsymbol{k_{LFV}} = 25.18 + 0.20\,T - 0.18\,\beta - 8.95\,pH + 1.11\,FP - 0.18\,CC - 0.003\,T^2 - 0.03\,(T \times FP) + 0.08\,(\beta \times CC) + 0.71\,pH^2$$

$$\boldsymbol{CM_\infty} = -159.32 - 2.82\,T + 15.67\,\beta + 75.66\,pH - 141.73\,FP + 48.59\,FP^2$$

$$\boldsymbol{k_{CM}} = 0.87 + 0.007\,T - 0.11\,pH$$

$$\boldsymbol{k} = 63.42 + 0.39\,T - 5.91\,\beta - 20.2\,pH + 2.73\,FP + 0.89\,(\beta \times pH) + 0.17\,(\beta \times CC) + 1.44\,pH^2 - 0.22\,(FP \times CC)$$

[1] CM_∞ = curd moisture (%) during syneresis at an infinite time; k_{LFV} = kinetic rate constant (min^{-1}) for the LFV sensor response during syneresis; k_{CM} = kinetic rate constant (min^{-1}) for curd moisture content changes during syneresis; k = ratio between k_{LFV} and k_{CM}.

T=temperature; β = cutting time factor; FP = fat/protein ratio; CC = calcium chloride addition level.

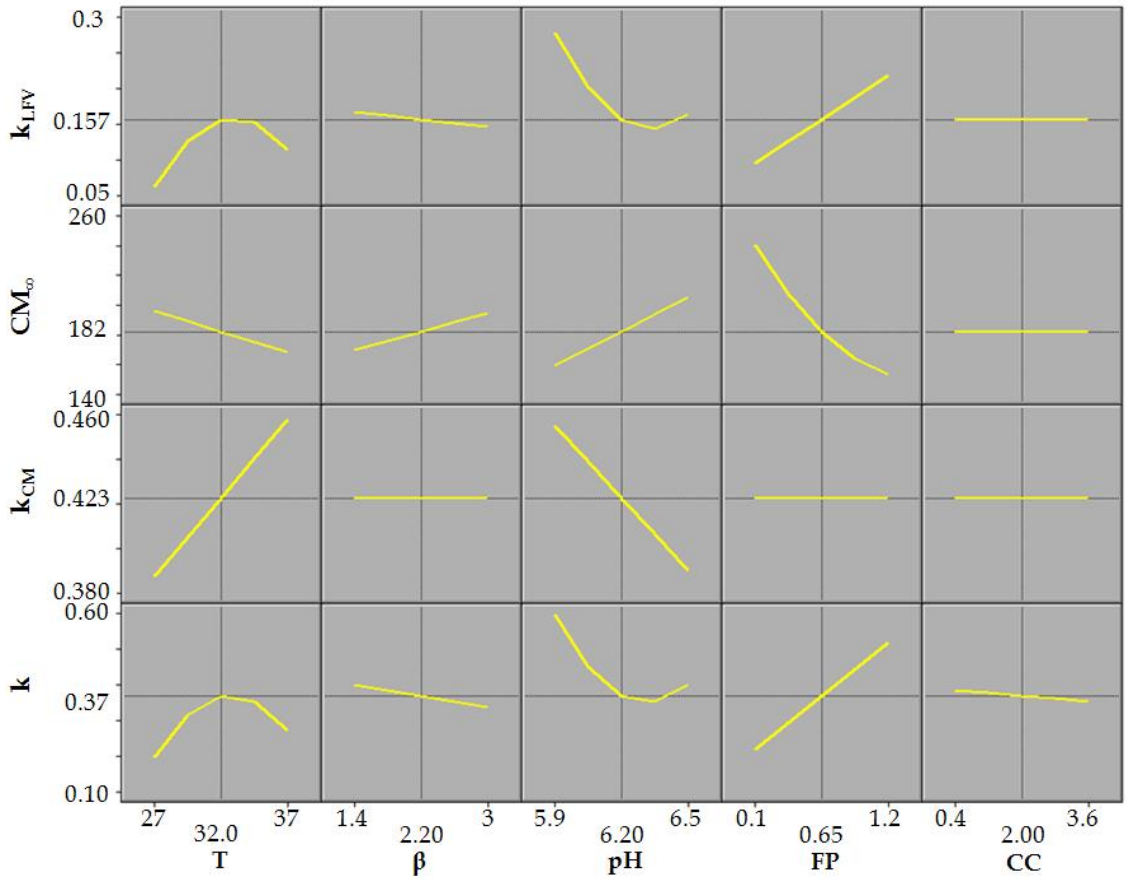

Figure 4.20 - Prediction profiler for the independents variables temperature (*T*), cutting time factor (β), pH, fat/protein ratio (*FP*), and calcium chloride addition level (*CC*) on k_{LFV}, CM_∞, k_{CM}, and *k*.

The prediction profiler graphs for k_{LFV}, CM_∞, k_{CM}, and *k* as a function of the independent variables are shown in Figure 4.20. Increasing the temperature was shown to decrease CM_∞, to increase k_{CM}, and to maximize k_{LFV} and *k* at 32˚C. Increasing cutting time was shown to increase CM_∞ and to decrease k_{LFV} and *k*. Increasing the pH was shown to minimize k_{LFV} and *k* at ~6.4, to increase CM_∞, and to decrease k_{CM}. Increasing the *FP* was shown to decrease CM_∞, and to increase k_{LFV} and *k*. *CC* was shown to slowly decrease *k*.

As expected CM_∞ follows the same trend as curd moisture before pressing. The kinetic constant rate for LFV sensor (k_{LFV}) can be associated with

the rate of syneresis but it is also related with the whey fat content. Increasing temperature up to 32˚C followed the increase in syneresis rate. Above 32˚C the fat release increased and the sensor sign dropped. Late cutting time decreases syneresis rate so decreased k_{LFV}. Increasing pH decrease syneresis rate so decreased k_{LFV}. The kinetic constant rate for curd moisture (k_{CM}) is directly related with casein aggregation speed which also affects syneresis. Lucey (2002) stated that the aggregation rate of rennet-altered micelles increases greatly with temperature and decrease with pH due to electrostatic repulsion.

(ii) Analysis of equation 4.5

Since only CM_∞ could be well explained by experimental conditions, a new approach needs to be finding so it can be applied in the industry.

Rearranging Equation 4.5 a relation between ratios was found as shown in Equation 4.6, where RR_t is the reflectance ratio 'ratio' as a function of time, RCM_t is the curd moisture ratio as a function of time, and k is a ratio between k_{LFV} and k_{CM}.

$$\left(\frac{R_t - R_\infty}{R_0 - R_\infty}\right) = \left(\frac{CM_t - CM_\infty}{CM_0 - CM_\infty}\right)^{\frac{k_{LFV}}{k_{CM}}} \rightarrow RR_t = (RCM_t)^k \qquad \text{Eqn.4.6}$$

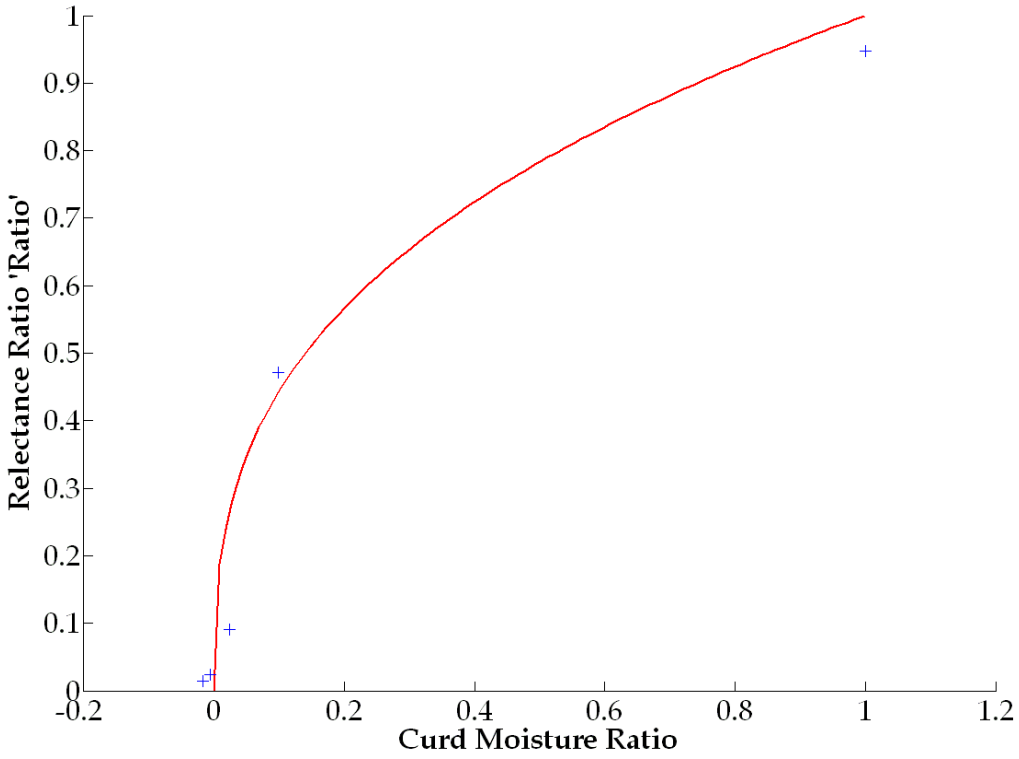

Figure 4.21 – Relation between ratio defined in Equation 4.6 at central point (T=32°C; β=2.2; pH=6.2; FP=0.65; CC=2mM. (—) Theoretical curve. (+) Experimental data.

Figure 4.21 shows an example of the relation between RR_t and RCM_t for a central point experiment. The curvature of the theoretical curve is related with the k value. Not enough data was obtained to do statistical analysis but it was visually observed that data points are usually close to the theoretical curve which indicate that this equation can be used to control curd moisture using LFV sensor response.

Chapter 5 : CONCLUSIONS

A CCD test design encompassing the primary factors (temperature, cutting time factor (β), pH, fat/protein ratio, and calcium chloride addition level) of concern in cheesemaking was developed and three replications conducted (33 tests per replication). The testing procedure required modifications and only data from replication 2 and 3 were used in the data analysis.

A sensor (LFV) was fabricated to measure the light scatter response (300 to 1100 nm) during both coagulation and syneresis steps used for cheesemaking. The response was greatest at 980 nm as indicated by the peak on coagulation and by a valley on syneresis step, so this wavelength was used exclusively for data analysis. The LFV sensor parameter t_{max} could be calculated as a function of the experimental factors as shown by the following equation:

$$\boldsymbol{t_{max}} = 1546.86 - 13.76\,T - 448.19\,pH - 0.54\,CC + 0.0755\,T^2 + 1.32\,(T \times pH) + 35.14\,pH^2$$

The effects of temperature, cutting time factor (β), pH, fat/protein ratio, and calcium chloride addition level on curd moisture content, whey fat losses, and curd yield were examined. Models for predicting those parameters were successfully developed (R^2>0.75) using the experimental factors as independent variables. Increasing temperature, decreasing cutting time, lowering pH, and increasing fat to protein content in the respective experimental ranges significantly decreased pressed curd moisture. Whey fat losses were predominantly affected by temperature and fat to protein ratio. Temperature, cutting time, pH, and fat to protein ratio significantly affected curd yield.

One of the objectives was the development of a method to use the light backscatter to control moisture content after pressing the curd. There was considerable scatter in the light backscatter response upon the beginning of

syneresis. The light backscatter response decreased exponentially as expected. The determination of a rate constant required manually selecting an exponential period (Tv) for each test. It was determined that pressed curd moisture also followed a first order response with syneresis time.

The Syneresis Monitoring Model was developed by combining the first order relations for pressed curd moisture and the light backscatter sensor response. The following is the Syneresis Monitoring Model:

$$\left(\frac{R_t - R_\infty}{R_0 - R_\infty}\right) = \left(\frac{CM_t - CM_\infty}{CM_0 - CM_\infty}\right)^{\frac{k_{LFV}}{k_{CM}}} \rightarrow RR_t = (RCM_t)^k$$

The data scatter during syneresis was the most limiting factor which obscured a clear model validation. Despite that, this model appeared to describe the relationship between curd moisture for pressed cheese and reflectance ratio response which is an important step on the improvement of the curd moisture control.

APPENDICES

Appendix A: Mat Lab Program

```
clc
clear all
cla

RsquaredRR=[];
Rinfinit=[];
Rzero=[];
k_LFV=[];
tend=[];

[data txt] = xlsread('DataRR.xlsx');

for i=1:2:131
    %get data for reflectance ratio as a function of time
selected
    %visually
    id = find(isnan(data(:,i)),1);
    if isempty(id)
       tr=data(:,i);
       RR=data(:,i+1);
    else
       tr = data(1:id-1,i);
       RR = data(1:id-1,i+1);
    end

    %to find Rinf, R0, k_LFV, and reflectance ratio predicted
    beta0=[1.2;0.5;0.5];
    [beta,r,J]=nlinfit(tr,RR,@funr,beta0);
    RRp=beta(1)+(beta(2)-beta(1))*exp(-beta(3)*tr);
    ESS=sum(r.^2);
    TSS=sum((RR-mean(RR)).^2);
    RsquaredRR(end+1,1)=1-ESS/TSS;
    save1=beta(1);
    save2=beta(2);
    save3=beta(3);
    save4=tr(end);
    Rinfinit(end+1,1)=save1;
    Rzero(end+1,1)=save2;
    k_LFV(end+1,1)=save3;
    tend(end+1,1)=save4;

    figure
      hold on
      plot(tr,RR,'*r')
      plot(tr,RRp,'b')
```

```
      xlabel ('Time from cutting (min)'); ylabel ('Reflectance
Ratio')
      hold off

end


RsquaredCM=[];
CMinfinit=[];
CMzero=[];
k_CM=[];
CM=[];

[data2 txt] = xlsread('DataCM.xlsx');
[data txt] = xlsread('DataR85.xlsx');

for j=2:1:67
    CMp=[];
    Rp=[];
    CMpp=[];
    tcmp=[];
    Tv=tend(1);
    tcm=data2(:,1); %10 data points for curd moisture at
0,5,15,25,35,45,55,65,75,and 85 min
    CMwb = data2 (1:10,j); %curd moisture wet basis
    CMdb=(CMwb./(1-(CMwb./100))); %curd moisture dry basis

    D=[tcm CMdb];
    %select data correspondent to reflectance ratio selected
visually
    for i=1:10
        if D(i,1)>Tv
           D(i,1)=0;
           D(i,2)=0;
        end
    end

    tcm=[0
         nonzeros(D(:,1))];
    CM=nonzeros(D(:,2));

    %to find CMinf, CM0,and k_CM
    beta0=[700;200;0.5];
    [beta,r,J]=nlinfit(tcm,CM,@funcm,beta0);
    ESS=sum(r.^2);
    TSS=sum((CM-mean(CM)).^2);
    RsquaredCM(end+1,1)=1-ESS/TSS;
    save4=beta(1);
    save5=beta(2);
    save6=beta(3);
    CMinfinit(end+1,1)=save4;
    CMzero(end+1,1)=save5;
```

```
    k_CM(end+1,1)=save6;

    CMinf=CMinfinit(1);
    CM0=CMzero(1);
    kCM=k_CM(1);
    Rinf=Rinfinit(1);
    kLFV=k_LFV(1);
    R0=Rzero(1);

    %to calculate curd moisture predicted and to make a plot
between
    %reflectance ratio and curd moisture predicted.

    for x=0:0.1:Tv;
        y=CMinf+(CM0-CMinf)*exp(-kCM*x);
        save7=x;
        save8=y;
        tcmp(end+1,1)=save7;
        CMpp(end+1,1)=save8;
    end

    figure
      hold on
      plot(tcm,CM,'*r')
      plot(tcmp,CMpp,'b')
      xlabel ('Time from cutting (min)'); ylabel ('Reflectance
Ratio')
      hold off

    x=[0 5 15 25 35 45 55 65 75 85];
    t=x';
    R = data (:,j);
    Rinitial= data (1,j);
    R5=sum(data (41:61,j))/21;
    R15=sum(data (141:161,j))/21;
    R25=sum(data (241:261,j))/21;
    R35=sum(data (341:361,j))/21;
    R45=sum(data (441:461,j))/21;
    R55=sum(data (541:561,j))/21;
    R65=sum(data (641:661,j))/21;
    R75=sum(data (741:761,j))/21;
    R85=sum(data (831:851,j))/21;
    y=[Rinitial R5 R15 R25 R35 R45 R55 R65 R75 R85];
    R=y';
    D=[t R];

    for i=1:10
        if D(i,1)>Tv
           D(i,1)=0;
           D(i,2)=0;
        end
    end
```

```
    t=[0
       nonzeros(D(:,1))];
    R=nonzeros(D(:,2));

    RRR=(R-Rinf)/(R0-Rinf);
    RCM=(CM-CMinf)/(CM0-CMinf);

    for x=CMinf:5:CM0;
        y=Rinf+(R0-Rinf)*((x-CMinf)/(CM0-CMinf))^(kLFV/kCM);
        save9=x;
        save10=y;
        CMp(end+1,1)=save9;
        Rp(end+1,1)=save10;
    end

    RRRp=(Rp-Rinf)/(R0-Rinf);
    RCMp=(CMp-CMinf)/(CM0-CMinf);

    figure
      hold on
      plot(RCMp,RRRp,'r')
      plot(RCM,RRR,'b*')
      hold off
end
```

REFERENCES

Brulé, G.; **Lenoir**, J. (**1987**): The coagulation of milk, pp. 1-21. In Eck, A. (Ed.): *Cheesemaking: Science and Technology*. Lavoisier,NY.

Calvo, M.M.; **Balcones**, E. (**2000**): Some Factors Influencing the Syneresis of Bovine, Ovine, and Caprine Milks. *Journal Dairy Science*, 83, 1733-1739.

Castillo, M.; Jordan, M.J.; Godoy, A.; Laencina, J.; Lopez, M.B. (**2000**): Kinetics of syneresis in freesh goat cheese. *Milchwissenschaft*, 55(10), 566-569.

Castillo, M.; Payne, F.A.; Hicks,C.L.; Lopez, M.B. (**2000b**): Predicting cutting and clotting time of coagulating goat's milk using diffuse reflectance: effect of pH, temperature and enzyme concentration. *International Dairy Journal*, 10, 551-562.

Castillo, M.; Payne, F.A.; López, M.B.; Ferrandini, E.; Laencina, J. (**2005**): Preliminary Evaluation of an Optical Method for Modeling the Dilution of Fat Globules in Whey During Syneresis of Cheese Curd. *Applied Engineering in Agriculture*, 21, 265-268.

Castillo, M.; Payne, F.A.; Shea, A. (**2005b**): Development of a combined sensor technology for monitoring coagulation and syneresis operation in cheesemaking. *Journal of Dairy Science*, 88-142.

Castillo, M.; Lucey, J.A.; Wang, T.; Payne, F.A. (**2006**): Effect of temperature and inoculums concentration on gel microstructure, permeability and syneresis kinetics. Cottage cheese-type gels. *International Dairy Journal*, 16, 153-163.

Castillo, M.; Lucey, J.A.; Payne, F.A. (**2006b**): Effect of temperature and inoculums concentration on rheological and light scatter properties of milk coagulated by a combination of bacterial fermentation and chymosin. Cottage cheese-type gels. *International Dairy Journal*, 16, 131-146.

Encyccheese: cheese production process. Art. *Encyclopædia Britannica Online*. Web. 14 Feb. 2011. <http://www.britannica.com/EBchecked/media/110232/The-cheese-making-process>.

Evervard, C.D.; O'Callaghan D.J.; Mateo, M.J.; O'Donnell, C.P.; M.; Castillo, M.; Payne, F.A. (**2008**): Effects of Cutting Intensity and Stirring Speed on Syneresis and Curd Losses During Cheese Manufacture. *Journal Dairy Science*, 91, 2575-2582.

Fagan, C.C. (**2006**): Process analytical technology tolls in natural and processed cheese manufacture. *PhD Thesis* University College Dublin, Dublin.

Fagan, C.C.; Leedy, M.; Castillo, M.; Payne, F.A.; O'Donnell, C.P.; O'Callaghan D.J. (**2007**): Development of a light scatter sensor technology for on-line monitoring of milk coagulation and whey separation. *Journal Dairy Science*, 90, 4499-4512.

Fagan, C.C.; Castillo, M.; Payne, F.A.; O'Donnell, C.P.; O'Callaghan D.J. (**2007b**): Effect of Cutting Time, Temperature, and Calcium on Curd Moisture, Whey Fat Losses, and Curd Yield by Response Surface Methodology. *Journal of Food Engineering*, 83, 61-67.

Fagan, C.C.; Castillo, M.; Payne, F.A.; O'Donnell, C.P.; Leedy, M.; O'Callaghan D.J. (**2007c**): Novel Online Sensor Technology for Continuous Monitoring of Milk Coagulation and Whey Separation in Cheesemaking. *Journal of Agricultural and Food Chemistry*, 55, 8836-8844.

Fagan, C.C.; Castillo, M.; O'Donnell, C.P.; O'Callaghan D.J.; Payne, F.A. (**2008**): On-line prediction of cheesemaking indices using backscatter of near infrared light. *International Dairy Journal*, 18, 120-128.

Foltmann, B. (**1993**): General and Molecular Aspects of Rennets, pp. 37-68. In P. F. Fox (Ed.): *Cheese: Chemistry, Physics and Microbiology*, Chapman and Hall.

Fox, P. F. (**1993**): Cheese: An Overview, pp. 1-36. In P. F. Fox (Ed.): *Cheese: Chemistry, Physics and Microbiology*, Chapman and Hall.

Fox, P.F.; Guinee, T.P.; Cogan, T.M.; McSweeney, P.L.H. (**2000**): *Fundamentals of Cheese Science*. Aspen, Gaithersburg; MD.

Guinnee, T.P.; **McSweeney**, P.L.H. (**2006**): Significance of Milk Fat in Cheese, pp. 377-440. In Fox, P.F. and McSweeney, P.L.H. (Ed.): *Advanced Dairy Chemistry, Volume 2: Lipids*. Springer,NY.

Guinnee, T.P.; Mulholland, E.O.; Kelly, J.; O'Callaghan D.J. (**2007**): Effect of Protein-to-Fat Ratio of Milk on the Composition, Manufacturing Efficiency, and Yield of Cheddar Cheese. *JournalDairy Science*, 90, 110-123.

Green, M. L.; Hobbs, D. G.; and Morant, S. V. (**1977**): The process of milk coagulation by rennet. *Biochemical Society Transactions*, 5, 1328-1330.

Green, M.L.; **Grandison**, A.S. (**1993**): Secondary (Non-enzymatic) Phase of Rennet Coagulation and Post-Coagulation Phenomena, pp. 101-140. In P. F. Fox (Ed.): *Cheese: Chemistry, Physics and Microbiology*, Chapman and Hall.

Johnson, M.E.; Chen, C.M.; Jaeggi, J.J. (**2001**): Effect of Rennet Coagulation Time on Composition, Yield, and Quality of Reduced-Fat Cheddar Cheese. *Journal Dairy Science*, 84, 1027-1033.

Lagoueyte, N.; Lablee, J.; Lagaude, A.; DeLaFuente, B.T. (**1994**): Temperature Affects Microstructure of Rennered Milk Gel. *Journal of Food Science*, 59, 956-959.

Lamb, A.M. (2010): The optical measurement of β-LG denaturation during thermal processing. Master thesis at University of Kentucky, KY, USA.

Lucey, J.A.; **Fox**, P. F. (**1993**): Importance of Calcium and Phosphate in Cheese Manufacture: A Review. *Journal Dairy Science*, 79, 1714-1724.

Lucey, J.A. (**2002**): Rennet Coagulation of Milk. University of Wisconsin-Madison, WI, USA

Lucey, J.A. (**2002b**): Formation and Physical Properties of Milk Protein Gels. *Journal Dairy Science*, 85, 281-294.

Lucey, J.A. (**2004**):, Formation, Structural Properties and Rheology of Acid-coagulation Milk Gels. pp. 105-122. In P. F. Fox; P.L.H. McSweeney; T.M. Cogan; T.P. Guinee (Ed.): *Cheese: Chemistry, Physics and Microbiology*, Elsevier.

Lee, W.J.; **Lucey**, J.A. (**2010**): Formation and Physical Properties of Yogurt. *Journal Animal Science*, 23, 1127-1136.

Marshall, R. (**1982**): An improved method for measurement of the syneresis of curd formed by rennet action on milk. *Journal of Dairy Research*, 49, 329-336.

McMahon, D.J.; Brown, R.J.; Richardson, G.H.; Ernstron, C.A. (**1984**): Effects of calcium, phosphate and bulk culture media on milk coagulation properties. *Journal Dairy Science*, 67, 930-938.

Mellema, M.; Walstra, P.; van Opheusden, J.H.J.; van Vliet, T. (**2002**): Effects of structural rearrangements on the rheology of rennet-induced casein particles gels. *Adv. Colloid Interface Science*, 98, 25-50.

Mishra, R.; Golvindasamy-Lucey, S.; **Lucey**, J.A. (**2005**): Rheological properties of rennet-induced gels during the coagulation and cutting process: impact of processing conditions. *Journal of Texture Studies*, 36, 190-212.

Scott, R.; Robinson, R. K.; Wilbey, R. A. (**1998**): *Cheesemaking practice*. Aspen Publishers Inc. Gaithersburg

Patel, M.C.; Lund, D.B.; Olson, N.F. (**1972**): Factors Affecting Syneresis of Renneted Milk Gels. *Journal of Dairy Science*, 55, 913-918.

Payne, F.A.; Hicks, C.L.; Madangopal, S.; Shear, S.A. (**1993**): Fiber optic sensor for predicting the cutting time of coagulation milk for cheese production. *Transactions of the ASAE*, 36(3), 841-847.

Payne, F.A.; Castillo, M. (**2007**): Light Backscatter Application in Milk Coagulation. *Encyclopedia of Agricultural, Food, and Biological Engineering*.

Renault, C.; Gastaldi, E.; Lagaude, A.; Cuq, J.L.; Tardo de La Fuente, B. (**1997**): Mechanisms of Syneresis in Rennet Curd without Mechanical Treatment. *Journal of Food Science*, 62, 907-910.

Tabayehnejad, N., Castillo, M., and Payne, F. A. (**2010**). Comparison of total milk-clotting activity measurement precision using the Berridge clotting time method and a proposed optical method. In review.

Tetra Pak (**1995**). Dairy Processing Handbook. Tetra Pak Processing Systems AB, Lund, Sweden.

Walstra, P.; van Dijk, H.J.M.; Geurts, T.J. (**1985**): The syneresis of curd. 1. Genreal considerations and literature review. *Milk Dairy Journal*, 39, 209-246.

Walstra, P. (**1993**): The Syneresis of Curd, pp. 141-191. In P. F. Fox (Ed.): *Cheese: Chemistry, Physics and Microbiology*, Chapman and Hall.

Weber, F. (**1987**): Curd drainage, pp. 22-36. In Eck, A. (Ed.): *Cheesemaking: Science and Technology*. Lavoisier,NY.

van den Bijgaart, H.J.C.M. (**1988**): Syneresis of rennet-induced milk gels as influenced by cheesemaking parameters. PhD Thesis Wageningen Agricultural University, Wageningen, the Netherlands.

Zviedrans, Z.; Graham, E.R.B. (**1981**): An improved tracer method for measuring the syneresis of rennet curd. *The Australian Journal of Diary Technology*, 117-120.

VITA

TATIANA GRAVENA FERREIRA

BIRTH DATE: June 9, 1983

BIRTH PLACE: Taubaté, SP - Brazil

EDUCATION

Bachelor of Food Engineering March 2003 to December 2007

Federal University of Viçosa, Minas Gerais, Brazil

PROFESSIONAL EXPERIENCE

Graduate Student Research Assistant, January 2008 to present - Biosystems and Agricultural Engineering, University of Kentucky, Lexington, KY

Engineering Intern, Sep 2005 - WOW, Caçapava, SP - Brazil

Undergraduate Research, June 2004 to June 2005

CERTIFICATIONS

Good Manufacturing Practice (GMP) and Hazard Analysis and Critical Control Points (HACCP).